

博士学位論文

氏名(本籍)

ALINA UUSIKU (NAMIBIA)

学位の種類

博士(工学)

学位記番号

博甲第159号

学位授与年月日

令和 2年3月31日

学位授与の要件

学位規則第4条第1項

学位論文題目

LOW TEMPERATURE FABRICATION OF
FUNCTIONAL THIN FILMS OF COPPER OXIDE
AND METALLIC COPPER *VIA* SPRAY
COATING: STUDY ON EFFECTIVE
USE OF LOCALLY PRODUCED COPPER IN
NAMIBIA

論文審査委員

主査 佐藤 光史

副査 大倉 利典

〃 阿相 英孝

〃 工藤 一秋(東京大学)

工学院大学大学院

SUMMARY OF THESIS

LOW TEMPERATURE FABRICATION OF FUNCTIONAL THIN FILMS OF COPPER OXIDE AND METALLIC COPPER *VIA* SPRAY COATING: STUDY ON EFFECTIVE USE OF LOCALLY PRODUCED COPPER IN NAMIBIA

Applied Chemistry and Chemical Engineering Program

ALINA UUSIKU

In this study, a molecular precursor aqueous solution was prepared by typical chemical synthesis and electrochemical methods, and sprayed on a quartz glass substrate at 180°C in air using a simple airbrush. Then, photocatalytic cuprous oxide (Cu₂O) under visible light irradiation and conductive metallic copper (Cu) thin films were fabricated. The purpose of the study was to contribute to the industrialization of Namibian raw material through effective utilization of copper metal which is one of the Namibia's main mineral resource.

First, aqueous ammonia solution containing copper formate was sprayed onto a quartz glass substrate kept at 180°C in air to fabricate Cu₂O thin films with oxygen deficiency, which is an important factor for high photocatalytic activity. It was demonstrated that the oxygen deficient Cu₂O thin film efficiently achieved the discoloration of methyl orange (MO) aqueous solution under visible light irradiation from a fluorescent lamp (0.45 mW cm⁻²). The O-defect site was found in the Raman spectra of these photocatalytic active thin films. Next, a direct preparation method of Cu₂O precursor aqueous solution from metallic copper was developed using an electrochemical method. A *p*-type Cu₂O semiconductor thin film obtained by spraying coating an electrochemically prepared aqueous solution at 180°C in air was identical to that fabricated using solution from starting material of copper formate. Furthermore, it was found that by adding ethylenediamine-*N*, *N*, *N'*, *N'*-tetraacetic acid (EDTA) into the electrochemically prepared aqueous solution result in a thin film of Cu single phase with the conductivity of the order 10⁻³ Ω cm *via* spray coating under same condition.

Heat treatment temperature of ca. 400°C and inert Ar gas were necessary for the formation of Cu₂O and Cu thin film by a conventional MPM. However, this study achieved their

formation only by spraying corresponding molecular precursor aqueous solutions onto substrate at 180°C in air.

This study consists of 6 chapters. Chapter 1 outline and summarized research background. Chapter 2 described the principles of characterization techniques for precursor aqueous solution and thin films, reagents used in the experiments and the equipment used for the measurement. Chapter 3 summarizes the low temperature fabrication and photocatalytic activity of spray coated *p*-type Cu₂O thin films using chemically synthesized molecular precursor aqueous solutions. Chapter 4 describes the preparation of Cu₂O precursor aqueous solution by electrochemical method, and Chapter 5 describes the selective formation of Cu₂O and Cu thin film by spray coating electrochemically prepared molecular precursor aqueous solution. In chapter 6, the research was summarized, its future development was proposed and described. A summary of each chapter is given below.

CHAPTER 1: GENERAL INTRODUCTION

Thin films can impart various functions such as electrical, magnetic, and optical to the material surface. From the viewpoint of resource and energy saving, such functional thin film is very important for the sustainable development which satisfies the needs of both present and next generation. Methods for the formation of a functional thin film can be roughly divided into a gas or liquid phase in which a raw material of a gas or liquid phase reacts with a substrate. In a gas phase method, the film is formed in the high vacuum which is necessary to transform the raw material into the gas phase state. On the other hand, the liquid phase method enables the formation of functional thin films without vacuum. The liquid phase formation process of functional thin films is also important for sustainable development. The molecular precursor method (MPM) is a wet chemical process for the formation of thin films of various metal oxides, metal and phosphate compounds by coating a precursor solution in which a metal complex is dissolved onto substrate followed by heat-treatment. It is based on the design of metal complexes in precursor solutions with excellent stability, homogeneity, miscibility and high coatability, amongst its many practical advantages. The formation of various metal oxide, phosphate compounds, and metal thin films has been reported by coating a precursor solution onto substrate using a spin coating method. The formation of Cu₂O and metallic Cu thin film which are the main objective of this study has been previously reported. When fabricating these thin films by spin coating, volatile organic compounds (VOCs) are generally used as solvents.

However, industrially, VOCs free solvents are desired because of the risk of ignition and adverse effects on human health and ecosystem associated with VOCs. From such viewpoint, the formation of Cu₂O and Cu thin films was attempted by preparing the molecular precursor aqueous solution and spraying it onto the substrate. Namibia is rich in resources such as diamond, uranium, gold, zinc, and copper. Copper in particular accounts for 50% of Namibia's annual export earnings. However, it is exported to foreign countries in its raw form for further processing into final products without being used in research and industrial fields inside the country. Therefore, it was considered that if functional thin films could be formed simply by using copper which is one of Namibia's rich natural resources, it will not only contribute to the sustainable development but also become an important asset to its value addition and industrialization in Namibia. In this study, Cu₂O precursor aqueous solution was prepared using metal salt as a starting material, and the formation of Cu₂O thin film at low temperature in air was achieved. In addition, a molecular precursor aqueous solution prepared from metallic copper plate using an electrochemical method was sprayed onto a substrate at 180°C in air to achieve the formation of a highly functional Cu₂O thin film and a conductive Cu thin film. The background and outline of these studies are summarized in Chapter 1.

CHAPTER 2: MATERIALS AND METHODOLOGY

Chapter 2, fully describes the preparation methods of precursor aqueous solution, the spray coating method for the preparation of thin films, the characterization and evaluation methods of formed thin films, and the measurement principles of measuring devices used under this study. The list of all chemical reagents, materials and equipment used is provided.

CHAPTER 3: Low Temperature Fabrication and Photocatalytic Activity of *p*-type Cu₂O Thin Films by Molecular Precursor Method

Single crystal of a *p*-type Cu₂O semiconductor has a band gap of about 1.9-2.3 eV. Cu₂O is one of the few *p*-type semiconductors among other oxides that absorbs visible light, therefore it is expected to be used as material for visible light-responsive photocatalysts and oxide solar cells. Its preference in those applications is due to its low toxicity, cost and minimum environmental loading. The fabrication of Cu₂O thin films by the conventional molecular precursor method has been achieved using alcohol-based system precursor solution such as ethanol. This is the first report on the formation of Cu₂O single phase thin film by liquid phase method *via* spray coating at 180°C in air. While even formation of *p*-type semiconductors by

gas phase method shows some general difficulties. Previously, Cu₂O thin film was formed by heat treatment of precursor film coated and dried on substrate by spin coating method, at 350°C in argon gas atmosphere. In Chapter 3, we prepared a novel Cu₂O aqueous precursor solution, and examined whether it could form a thin film by spray coating it onto a substrate at 180°C in air. The photocatalytic activity of the formed thin film was examined under visible light irradiation. Specifically, the precursor aqueous solution were prepared in a diluted ammonia solution by dissolving Cu(II) formate and ammonium formate whose molar ratios to Cu(II) ion were 0, 2, 6 and 14. The aqueous precursor solution were sprayed onto a quartz glass substrate at 180°C in air using an airbrush to form thin films which adhered well to the substrate. The films formed were Cu₂O single phase, and their Hall effect measurements showed that both films were *p*-type semiconductors. It was found that the films became thicker and porous with increasing ammonium formate content in the aqueous precursor solution. The photocatalytic activity of the thin films was investigated by a discoloration test with visible light irradiation on the films immersed in methyl orange aqueous solution. In the cases of the molar ratios at 6 and 14, the Cu₂O thin films of 140 and 350 nm thickness respectively indicated a highly photocatalytic activity under visible-light irradiation of 0.45 mW cm⁻², and the pseudo-first-order rate constants of 0.056 and 0.087 min⁻¹ were respectively obtained by tracing the discoloration of a methyl orange solution. The O-defect site was found in the Raman spectra of these photocatalytic thin films whose adhesion strength onto the quartz substrate were larger than 5.6 N.

CHAPTER 4: Preparation of aqueous Cu₂O precursor solution using electrochemical method

In Chapter 4, the direct preparation of Cu₂O precursor aqueous solution from metal copper plate was tried as a model of refined copper blister using electrochemical method. Concretely, ammonium formate aqueous solution was put into a glass vessel cell as an electrolytic solution, copper plates electrodes were immersed in electrolytic solution as both an anode and cathode, and a potential difference of 18 V was applied for 2 hours. The electrolytic solution changed from colorless to blue. However, precipitates thought to be copper hydroxide were formed in the solution. Additionally, two glass containers were connected through the partition of cellulose semipermeable membrane, ammonium formate aqueous solution and copper plate electrodes were placed in each glass container, and a potential difference of 18 V was applied. The aqueous solution in the anode glass vessel cell changed with time from colorless to blue,

and no precipitation occurred. On the other hand, gas was generated from the copper plate without coloring the aqueous solution in the cathode glass vessel cell. The gas generated from the surface of cathode electrodes was identified as hydrogen. The absorption spectrum of the precursor aqueous solution obtained from the anode glass cell was in agreement with the absorption wavelength of the molecular precursor aqueous solution used in Chapter 3. Higher concentration of the Cu(II) complex was obtained in the precursor solution. Thus, an aqueous solution containing Cu(II) complex was obtained. The Cu₂O precursor aqueous solution, was prepared in one step by an electrochemical method using metallic copper.

CHAPTER 5: Selective Low Temperature Fabrication of Cu and Cu₂O Thin Films by Spray Application of Aqueous Solution Prepared by Electrochemical Method

The aqueous complex solution prepared in Chapter 4 was applied under the spray conditions of Chapter 3 to form a thin film. The formed thin films were Cu₂O single-phase *p*-type semiconductors identical to those formed in Chapter 3. On the other hand, ethylenediamine-N, N, N', N'-tetraacetic acid (EDTA) was added to the same aqueous solution containing Cu(II) complex, and the resultant spray solution was sprayed under the same conditions to form a thin film. The resulting thin film was of a single-phase metallic Cu with a thickness of 170 nm, and its electrical resistivity was $8.9(2) \times 10^{-3} \Omega \text{ cm}$. Its adhesion strength to the quartz glass substrate showed 12(7) MPa. It was clarified that the fabricated conductive metallic Cu thin film could be selectively formed by the addition of EDTA to the aqueous solution containing Cu(II). Thus, we have developed a method to directly prepare precursor aqueous solution from metallic copper by electrochemical method. In addition, either by using electrochemically prepared precursor solution itself or that obtained by the simple method of adding EDTA to it, the selective thin film formation of Cu₂O semiconductor and metallic Cu could be achieved *via* spray coating at 180°C in the air.

CHAPTER 6: Summary and Future Developments

In this study, molecular precursor aqueous solution prepared using synthetic chemical method and electrochemical method will be sprayed on the quartz glass substrate at 180°C in air, to achieve the formation of high-performance Cu₂O thin film and conductive Cu thin film, respectively. In the future, the preparation of similar molecular precursor aqueous solution will be attempted using electrodes of crude copper mined and refined from Tsumeb mine in

Namibia. The resultant solution will be used in the fabrication of catalytically active Cu₂O thin film by visible light and conductive Cu thin film. The fabricated films will not only be considered to be applicable material in energy devices such as thin film solar cells and flexible electronic devices, but also for application such as their formation of antibacterial materials for environmental purification and immobilized photocatalysts.

PUBLICATIONS FROM THE MAJOR RESULTS

1. Alina Uusiku, Hiroki Nagai, and Mitsunobu Sato “Highly photo-reactive p-type Cu₂O thin films fabricated on a quartz glass substrate at 180°C in air, by spraying aqueous precursor solutions involving Cu(II) complexes.”, *Material Technology: “Advanced Performance Materials”*, **00**, 1–12 (2019).
2. Alina Uusiku, Hiroki Nagai, and Mitsunobu Sato, “Selective deposition of p-type Cu₂O or conductive Cu thin film at 180°C in air on a quartz glass substrate: Development of an aqueous spray solution using two-compartment electrolysis system.”, *Functional Material Letters*”, **13(03)**, 1–7 (2020). Full length article.

博士論文概要書

スプレー塗布による銅酸化物および金属銅機能性薄膜の低温形成

－ナミビア産銅の有効利用に関する研究－

大学院工学研究科化学応用学専攻

ALINA UUSIKU

本研究は、典型的な化学合成法と電気化学的方法を用いて分子プレカーサー水溶液を調製し、空气中で簡便なエアブラシを用いて 180°C の基板上にスプレー塗布し、可視光照射下で触媒活性な酸化銅 (Cu₂O) 半導体薄膜と導電性銅 (Cu) 金属薄膜の形成を達成した。ナミビア国の主要鉱物資源である銅の有効利用に資することを目的に実施した。

先ず、ギ酸銅を含むアンモニア水溶液を 180°C に保った石英ガラス基板上に空气中でスプレー塗布し、高い光触媒能に重要な因子である酸素欠損をもつ Cu₂O 薄膜を形成した。その酸素欠損 Cu₂O 薄膜は、蛍光灯の光照射によってメチルオレンジ水溶液を効率良く退色させることを実証し、さらにラマンスペクトルを用いてその要因を解明した。次に、電気化学的方法を用いて金属銅からの Cu₂O プレカーサー水溶液の直接調製法を開発した。この水溶液を用いて同条件下でスプレー塗布して得た Cu₂O 膜は、ギ酸銅を出発原料とする先のプレカーサー水溶液と同様に *p* 型半導体だった。さらに、電気化学的に得た溶液にエチレンジアミン四酢酸を添加した水溶液を同条件で塗布した膜が、10⁻³ Ω cm レベルの導電性をもつ Cu 単一相であることを見出した。これまで分子プレカーサー法によっても、Cu₂O や Cu 薄膜形成には 400°C 程度の熱処理温度と不活性ガスを必要とした。本研究は、180°C の空气中でのスプレー塗布のみでの形成を達成した。

本論文は、全 6 章からなる。第 1 章は、研究背景と概要をまとめた。第 2 章は、実験で用いた試薬や測定に用いた装置の原理に関して述べた。第 3 章は、化学合成した分子プレカーサー溶液による *p* 型 Cu₂O 薄膜の低温形成と光触媒活性についてまとめた。第 4 章は、電気化学的方法による Cu₂O プレカーサー水溶液の調製を、第 5 章では、その水溶液を用いたスプレー塗布による Cu₂O と Cu 薄膜の選択的形成について述べた。第 6 章では研究を総括し、今後の展開に関して述べた。各章の概要を以下に記載する。

第 1 章 研究背景と概要

薄膜は、電気的、磁氣的、光学的などの多様な機能を材料表面に付与できる。このような機能性薄膜は、現在のみならず次世代のニーズも満足させられる開発（持続可能な開発）にとって、省資源、省エネルギーの観点からも非常に重要である。このような機能性薄膜の形成法は、一般に気相の原料と基板を反応させる気相法と、液相の原料と基板を反応させる液相法に大別できる。気相法は、原料を気相状態にする必要性から高真空中で成膜される。一方で液相法は、真空無しでの機能性薄膜の形成が可能である。このような機能性薄膜の形成プロセスも持続可能な開発には、重要である。

分子プレカーサー法 (MPM) は、金属錯体が溶解したプレカーサー溶液を塗布、熱処理して金属や金属酸化物、リン酸化合物の薄膜を形成する方法である。MPM は、プレカーサー溶液中の金属錯体の設計を基盤としており、安定性、均一性、混和性、塗布性の高さなどにおいて実用的な利点をもつ。これまでにスピコート法でプレカーサー溶液を塗布し、様々な金属酸化物、リン酸化合物、金属薄膜の形成を報告してきた。これまでに本研究で対象としている Cu₂O 薄膜や Cu 薄膜の形成も報告している。スピコート法で塗布する場合は、一般的に揮発性有機化合物 (VOCs) を溶媒として用いる。しかし、工業的には、引火の危険性や人間の健康と生態系に悪影響を与えることから、VOCs フリーの溶媒が望まれる。このような観点から、

分子プレカーサー水溶液を調製し、その溶液をスプレー塗布して金属や金属酸化物、リン酸化合物薄膜の形成を試みた。

さて、出身国のナミビアには、ダイヤモンド、ウラン、金、亜鉛、銅などの資源が豊富である。特に銅は、ナミビアの年間輸出収益の 50%を占めている。しかし、現地での利用や最終製品にならないまま諸外国に輸出している。したがって、ナミビアの豊富な資源である銅を用いて簡便に機能性薄膜を形成できれば、持続可能な開発に貢献できるだけでなく、ナミビアの工業化にも重要と考えた。

これらのことから本研究では、先に金属塩を原料とする Cu_2O プレカーサー水溶液を調製し、低温かつ空気中での Cu_2O 薄膜形成を試みた。さらに、電気化学的方法を用いて金属銅から調製した分子プレカーサー水溶液を 180°C の基板に空気中でスプレー塗布し、高機能な Cu_2O 薄膜と導電性をもつ Cu 薄膜の形成を達成した。これらの研究背景と概要を第 1 章にまとめた。

第 2 章 使用試薬と測定装置

第 2 章では、本研究で使用した試薬リスト、プレカーサー水溶液の調製方法や形成した薄膜の特性評価方法とその測定装置の測定原理について述べた。

第 3 章 分子プレカーサー法による p 型 Cu_2O 薄膜の低温形成と光触媒活性

Cu_2O 単結晶は、バンドギャップが $1.9\text{--}2.3\text{ eV}$ 程度の p 型半導体である。可視光を吸収することや酸化物半導体として数少ない p 型半導体であることから、可視光応答型光触媒や酸化物太陽電池などへの利用が期待されている。また、毒性が低く、安価で環境負荷が小さい。

従来分子プレカーサー法による Cu_2O 薄膜形成は、エタノール溶媒系のプレカーサー溶液で達成されてきた。気相法でも一般に困難を伴う p 型半導体を示す Cu_2O 単一相薄膜を液相法で形成した最初の報告である。この Cu_2O 薄膜は、スピコート法で塗布・乾燥したプレカーサー膜をアルゴンガス雰囲気中 450°C の熱処理で形成した。第 3 章では、新たに Cu_2O プレカーサー水溶液を調製し、 180°C の空気中でのスプレー塗布で形成可能か調べた。また、形成した薄膜の可視光照射下における光触媒活性について調べた。具体的には、 Cu(II) イオン（ギ酸銅）に対して物質量比が 0, 2, 6, 14 となるようにギ酸アンモニウムを溶解したプレカーサー水溶液を調製した。その溶液を 180°C の石英ガラス基板にエアブラシを用いて空気中でスプレー塗布し、基板に良く密着した薄膜を形成した。形成した薄膜は、 Cu_2O 単一相で、これらの膜の Hall 効果測定は、いずれの膜も p 型半導体であることを示した。また、水溶液中に含まれるギ酸アンモニウム量の増加で膜は厚くなり、多孔質になった。これらの膜の光触媒活性は、メチルオレンジ（MO）水溶液に浸漬した膜への可視光照射による退色試験で調べた。 Cu(II) イオンに対して物質量が 6, 14 倍のギ酸アンモニウムを含む水溶液から形成した 140 と 350 nm の膜厚をもつ Cu_2O 薄膜は、 0.45 mW cm^{-2} の可視光照射下で高い光触媒活性を示した。メチルオレンジ水溶液の擬一次退色速度定数は、それぞれ $0.056, 0.087\text{ min}^{-1}$ だった。また、高い光触媒活性を示したこれらの膜は、酸素欠損 Cu_2O を含むことをラマンスペクトルによって明らかにした。

第 4 章 電気化学的方法を用いた Cu_2O プレカーサー水溶液の調製

第 4 章では、電気化学的方法を用いて、精錬銅プリスターのモデルとして金属銅板から Cu_2O プレカーサー水溶液の直接調製を試みた結果をまとめた。具体的には、ガラス容器にギ酸アンモニウム水溶液を電解液として入れ、液中に陽極と陰極として銅板を浸漬し、18 V の電圧を 2 時間印加した。溶液は、無色から青色に変化した。しかし、溶液中には水酸化銅と考えられる沈殿物を生じた。そこで、二つのガラス容器をセルロー

ス半透膜の隔壁を通して連結し、各ガラス容器にギ酸アンモニウム水溶液と銅板を入れて 18 V の電圧を印加した。陽極側のガラス容器内の水溶液は、時間変化に伴って無色から青色に変化し、沈殿は生じなかった。一方で、陰極側のガラス容器内の水溶液は着色することなく、銅板から気体が発生した。検知管で調べたところ、陰極から発生した気体は、水素だった。陽極側の水溶液の吸収スペクトルは、第 3 章で用いた分子プレカーサー水溶液の吸収波長と一致し、より高濃度の錯体溶液が得られた。このように、金属銅を用いた電気化学的な方法で Cu₂O プレカーサー水溶液となり得る錯体水溶液を 1 段階で調製できた。

第 5 章 電気化学的方法で調製した水溶液のスプレー塗布による Cu と Cu₂O 薄膜の選択的低温形成

第 4 章で調製した錯体水溶液を第 3 章のスプレー条件で塗布して薄膜を形成した。形成した薄膜は、第 3 章で形成した膜と同様に p 型半導体の Cu₂O 単一相膜だった。一方、同一の錯体水溶液にエチレンジアミン-N, N, N', N'-四酢酸 (EDTA) を加えて、同条件でスプレー塗布し、薄膜を形成した。結果として得られた薄膜は、厚さ 170 nm の Cu 単一相で、その電気抵抗率は、 $8.9 (2) \times 10^{-3} \Omega \text{ cm}$ だった。また、石英ガラス基板への密着強度は、12(7) MPa を示し、錯体水溶液への EDTA 添加で導電性を示す Cu 薄膜を選択的に形成できることを明らかにした。

以上のように、電気化学的方法によって、金属銅からプレカーサー水溶液を直接調製する方法を開発した。さらに当該溶液そのもの、および EDTA を加える簡便な方法で得た溶液を用いることによって、半導体の Cu₂O と金属 Cu の選択的薄膜形成を 180°C の空气中で達成した。

第 6 章 総括および今後の展開

本研究は、合成化学的方法と電気化学的方法を用いて調製した分子プレカーサー水溶液を、180°C の基板に空气中でスプレー塗布し、高機能な Cu₂O 薄膜と導電性 Cu 薄膜の形成を達成した。今後は、ナミビアのツメブ鉱山で採掘され精錬した粗銅を用いて同様の分子プレカーサー水溶液の調製を試みる。また、その溶液を用いて可視光で触媒活性な Cu₂O 薄膜と導電性 Cu 薄膜の形成を試みる。これらは、薄膜太陽電池などのエネルギーデバイスやフレキシブルな電子デバイスなどへの応用のみならず、環境浄化用の抗菌材料や固定化光触媒の形成に利用可能と考えられる。

PUBLICATIONS FROM THE MAJOR RESULTS

1. Alina Uusiku, Hiroki Nagai, and Mitsunobu Sato “Highly photo-reactive p-type Cu₂O thin films fabricated on a quartz glass substrate at 180°C in air, by spraying aqueous precursor solutions involving Cu(II) complexes.”, *Material Technology: Advanced Performance Materials*, **00**, 1-12 (2019).

2. Alina Uusiku, Hiroki Nagai, and Mitsunobu Sato, “Selective deposition of p-type Cu₂O or conductive Cu thin film at 180°C in air on a quartz glass substrate: Development of an aqueous spray solution using two-compartment electrolysis system.”, *Functional Material Letters*, **13(03)**, 1–7 (2020). Full length article.

Ph. D. THESIS

**LOW TEMPERATURE FABRICATION OF FUNCTIONAL
THIN FILMS OF COPPER OXIDE AND METALLIC COPPER
VIA SPRAY COATING: STUDY ON EFFECTIVE USE OF
LOCALLY PRODUCED COPPER IN NAMIBIA**

Applied Chemistry and Chemical Engineering Program

ALINA UUSIKU

OUTLINE OF THESIS

CHAPTER 1: GENERAL INTRODUCTION1

- 1.1. Brief introduction
- 1.2. Properties and application of Cu₂O nano structural materials
- 1.3. Molecular precursor method (MPM) for fabrication of Cu₂O thin film
 - 1.3.1. Spin coating
 - 1.3.2. Spray coating
- 1.4. Properties and applications of copper nano materials and Cu thin film
- 1.5. Motivation of study
- 1.6. Aims and objectives
- References

CHAPTER 2: MATERIALS AND METHODOLOGY.....15

- 2.1. Materials and Instruments
- 2.2. Characterization of precursor solution and thin films
 - 2.2.1. Absorbance and optical transmittance by UV-Vis spectrophotometry
 - 2.2.2. Determination of concentration of Cu(II) in spray solution by Beer Law plot
 - 2.2.3. Optical characterization of thin films
 - 2.2.4. pH
- 2.3. Structural characterization
 - 2.3.1. X-ray diffraction for thin film characterization
- 2.4. Chemical characterization
 - 2.4.1. Auger Electron Spectroscopy
 - 2.4.2. Raman spectroscopy
- 2.5. Morphology and thickness
- 2.6. Electrical properties
 - 2.6.1. Hall effect measurement
 - 2.6.2. Four probe measurement
- 2.7. Physical properties
 - 2.7.1. Thickness of Cu thin films
 - 2.7.2. Adhesion strength by scratch test
- 2.8. Photocatalytic properties
- 2.9. Summary

References

CHAPTER 3: LOW TEMPERATURE FABRICATION AND PHOTOCATALYTIC ACTIVITY OF P-TYPE Cu_2O THIN FILMS BY MOLECULAR PRECURSOR METHOD41

- 3.1. Introduction on p-type semiconductors
- 3.2. Properties and application of Cu_2O semiconductors
- 3.3. Cu_2O thin films
- 3.4. Preparations of Cu(II) in spray solution solutions with various ratio of HCOONH_4
- 3.5. Fabrication of Cu_2O thin films at 180°C in air by via spray coating
- 3.6. UV-Vis absorption of spray solution
- 3.7. Characterization of the fabricated thin films
 - 3.7.1. Crystal structure of the low temperature fabricated thin films
 - 3.7.2. Morphologies and adhesion strength of the low temperature fabricated thin films
 - 3.7.3. Electrical properties of the low temperature fabricated thin films
 - 3.7.4. Chemical composition of the low temperature fabricated thin films
 - 3.7.5. Raman spectra of the low temperature fabricated thin films
 - 3.7.6. Optical and photocatalytic of the low temperature fabricated thin films
- 3.8. Results and discussions
 - 3.8.1. Spray precursor solutions
 - 3.8.2. Fabrication and purity of the low temperature fabricated thin films
 - 3.8.3. crystal growth of Cu_2O , morphology and adhesion strength of thin films
 - 3.8.4. Electrical and optical properties of Cu_2O thin films
 - 3.8.5. Application of Cu_2O thin films in photocatalytic degradation of MO under visible light
- 3.9 Summary

References

CHAPTER 4: PREPARATION OF AQUEOUS Cu_2O PRECURSOR SOLUTION USING ELECTROCHEMICAL METHOD67

- 4.1. Introduction
 - 4.1.1. Introduction on copper(II) metal complexes
 - 4.1.2. Fundamental principle of electrochemical process for the coating applications
 - 4.1.3. Electrochemical process for preparation of coating solution containing Cu(II) complexes for MPM

4.2. Experimental	
4.2.1 Preparation of electrolytic solutions; ES	
4.2.2. Electrochemical preparation of precursor solution in a single electrolytic compartment	
4.2.3. Electrochemical preparation of Cu(II) complexes containing EDTA in a two electrolytic compartments	
4.2.4. Preparation of reference solutions; S _r	
4.3. Results	
4.3.1. UV-Vis spectra, pH and determination of concentration of Cu ²⁺ in aqueous precursor solution	
4.3.1.1. One compartment electrolysis system	
4.3.1.2. Two compartments electrolysis system	
4.4. Discussion	
4.4.1. Aqueous precursor solutions of Cu ²⁺ complex involving NH ₃ and HCOO ⁻ counter ions	
4.4.1.1. One compartment electrolysis system	
4.4.1.2. Two compartments electrolysis system	
4.5. Summary	
Reference	

CHAPTER 5: SELECTIVE LOW TEMPERATURE FABRICATION OF Cu AND Cu₂O THIN FILMS BY SPRAY APPLICATION OF AQUEOUS SOLUTION PREPARED BY ELECTROCHEMICAL METHOD.....85

5.1. Introduction	
5.1.1. Introduction on metallic copper thin films	
5.1.2. Fabrication methods of Cu thin film and their simple advantages	
5.1.3. Molecular Precursor Method employing alcohol and aqueous solvents	
5.1.4. Application of electrochemical prepared Cu ₂ O precursor solution	
5.2. Experimental	
5.2.1. Preparation of electrolytic solutions	
5.2.2. Electrochemical preparation of precursor aqueous solutions	
5.2.3 Fabrication of thin films	
5.3. Results and their discussion	

- 5.3.1. Direct preparation of aqueous solutions involving Cu(II) complexes by electrochemical process
- 5.3.2. Absorption spectra and pH values of spray solutions
- 5.3.3. The role of EDTA in selective formation of Cu₂O, Cu or composite Cu/Cu₂O thin films by spray deposition
- 5.3.4. Surface morphology, and the influence of chemical composition mainly atomic ratio of oxygen to copper on adhesion strength of thin films
- 5.3.5. The influence of chemical composition mainly, atomic ratio of carbon to copper on the electrical resistivity of the thin films
- 5.4. Photocatalytic activity of F₁ fabricated using electrochemically prepared precursor solution
 - 5.4.1. The effect of irradiation time and increased size of Cu₂O thin films on the photocatalytic activity of the Cu₂O thin films under visible light
 - 5.4.2. The effect of pH on the photocatalytic activity of the Cu₂O thin films under visible light
- 5.5. Fabrication of Cu₂O thin film at spraying temperature of 100 – 150°C
- 5.6. Merit of Spray coating for fabrication of thin films at low temperature
- 5.7. Summary
- Reference

CHAPTER 6: SUMMARY AND FUTURE DEVELOPMENT.....111

6.1. Fabrication of Highly photocatalytic *p*-type Cu₂O semiconductor at low temperature from the chemical synthesized precursor aqueous solution

6.1.1 Recommendations and future development

6.2. Selective fabrication of Cu₂O and Cu thin films at low temperature from electrochemically prepared precursor aqueous solution

6.2.1 Recommendations and future development

ACADEMIC ACHIEVEMENTS120

Publications

Oral presentations

Poster presentations

Academic awards

ACKNOWLEDGEMENTS

CHAPTER 1
General Introduction

CHAPTER 1: GENERAL INTRODUCTION

1.1. General introduction

This study presents the methods for the (1) Preparation of precursor aqueous coating solution using copper salts and the fabrication of *p*-type Cu₂O thin films by molecular precursor method (MPM) at 180°C in air, (2) Electrochemical preparation of spray precursor solutions using one and two compartments electrolysis system at ambient temperature, (3) Fabrication of functional Cu₂O thin films *via* spray coating of an electrochemically prepared aqueous spray solution, (4) Fabrication of conductive metallic Cu thin films *via* spray coating of an electrochemically prepared aqueous spray solution. The two main methods used in preparation of coating solution are fully studied. The first method is the well-known chemically conventional route of preparing coating solution within the MPM, whereby an isolated Cu(II) complex containing EDTA ligand and/or metal salts such as copper acetate and formate are reacted in a solvent such as water and ethanol. The second and newly incorporated method for the preparation of coating solution within MPM is use of electrochemical process to dissolve metal copper plate in aqueous solutions containing EDTA and NH₃ ligands *via* a simple two compartment electrolysis system. Copper plates and/or lumps of copper blister are used as starting materials and sources of dissolved Cu²⁺ ion in the precursor solution instead of copper salts.

Copper is one of Namibia's main mining products in addition to diamonds, uranium, gold, and zinc. Copper specifically contribute ca. 50% of Namibia's annual export earnings. However, they are usually exported in the semi-finished state which highlights a great need to add value and process crude copper mined in Namibia into finished products before local utilization or exportation. From this point of view, the fabrication of functional thin films using Namibian crude copper as a starting material will contribute to its value addition and local industrialization. Figure 1 shows the geographical location of Namibia and its mining and smelting site for crude copper.

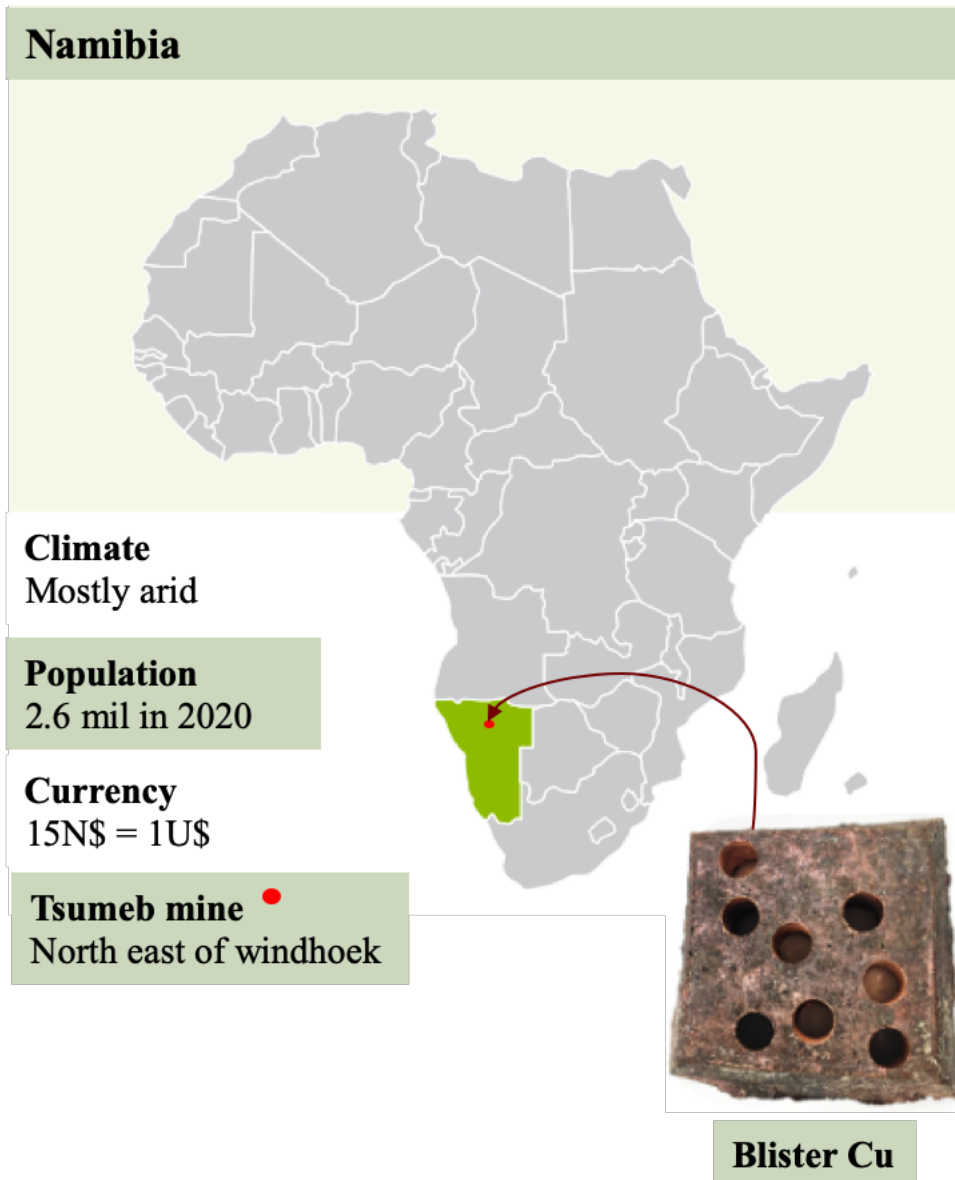


Figure 1. Geographical location of Namibia and its mining and smelting site for blister Cu.

The MPM utilizing electrochemically prepared aqueous precursor solution from copper blister can easily form a copper thin film on a glass substrate. The procedure will not only contribute to the industrialization of Namibia’s mined raw products, but also has a potential to solve the cost problems associated with fabricating copper thin films at high temperature by using a simple system. Some of the important practical advantages of fabricating copper thin film using the MPM is its ability to do so on substrates of various shapes and easily optimizing of thin film’s thickness by controlling the concentration of copper complexes in the precursor solution [1]. For such reasons it makes the goals of fabricating the conductive metallic copper thin films for applications in heating and transportation water tubes and in ozone generator necessary for water purification in Namibia.

Fabrication of a desired single crystal phase of copper based thin films is the key target in preparation of a copper oxide thin films. While the fabrication of a single phased copper oxide thin films can be challenging, few various fabrication methods had achieved it. The Cu₂O thin films can be achieved by many deposition techniques, which includes; physical processes such as magnetic sputtering deposition [2, 3], pulse laser deposition [4]. As well as wet chemical processes such as; nebulizer spray technique [5], spray pyrolysis [6] and electrochemical deposition [7].

1.2. Properties and application of Cu₂O nano-structural materials

Cuprous oxide (Cu₂O) is a well-known *p*-type semiconductor with a direct band gap of 2.2 eV which allows its [8] applications in solar energy conversion [9–12], as an electrode for lithium ion battery [13–14], gas sensors [15] and photocatalytic degradation of organic pollutants and decomposition of water under visible light [16–20]. Over the last few decades, Cu₂O nanoparticle powders have alarmingly emerged as one of the effective *p*-type semiconductors for photocatalytic degradation of Methyl Orange (MO) under visible light irradiation. The Cu₂O nanoparticles with different nano-structural sizes and morphologies have been mostly prepared by a typical facile chemical synthesis. It has been used as a photocatalyst because of its several advantages. Firstly; it has low toxicity, inexpensive, environmentally friendly, it is plentiful and readily available [21]. Secondly; the band gap of Cu₂O can be modified by factors such as particle size [22–23]. Thirdly; it directly utilizes visible light as photocatalyst [20]. Fourthly; it has a powerful adsorption capacity for molecular O₂ which can harvest photoelectron to prevent the recombination of electrons and holes [20].

Many researchers have already investigated photocatalytic properties and the optimized experimental parameters (i.e. type of Cu²⁺ reductants, synthetic temperature, copper salts, pH and reaction rate) dependent on particle sizes and morphologies of Cu₂O nanoparticles. Nanoparticle powders can be prepared by various methods such as liquid phase chemical synthesis [21, 25–28], electrodeposition method [29–32], chemical dealloying [33, 34] and irradiation process [35]. On the other hand, it was found that Cu₂O nanocomposite powders with TiO₂ have a better photocatalytic property toward MO degradation than single phased Cu₂O, as coupling the Cu₂O and TiO₂ extend the absorption range to visible light region and promotes electron-hole pair separation [36–38].

The pH of test solution, and surface area and particle size of Cu₂O nanoparticle powder play a very sensitive role to determine the degradation rate of MO as a model of pollutant dye by the powders under visible light. While much attention on Cu₂O photocatalytic material had

been focused on the structural shape of nanoparticle powder, there is no report on Cu₂O thin films fabricated *via* coating of its crystallized phase onto substrate by various methods. This study focuses on the photocatalytic and visible light-responsive properties of Cu₂O thin films at neutral pH of MO solution.

1.3. Molecular precursor method (MPM) for fabrication of Cu₂O and metallic Cu thin film

1.3.1. Spin coating

The procedures for thin film fabrication using MPM have been vigorously reported by our research team. The MPM is a wet process for the thin film fabrication of various metal oxides, metals, and phosphate compounds which is based on the design of metal complexes in coating solutions with excellent stability, homogeneity, miscibility, coatability, amongst other many practical advantages [39]. Volatile organic-solvent based precursor solutions are favorable for spin-coating method, because aqueous solutions are generally inadequate to spread onto various substrates due to high surface tension [40, 41]. Previously, an alcohol based coating solution containing a dibutylammonium salt of Cu(II) complex with EDTA ligand and a Cu(II) formate dissolved with propylamine was used to successfully fabricate a conductive metallic Cu thin film with thickness of 40 nm *via* MPM [42]. In addition a precursor solution involving copper(II) complex of EDTA, dibutylamine in ethanol was spin coated on a quartz glass substrate to fabricate a *p*-type Cu₂O film with thickness of 50 nm [43]. Furthermore, a precursor solution involving Cu(II) formate, propylamine, ethylenediamine in ethanol was used to fabricate a *p*-type Cu₂O film by ultraviolet (UV) irradiation [44]. Figure 2 shows the schematic route for fabrication of copper oxides by MPM *via* spin coating.

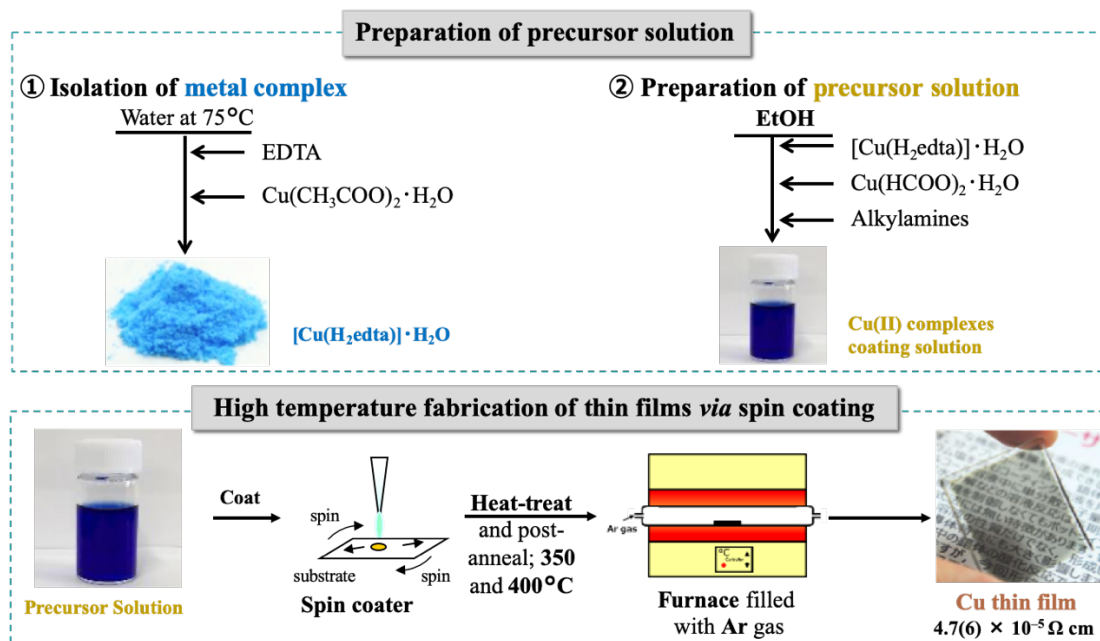


Figure 2. Schematic route for fabrication of copper oxides by MPM *via* spin coating [42].

1.3.2. Spray coating

Alcohol-based precursor solutions are generally favorable for spin coating [41]. Spray coating is a coating procedure within MPM which is applicable to coating of aqueous based solution due to controllable temperature of substrate, thus depositing the precursor compounds onto the substrate without spontaneous evaporation of solvent at room temperature [45]. The advantages of the spray coating method to deposit precursor films on quartz glass substrate includes; it's simple and inexpensive instrumental set-up, reduced material loss and its adjustability for a large area deposition [45–46]. The spray deposition has been previously used by our research team to fabricate thin films of different metal precursors by MPM. It has first been utilized by MPM to deposit carbonate containing apatite film on a Ti plate by spraying an aqueous based solution of $\text{Ca}(\text{OH})_2$ and phosphoric acid [47, 48]. It has resulted in the fabrication of a highly conductive and well adhered Cu thin film on a quartz glass substrate coated with ammonium aqueous solution containing $\text{Cu}(\text{HCOO})_2 \cdot 4\text{H}_2\text{O}$ and Cu(II) complex of EDTA [45]. Figure 3 shows a simple experimental design of spray coating method and its application to fabricate metallic Cu thin film by depositing aqueous precursor solution onto substrate.

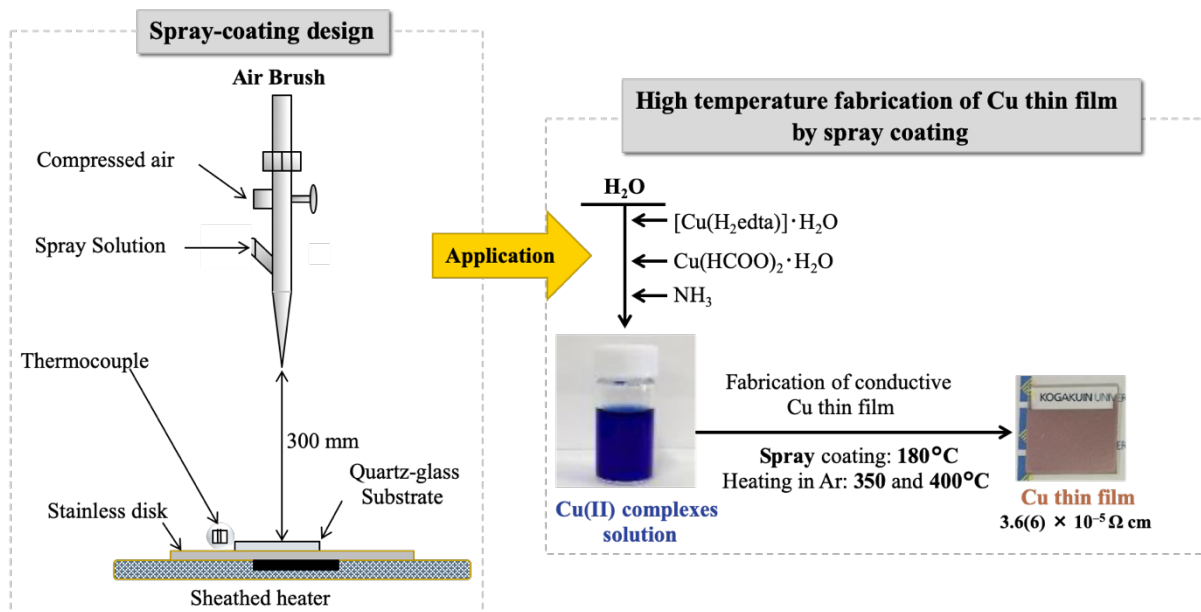


Figure 3. Simple experimental design of spray coating method and its application to deposit aqueous precursor solution in fabrication of metallic Cu thin film [45].

Under this study, the fabrication of *p*-type Cu₂O thin-films on a quartz glass substrate heated at 180°C in air directly by spraying aqueous precursor solutions, which were prepared by dissolving Cu(II) formate and ammonium formate is fully studied. It also covers the fabrication of *p*-type Cu₂O thin film by MPM using an electrochemically prepared aqueous based precursor solution containing Cu(II) complexes of NH₃ ligand and HCOO⁻ ions. Cu₂O thin film could be fabricated at low temperature in air by spray coating a quartz glass substrate with precursor solution prepared by chemical synthesis and that derived directly from conversion of Cu metal sheet into Cu(II) complexes with no isolation of solid Cu(II) complexes or salts. The resultant Cu₂O thin films were characterized by the electrical and optical properties, chemical composition, morphologies, and bonding vibration analyses and compared to those of Cu₂O films fabricated at high temperature using coating solutions prepared by the chemical synthesis. The photocatalytic degradation of methyl orange (MO) by the fabricated Cu₂O thin film were fully evaluated.

1.4. Properties and applications of copper nanosized materials and Cu thin film

Metallic copper-based nanosized materials exhibit superior magnetic and thermal properties [49]. They have also attracted much attention for over a decade because of their photocatalytic and optical properties, high electrical and thermal conductivity [50], which contribute attractive prospects in the design of many new devices requiring such functionalities. Particularly,

conductive copper thin film is a suitable material for its applications in electrodes or conductive patterns in multilayered electronic parts, printed circuit boards and hybrid integrated circuit in electronic industries [50, 51]. In addition, copper nanosized material's various application makes a good substitute for conductive and expensive noble metals like gold and silver in the chemical and metallurgical process [52, 53].

However, the attractive properties of copper nanomaterial and thin films owes it to those of bulk copper such as its abundant availability, less toxicity, versatility, malleability and resistance to corrosion and good electrical and thermal conductivity [54, 55]. The physical and chemical properties of copper nanomaterial are also different from those of bulk copper material due the high surface area to volume ratio [56]. It is interesting to note that the fabrication methods for metallic copper thin films are basically identical to those of Cu₂O thin films with the exception of starting materials, in this study.

1.5. Motivation of study

Recently, spray coating technique has evolved in utilization of aqueous-based coating solution of copper precursor and used in fabrication of metallic Cu [45] and of highly photo-reactive *p*-type Cu₂O thin film [57] *via* spray deposition at low temperature.

Although, the aqueous spray solutions containing Cu(II) complexes of EDTA and amine used in the previous studies were synthesized from various Cu(II) salts as starting material. Cu²⁺ ions in aqueous solution can also be generated by electrochemical dissolution of metallic Cu anode. For example, the preparation of a Cu(II) salt from electrochemical oxidation of metallic Cu anode in CH₂COONH₄ with palm-based stearic acid [58] and oleic acid [59] electrolytes has been reported, although the yields are terribly low.

In this study, we attempted a novel method for the preparation of copper aqueous precursor solution from metallic copper. The aqueous precursor solution involving Cu(II) complex species was electro-synthesized by oxidation of anodic copper electrode in an electrolytic solution containing ammonium formate and ammonia at room temperature. The ethylenediamine-*N, N, N', N'*-tetraacetic acid (EDTA) was added to the electrochemically prepared solution and then spray-coated onto a quartz glass substrate at 180°C in air to result in a conductive metallic Cu thin film. A two-compartment-electrolysis apparatus was newly contrived to efficiently achieve an electrochemical production of the precursor solution.

1.6. Aims and objectives

Over the years MPM has been developed as a convenient wet chemical procedure for the fabrication of nanocrystalline thin films of various metals, metal oxides and phosphate compounds. The procedure mainly involves two important steps. Firstly; the preparation and design of metal complexes in coating precursor solutions with practical advantages such as; excellent stability, homogeneity, miscibility and coatibility. Secondly; coating of resultant precursor solution onto substrate to form an amorphous precursor film using different coating procedures. Here, the precursor film involving a metal complex should be amorphous in order to obtain a resulting metal oxide thin film spread homogeneously on substrate by subsequent heat-treatment, as per such procedure's advantage. However, it was revealed through coating procedures with MPM that a crystallite metal oxide can be formed directly without first formation of the homogeneous amorphous precursor film *via* spray coating. Spraying an aqueous precursor solution onto pre-heated substrate at 180°C can form a metal polycrystalline thin film with no further heat-treatment of sprayed film under inert gases. The well-developed spray coating method within MPM have advantages such as fewer material losses, simple experimental set-up, suitability to coating of VOC-free solutions and less cost.

Highly conductive metallic copper thin films had been previously formed at high temperature under inert gases from alcohol- and aqueous-based solutions, using spin and spray coating procedures, respectively. Previously, after spray coating of precursor aqueous solution onto pre-heated substrate, further heat treatment of sprayed film is necessary to obtain a conductive metallic Cu thin film. Fabrication of Cu and Cu₂O thin films by spray application of aqueous solution at low temperature of 180°C in air with no further subjection of sprayed film to high temperature treatment under inert gas is still not investigated. The world continues to uphold sustainable development programs while striving for the realization of low-cost energy techniques and its requiring devices. It is important to consider the input energy towards production of such devices.

Bulk copper is regarded as an important metal due to its strength, fatigue resistance, and ability to take a good finish, its alloys and born nanocrystalline materials such as thin films possesses properties of electrical and thermal conductivity, corrosion resistance, color and ease of fabrication. The metal ore is available in many parts of the world including Namibia. The Namibian copper raw material is exported to foreign countries for fully processing into finished products without being used inside the country. It's important to add value to Namibian raw material such as copper inside the country. Therefore, the main objective of this study is to attempt to add value to Namibian crude copper through low temperature formation of

nanocrystalline thin films of metallic Cu and copper oxides. The summary of the objectives of the study is:

- 1.1 Preparation of stable Cu₂O precursor solution by dissolving copper formate and ammonium formate in ammonia aqueous solution.
- 1.2 Fabrication of *p*-type Cu₂O thin film by spray coating the chemical synthesized precursor aqueous solution onto pre-heated quartz glass substrate at 180°C in air.
- 1.3 Application of *p*-type Cu₂O thin film semiconductor in visible-light-driven photocatalytic discoloration of MO as a model organic pollutant.
- 1.4 Preparation of molecular precursor solution from direct conversion of Cu metal into Cu(II) complexes with no isolation of solid Cu(II) complexes or salts, *via* an electrochemical process in an electrolytic solution involving H₄edta and NH₃ ligands.
- 1.5 Selective fabrication of functional *p*-type Cu₂O and conductive Cu thin films by spraying electrochemically prepared precursor solution onto pre-heated quartz glass substrate at 180°C in air.
- 1.6 Consideration for the application of fabricated thin films as a candidate material in energy devices such as thin film solar cells and flexible electronic devices, formation of antibacterial materials for environmental purification and immobilized photocatalysts (Future work).
- 1.7 Electrochemical production, harvesting and application of H₂ gas as a driving energy in fuel cells (Future work).

References

- [1] Nagai, H.; Suzuki, T.; Nakano, T.; Sato, M. Embedding of copper into submicrometer trenches in a silicon substrate using the molecular precursor solutions with copper. *Mater. Lett.* **2016**, *182*, 206–209.
- [2] Hojabri, A.; Hajakbari, F.; Moazzen, M.; Kadkhodaei S. Effect of Thickness on Properties of Copper Thin Films Growth on Glass by DC Planar Magnetron Sputtering. *Sid.Ir.* **2012**, *2*, 107–112.
- [3] Mistry, S.; Cropper, M.; Valizadeh, R.; Jones, L.B.; Middleman, K.J.; Hannah, Militsyn, B.L.; Noakes, T.C.Q. A comparison of surface properties of metallic thin film photocathodes. *IPAC 2016 - Proc. 7th Int. Part. Accel. Conf.* **2016**, 3691–3694.
- [4] Aadim, K.A.; Hussain, A.A.K.; Abdulameer, M.R. Effect of Laser Pulse Energy on the Optical Properties of Cu₂O Films by Pulsed Laser Deposition. *Acta Phys. Pol.* **2015**,

- 128, 419–422.
- [5] Prabu, R.D. Studies on copper oxide thin films prepared by simple nebulizer spray technique. *J. Mater. Sci. Mater. Electron.* **2017**, *28*, 1–9.
- [6] Osorio-Rivera, D.; Torres-Delgado, G.; Márquez-Marín, J.; et al. Cuprous oxide thin films obtained by spray-pyrolysis technique. *J. Mater. Sci. Mater. Electron.* **2018**, *29*, 851–857.
- [7] Norziehana, N.; Isa, C. Electrodeposition and Characterization of Copper Coating on Stainless Steel Substrate from Alkaline Copper Solution Containing Ethylenediaminetetraacetate (EDTA). *J. Mech. Eng.* **2017**, *2*, 127–138.
- [8] Ding, J.; Sui, Y.; Fu, W.; et al. Applied Surface Science Synthesis and photoelectric characterization of delafossite conducting oxides CuAlO_2 laminar crystal thin films via sol – gel method. *Appl. Surf. Sci.* **2010**, *256*, 6441–6446.
- [9] Katayama, J.; Ito, K.; Matsuoka, M.; et al. Performance of $\text{Cu}_2\text{O}/\text{ZnO}$ solar cell prepared by two-step electrodeposition. *J. Appl. Electrochem.* **2004**, *34*, 687–692.
- [10] Fernando, C.A.N.; Bandara, T.M.W.J.; Wethasingha, S.K. H_2 evolution from a photoelectrochemical cell with n- Cu_2O photoelectrode under visible light irradiation. *Sol. Energy Mater. Sol. Cells.* **2001**, *70*, 121–129.
- [11] Zhu, Q.; Zhang, Y.; Wang, J.; et al. Microwave Synthesis of Cuprous Oxide Micro-/Nanocrystals with Different Morphologies and Photocatalytic Activities. *J. Mater. Sci. Technol.* **2011**, *27*, 289–295.
- [12] Hung, L.; Tsung, C.; Huang, W.; et al. Room-temperature Formation of Hollow Cu_2O Nanoparticles. *Communication.* **2010**, *22*(17), 1–17.
- [13] Hasan, M.; Chowdhury, T.; Rohan, J.F. Nanotubes of Core/Shell $\text{Cu}/\text{Cu}_2\text{O}$ as Anode Materials for Li-Ion Rechargeable Batteries. *J. Electrochem. Soc.* **2010**, *157*, A682.
- [14] Chen, R.; Wang, Y.; Nuli, Y.; et al. Cu_2O nanowires as anode materials for Li-ion rechargeable batteries. *Sci. China Technol. Sci.* **2014**, *57*, 1073–1076.
- [15] Zhang, J.; Liu, J.; Peng, Q.; et al. Nearly Monodisperse Cu_2O and CuO Nanospheres: Preparation and Applications for Sensitive Gas Sensors . *Chem. Mater.* **2006**, *18*, 867–871.
- [16] Hara, M. Cu_2O as a photocatalyst for overall water splitting under visible light irradiation. *Chem. Commun.* **1998**, *2*, 357–358.
- [17] Yang, Y.; Xu, D.; Wu, Q.; et al. $\text{Cu}_2\text{O}/\text{CuO}$ bilayered composite as a high-efficiency photocathode for photoelectrochemical hydrogen evolution reaction. *Sci. Rep.* **2016**, *6*, 1–13.

- [18] Pan, L.; Kim, J.H.; Mayer, M.T.; et al. Boosting the performance of Cu₂O photocathodes for unassisted solar water splitting devices. *Nat. Catal.* **2018**, *1*, 412–420.
- [19] Paracchino, A.; Laporte, V.; Sivula, K.; et al. Highly active oxide photocathode for photoelectrochemical water reduction. *Nat. Mater.* **2011**, *10*, 456–461.
- [20] Xu, H.; Wang, W.; Zhu, W. Shape evolution and size-controllable synthesis of Cu₂O octahedra and their morphology-dependent photocatalytic properties. *J. Phys. Chem. B.* **2006**, *110*, 13829–13834.
- [21] Huang, L.; Peng, F.; Yu, H.; et al. Preparation of cuprous oxides with different sizes and their behaviors of adsorption, visible-light driven photocatalysis and photocorrosion. *Solid State Sci.* **2009**, *11*, 129–138
- [22] Schä, P.; Van Der Veen, M.A.; Domke, K.F. Unraveling a two-step oxidation mechanism in electrochemical Cu-MOF synthesis. *Chem. Commun.* **2016**, 4722, 4722–4725.
- [23] Chang, Y.; Teo, J.J.; Zeng, H.C. Formation of colloidal CuO nanocrystallites and their spherical aggregation and reductive transformation to hollow Cu₂O nanospheres. *Langmuir.* **2005**, *21*, 1074–1079.
- [24] Feng, L.; Zhang, C.; Gao, G.; et al. Facile synthesis of hollow Cu₂O octahedral and spherical nanocrystals and their morphology-dependent photocatalytic properties. *Nanoscale Res. Lett.* **2012**, *7*, 1–10.
- [25] Wang, Y.; Huang, D.; Zhu, X.; et al. Surfactant-free synthesis of Cu₂O hollow spheres and their wavelength-dependent visible photocatalytic activities using LED lamps as cold light sources. *Nanoscale Research Letters.* **2014**, *9*, 36–38.
- [26] Gao, R.J.; Ding, T.; Duan, X.J. Kinetics Study on Photocatalytic Degradation of Methyl Orange Catalyzed by Sea Urchin-Like Cu₂O. *Journal of Material Science and Chemical Engineering.* **2016**, *4*, 35–40.
- [27] Sun, W.; Sun, W.; Zhuo, Y.; et al. Facile synthesis of Cu₂O nanocube/polycarbazole composites and their high visible-light photocatalytic properties. *J. Solid State Chem.* **2011**, *184*, 1638–1643.
- [28] Zhang, X.; Song, J.; Jiao, J.; et al. Preparation and photocatalytic activity of cuprous oxides. *Solid State Sci.* **2010**, *12*, 1215–1219.
- [29] Tang, A.; Xiao, Y.; Ouyang, J.; et al. Preparation, photo-catalytic activity of cuprous oxide nano-crystallites with different sizes. *J. Alloys Compd.* **2008**, *457*, 447–451.
- [30] Khattar, H.K.; Jouda, A.M.; Alsaady, F. Preparation of Cu₂O Nanoparticles as a Catalyst in Photocatalyst Activity Using a Simple Electrodeposition. *Nano Biomed Eng.* **2018**,

- 10, 406–416.
- [31] Singh, D.P.; Singh, J.A.I.; Mishra, P.R.; et al. Synthesis , characterization and application of semiconducting oxide (Cu₂O and ZnO) nanostructures. *Bull. Mater. Sci.* **2008**, *31*, 319–325.
- [32] Saini, K.; Pandey, R.S. Concentration-dependent electrochemical synthesis of quantum dot and nanoparticles of copper and shape-dependent degradation of methyl orange. *Advanced Materials Letters.* **2017**, *8*, 1080–1088.
- [33] Dong, C.; Zhong, M.; Huang, T.; et al. Photodegradation of methyl orange under visible light by micro-nano hierarchical Cu₂O structure fabricated by hybrid laser processing and chemical dealloying. *ACS Appl. Mater. Interfaces.* **2011**, *3*, 4332–4338.
- [34] Dan, Z.; Yang, Y.; Qin, F.; Wang, H.; Chang, H. Facile Fabrication of Cu₂O Nanobelts in Ethanol on Nanoporous Cu and their Photodegradation of Methyl Orange. *Material.* **2018**, *11*, 1–14.
- [35] Xiangfeng; L.I.N.; Ruimin, Z.; Xiaohai, S.; et al. Cu₂O nanoparticles : Radiation synthesis , and photocatalytic activity. *Nuclear Science and Techniques.* **2010**, *21*, 146–151.
- [36] Zhang D. Synergetic effects of Cu₂O photocatalyst with titania and enhanced photoactivity under visible irradiation. *Acta Chimica Slovaca.* **2013**, *6*, 141–149.
- [37] Jaber, S.H. Synthesis of TiO₂ and Cu₂O nanoparticles and TiO₂/Cu₂O nanocomposite and study the ability to remove pollutants from aqueous solution. *Scientific Conference.* **2017**, *3*, 137-146.
- [38] Janczarek, M.; Kowalska E. On the Origin of Enhanced Photocatalytic Activity of Copper-Modified Titania in the Oxidative. *Catalyst.* **2017**, *7*, 1 – 26.
- [39] Nagai, H.; Sato, M. Heat Treatment in Molecular Precursor Method for Fabricating Metal Oxide Thin Films. *Heat Treat. – Conv. Nov. Appl.* Intech 2012.
- [40] Wu. H.J.; Tomiyama, N.; Nagai, H.; et al. Fabrication of a *p*-type Cu₂O thin-film via UV-irradiation of a patternable molecular-precursor film containing Cu(II) complexes. *J. Cryst. Growth.* **2019**, *509*, 112–117.
- [41] Nagai, H.; Sato, M. Molecular Precursor Method for Fabricating *p*-Type Cu₂O and Metallic Cu Thin Films. *Mod. Technol. Creat. Thin-film Syst. Coatings.* 2017.
- [42] Nagai, H.; Mita, S.; Takano, I.; et al. Conductive and semi-transparent Cu thin film fabricated using molecular precursor solutions. *Mater. Lett.* **2015**, *141*, 235–237.
- [43] Nagai, H.; Suzuki, T.; Hara, H.; et al. Chemical fabrication of *p*-type Cu₂O transparent thin film using molecular precursor method. *Mater. Chem. Phys.* **2012**, *137*, 252–257.

- [44] Wu, H.; Tomiyama, N.; Nagai, H.; et al. Fabrication of a *p*-type Cu₂O thin- film via UV-irradiation of a patternable molecular-precursor film containing Cu(II) complexes. *Journal of Crystal Growth*. **2019**, *509*, 112–117.
- [45] Hishimone, P.; Nagai, H.; Morita, M.; et al. Highly-Conductive and Well-Adhered Cu Thin Film Fabricated on Quartz Glass by Heat Treatment of a Precursor Film Obtained Via Spray-Coating of an Aqueous Solution Involving Cu(II) Complexes. *Coatings*. **2018**, *8*(10), 1–10.
- [46] Hishimone, P.N.; Watarai, K.; Nagai, H.; et al. Thin Film Fabrication and Characterization of Layered Rock Salt LiCoO₂ on Quartz Glass Spray-Coated with an Aqueous Ammonia Solution Involving Metal Acetates. *Coatings*. **2019**, *9*(2), 1–10.
- [47] Mochizuki, C.; Hara, H.; Takano, I.; et al. Application of carbonated apatite coating on a Ti substrate by aqueous spray method. *Mater. Sci. Eng. C*. **2013**, *33*, 951–958.
- [48] Mochizuki, C.; Hara, H.; Oya, K.; et al. Behaviors of MC3T3-E1 cells on carbonated apatite films, with a characteristic network structure, fabricated on a titanium plate by aqueous spray coating. *Mater. Sci. Eng. C*. **2014**, *39*, 245–252.
- [49] Ahmed, R.A.; Alzahrani E. Synthesis of Copper Nanoparticles with Various Sizes and Shapes : Application as a Superior Non-Enzymatic Sensor and Antibacterial Agent. *Int. J. Electrochem. Sci*. **2016**, *11*, 4712–4723.
- [50] Hashemipour, H.; Zadeh, M.E.; Pourakbari, R.; et al. Investigation on synthesis and size control of copper nanoparticle via electrochemical and chemical reduction method. *Int. J. Phys. Sci*. **2011**, *6*, 4331–4336.
- [51] Yu, L.; Sun, H.; He, J.; et al. Electro-reduction of cuprous chloride powder to copper nanoparticles in an ionic liquid. *Electrochemistry Communications*. **2007**, *9*, 1374–1381.
- [52] Song, X.; Sun, S.; Zhang, W.; et al. A method for the synthesis of spherical copper nanoparticles in the organic phase. **2004**, *273*, 463–469.
- [53] Lee, Y.; Choi, J.; Lee, K.J.; et al. Large-scale synthesis of copper nanoparticles by chemically controlled reduction for applications of inkjet-printed electronics. *Nanotechnology*. **2008**, *19*, 1–7.
- [54] Tegoni, M.; Valensin, D.; Toso, L.; et al. Copper Chelators : Chemical Properties and Bio-medical Applications. *Current Medicinal Chemistry*. **2014**, *21*, 3785–3818.
- [55] Touabi, N.; Martinez, S.; Bounoughaz, M. Optimization of Electrochemical Copper Recovery Process : Effect of the Rotation Speed in Chloride Medium of pH = 3. *Int. J. Electrochem. Sci*. **2015**, *10*, 7227–7240.

- [56] Yang, X.; Chen, S.; Zhao, S.; et al. Synthesis of copper nanorods using electrochemical methods. *J.Serb.Chem.Soc.* **2003**, *68*, 843–847.
- [57] Uusiku, A.; Nagai, H.; Sato, M. Highly photocatalytic *p*-type Cu₂O thin films fabricated on a quartz glass substrate at 180°C in air, by spraying aqueous precursor solutions involving Cu(II) complexes. *Mater. Technol.* **2019**, *00*, 1–12.
- [58] Nordin, N.; Hasan, S.Z.; Zakaria, Z.; et al. Effect of applied voltage on slow-release of Cu(II) ions on the synthesis of Copper(II) stearate complex by electrochemical technique. *J. Braz. Chem. Soc.* **2015**, *26*, 1115–1123.
- [59] Kuprum, P.; Karboksilat, I.I.; Berasaskan, O.; et al. Synthesis and Characterization of Copper(II) Carboxylate with Palm-Based Oleic Acid by Electrochemical Technique. *Malaysian Journal of Analytical Science.* **2015**, *19*, 236–243.

CHAPTER 2
Materials and methodology

CHAPTER 2: Materials and methodology

The materials, apparatus, chemical reagents and measuring instruments and their operational functions used in provision of the results under this study are fully described in this chapter. Two different routes used for the preparation of coating solutions and specific detailed concentrations of mixed reagents in resultant precursor solutions, are described in their corresponding chapters in which they were utilized by spray coating method to fabricate respective functional thin films. The sections also cover the measurements for the characterization of precursor solution derived from copper salts. As well as, of these derived from solid metal plate or blister. The method for determining the concentration of Cu(II) complexes in the coating solution prepared by a newly established and incorporated route of electrochemical process within MPM is described. An overview of the adapted spray coating method used to spray the resultant aqueous spray precursor solutions prepared by the two routes, is also presented in respective chapters. The chapter summarizes all the measurements and characterizations of the fabricated functional thin films of metallic Cu and copper oxides at low temperature in air.

2.1 Materials and instruments

The summary of all the essential materials, chemical reagents and measuring instruments are described in Table 1.

Table 1. Summary of the chemical reagents, materials, and measuring instruments used in this study.

Chemical reagents, and measuring instruments	Formula/Abbreviation*¹	Formula weight or model	Company supplier	Modification prior to use*²
2-propanol	(CH ₃) ₂ CHOH (IPA)	60.10	Kanto Chemical Co., Inc	-
28 % Ammonium hydroxide	28 % NH ₄ OH	17.03	Taisei Chemical Co. Ltd	-

Ammonium formate	HCOONH ₄	63.06	Wako Pure Chemical Industry	-
Acetone	CH ₃ COCH ₃	58.08	Kanto Chemical Co., Inc	-
Ethanol	(CH ₂) ₂ OH	46.07	Kanto Chemical Co., Inc	-
Deionized water	H ₂ O		Kyoei Co., Ltd	-
Copper plate	Cu	63.55	Hikari Co., Ltd	cleaned*4
Copper formate	Cu(HCOO) ₂ ·4H ₂ O	225.64	Kanto Chemical Co., Inc	-
Ethylenediamine–N, N, N', N'-tetraacetic acid	[-CH ₂ N(CH ₂ COOH) ₂] ₂ EDTA	292.25	Kanto Chemical Co., Inc	-
Ethylenediamine	(CH ₂) ₂ (NH ₂) ₂ (En)	60.10	Wako Pure Chemical Corporation	-
Methyl orange	MO	327.34	Kanto Chemical Co., Inc	-
External Electric DC supplier	DC supplier			-
Cellulose membrane	-	-	Nihon Medical, Inc	-
Quartz glass Electrolytic cell	-	-	EIKOH Co., Ltd	-
Spray air brush	-	Revolution HP-SAR	ANEST IWATA Co.,	-

			Kanagawa, Japan	
Chrome-alum thermocouple	-	A3-K-Q, TGK	Tokyo, Japan)	-
Quartz glass substrate	Qz	-	Akishima glass Co., Ltd	cleaned* ⁵
UV-Vis spectrophotometer	UV-Vis	U-2800	Hitachi, Tokyo, Japan	-
pH meter	pH	GST- 2729C	DKK-TOA Corporation, Tokyo, Japan	-
Tubular furnace	-	EPKRO- 12K	Isuzu, Toyota, Japan	-
Fluorescent Lamp	-	FS2015E- H	Hitachi, Tokyo, Japan	-
Digital illuminometer	-	M-101	MonotaRO Co., Ltd., Amagasaki, Japan	-
UV-Vis spectrophotometer	UV-Vis	U-2800	Hitachi, Tokyo, Japan	-
XRD-diffractometer	XRD	-	Rigaku	-
Auger electron spectrophotometer	AES	JAMP- 9500	Tokyo, Japan JEOL	
Fourier-Scanning electron microscope	FE-SEM	JSM- 6701F	JEOL, Tokyo, Japan	-

Four probes’ DC power supply,	PAB32-1.2,	DC	Kikusui Electronic Corp., Kanagawa, Japan;	-
Four probes’ Multimeters	VOAC7512	MM	Iwatsu Electric Corp., and Keithley Electric Co., Ltd., Tokyo, Japan	-
Scratch tester	-	HEIDON- 22	Shinto Scientific, Tokyo, Japan	-
Razor Scanning microscope	RSM	-	-	-
Raman spectrometer	-	LaBRAM HR800	Horiba, Kyoto, Japan	-
HL5500 Hall system	-	Accent	London, UK	-

*¹ Acceptable abbreviations in chemical production industries.

*² Modifications and procedures for cleaning substrates and copper plates electrodes are described in their respective chapters.

2.2. Characterization of precursor solution and thin films

2.2.1. Absorbance and optical transmittance by UV-Vis spectrophotometry

UV-Vis spectroscopy is the study of interaction of radiation from the visible region ($\lambda = 380\text{--}720$) of the electromagnetic spectrum with a chemical species. The technique quantifies the interaction of visible light with a chemical sample which allows for the determination of unknown solution concentration, the monitoring of reaction progress as a function of time and other quantitative uses.

UV-Vis spectrophotometry has been previously used in various studies to characterize the metal complexes of copper in solution; *via* (1) measuring the temperature dependence of electronic absorption of cupric acetate in EPA solution [1]. Determination of trace amount and concentration of Cu(II) in synthetic mixture and water samples [2, 3], environmental samples [4], biological, food and soil samples [5]. The simple interpretations of how the UV-Vis spectrophotometry work is based on the principle of light energy. Light travels in packets of energy called photons and each photons has specific energy related to a certain frequency of wavenumber ($E = h c/\lambda$), the visible light consist of wavelengths ranging from 380–720 nm and when they are all present the light appears as white color, and if any wavelength is removed or absorbed, the remaining combination of wavelength is perceived as the complimentary color. For example, if white light passes through a test tube containing a solution of copper (II) sulfate (CuSO_4), the solution will be blue because the Cu^{2+} ion strongly absorb orange photons of light with $\lambda = \text{ca. } 600 \text{ nm}$.

The absorption of photon of colored light by the sample compound causes an electron transition from lower (ground state) to a higher (excited state) energy orbital, and the released energy of absorbed radiation is equal to the difference between the highest energy electronic occupied molecular orbital (HOMO) and the lowest/closest unoccupied molecular orbital (LUMO) as expressed by equation (1). The wavelength and the energy difference of the absorbed photon required to promote an electron from the ground to the excited state is specifically unique to the chemical species within the test sample of material or solution. That is why the measured absorption or transmittance of the material can be able to identify its unique chemical species or concentration within it.

$$E_{\text{light}} = h \nu_{\text{light}} = hc/\lambda_{\text{light}} = \Delta E = E_{\text{LUMO}} - E_{\text{HOMO}} \quad (1)$$

Where; E , h , ν , c , λ , and ΔE are defined as energy of light, plank's constant, velocity of light, speed of light, wavelength, and difference of energy of light, respectively.

This measuring absorbance method requires the compound to be dissolved in a solution and the amount of a particular energy of light passing through that solution is quantified as transmittance (T), which is calculated from the ratio of light intensity leaving the chemical sample (I) to that entering the it (I_0); equation (2). While the amount of light absorbed (A) by the chemical sample can be calculated from the transmittance equation (3).

$$A = \log (1/T) = -\log T \quad (2)$$

$$A = 2.00 - \log \%T \quad (3)$$

Absorbances are measured by the UV-Vis spectrophotometer, which contains a light source, focusing lenses, diffraction grating or prism to split light into different wavelength a sample holder “cell” a photosensitive detector measuring the light passing through the sample and an output device meter or recorder. The diagram for the presentation of UV-Vis spectrophotometer features and the principle of absorption of light involved in electron excitation are shown in Figure 1. Many transition metals complexes and large conjugated organic molecules are brightly colored because their absorbed energy difference is equal to an energy within the visible region.

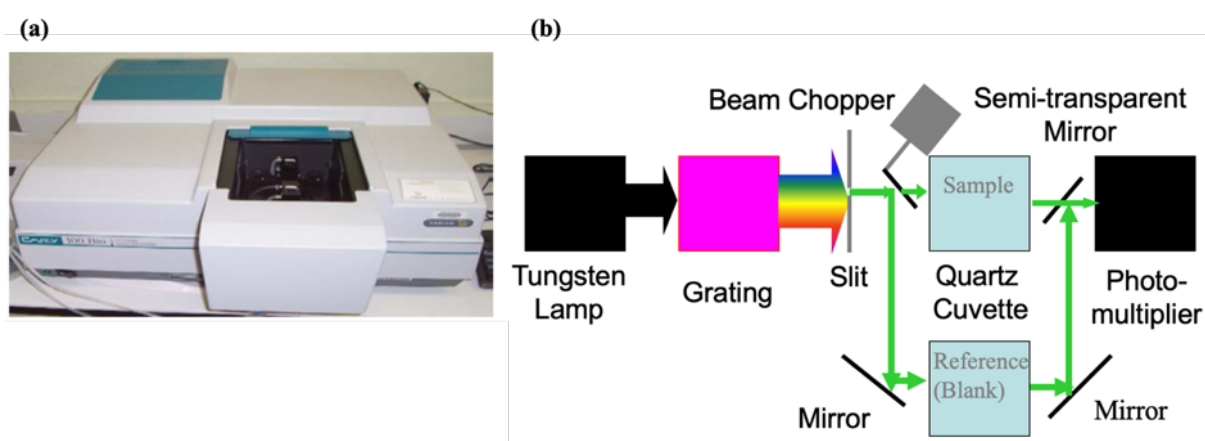


Figure 1. The schematic representation of the (a) outside and (b) inside arrangement and operational principle of double beam UV-Vis spectrophotometer.

2.2.2. Determination of concentration of Cu(II) in spray solution by Beer Law plot

The Beer’s Law described by equation (4) below, states that the amount of light absorbed at a specific wavelength is directly proportional to the concentration of the solution.

$$A = \varepsilon \times C \times l \quad (4)$$

Where; A , ε , C , and l are defined as absorbance, molar absorptivity coefficient, concentration of absorbing species, and path length, respectively.

Its plot is a calibration curve of absorption plotted as a function of concentration and its phenomenon is used in determination of unknown concentrations of metal ions in material or dissolved in solution. An absorption spectrum of solution containing unknown concentration of Cu(II) must be acquired first to determine the wavelength of their maximum absorbance λ_{\max} . All the absorbance is acquired at λ_{\max} .

UV-Vis spectrophotometry was used under this study to determine and confirm the concentration of Cu(II) complexes in electrochemically prepared coating spray solutions

derived from both copper salt and metal. It was also used to identify and confirm the presence of Cu(II) complexes present in resultant spray coating solutions, based on their absorbance spectra within the visible region. The absorbance of Cu(II) complexes in spray solutions were measured with a UV-Vis spectrophotometer (U-2800, Hitachi, Tokyo, Japan) in the double beam mode and wavelength range of 1100–300 nm. A quartz glass cell of a 10 mm path was used as sample holder, and deionized water was used as a reference.

The Beer Lampard plot was constructed using absorbance values of the least five solutions with known concentration of Cu(II) as 0.01, 0.02, 0.03, and 0.05 mmol g⁻¹. A graph of absorbance versus concentration is first constructed and a best fit straight line was drawn through the data point. The absorbance of spray solution containing the unknown concentration of Cu(II) is also measured and its concentration is determined by comparison to the Beer Lampard Law plot. The unknown concentration of Cu(II) in spray solution was therefore extrapolated from the best fit straight line of the Beer Lampard Law plot by drawing a horizontal line from the value of the experimentally found absorbance on the y-axis to the calibration curve, and a vertical line to the x-axis to determine the value of the independent variable which is the unknown concentration of Cu(II) in this case. The unknown concentration of Cu(II) in spray solution can also be determined as the value of the slope calculated from the equation of best fitted straight line of the Beer Lampard Law plot.

2.2.3. Optical Characterization of thin films

UV-Vis spectrophotometry was also used to measure and analyze the absorbance and optical transmittances of Cu₂O thin films fabricated using precursor spray solution derived from copper salts. The optical transmittances data was used to calculate the band gap of the thin films. The optical band gap of each Cu₂O thin film was calculated from the corresponding transmittance data at a given wavelength, based on the Tauc expression, indicated by equation (5) below:

$$\alpha = \frac{A(E-E_g)^2}{E} \quad (5)$$

Where; E_g , E , A and α are defined as the optical band gap, photon energy ($h\nu$), constant related to material and absorption coefficient at a given wavelength, respectively [6, 7].

The band gap energy is related to the electron excitation of the Cu₂O thin films under UV or visible light irradiation. The optical transmittance of thin films was measured using the same UV-Vis spectrophotometer, in the wavelength range of 1100–300 nm and in double beam mode.

2.2.4. pH

The chemical stability of the metal complexes in dissolved solution determine its life time for storage of the coating solutions. The metal ions can exist as unstable metal salt or complex, respectively based on the pH of their dissolved solutions. The pH of the prepared coating spray solutions under this study was measured in order to determine the stability of their constituted Cu(II) complexes. The pH of spray solutions was measured using a pH meter (GST-2729C, DKK-TOA Corporation, Tokyo, Japan).

2.3. Structural Characterization

2.3.1. X-ray diffraction for thin film characterization

X-ray measurement technique is well developed and widely used for the characterization of various thin film materials and devices. The instrument that is used to measure the unknown diffraction angle of material is known as the XRD diffractometer. Based on Inaba *et al.*, who studied the X-ray thin-film measurement techniques; X-ray diffraction method as a tool for characterizing materials including thin film surfaces has been remarkable when compared to other methods such as electron beam diffraction method due to its merit such as; (1) non-destructive measurement and no requirement of special sample preparation, (2) performance applicable to both atmospheric, high temperature and/or high pressure condition, (3) allowance of the information extraction on the average structure in a relatively large surface area, (4) no irradiation damages in organic materials, (5) controllability of the analysis depth by the incident angle onto the surface and characterization of buried interface structure specifically in thin films [8].

The measurement of thin films by the XRD diffractometer is based on their two-dimensional formation on the substrate surface, basing its characterization discussion along two stacking and in-plane direction. The technique also provides analysis of thin film information such as; lattice constant and distortion, crystal orientation, and crystallite size [8]. Figure 2 (a) shows main components of the X-ray diffractometer includes; measurement axial, sample position adjustment axes, X-ray source, incident optical system, goniometer, receiving optical system and detection section among others.

(a)

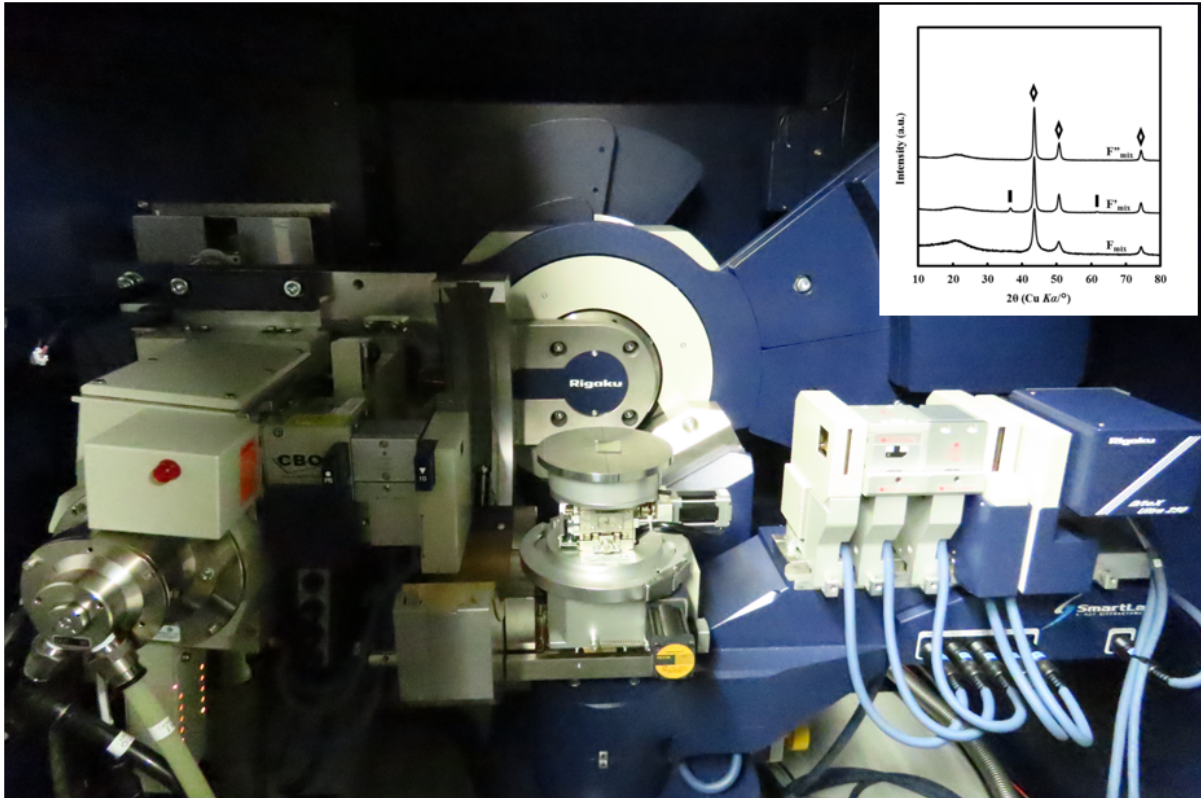


Figure 2. (a) The schematic diagram of X-ray diffractometer equipped with 2θ and containing inset for the pattern of copper thin films fabricated by MPM *via* spray coating [9].

During thin film measurement the selection of X-ray geometry is important. Para focusing X-ray geometry is used for analyzing a powder sample while in quantitative analysis of thin films, it is not focused incident X-ray but rather parallel incident X-rays that are more suitable [10]. To characterize the crystallinity of thin film an extremely small width profile from high resolution measurement is required.

The XRD patterns of a substance is a characteristic of that substance and form a sort of fingerprint by which the substance may be identified. However, it is a collection of diffraction patterns that allows the identification of unknown by recording its diffraction pattern and locating in the file of unknown patterns the one that it matches. Two main important parameters in X-ray measurements of thin films are the phase identification by X-ray diffraction and determination of crystal structures. X-ray diffraction is due essentially to the existence of certain phase relation between two or more light waves. It's the difference in the length of the path traveled that leads to the difference in phase of which introduction produce a change in amplitude. The greater the path difference leads to its greater difference in phase. Therefore,

two rays are completely in phase whenever their path lengths differ either by zero or by a whole number of wavelengths. While the difference in the path length of various rays arose naturally when considering how a crystal diffracts X-rays. Figure 2 (b) is a representation of a crystal whereby its atom is arranged on a set of parallel beam A, B, C, D normal to the plane of drawing and spaced a distance d' apart. Assuming that a beam of perfectly parallel and monochromatic X-ray of wavelength is incident on this crystal at an angle θ , called Bragg angle and where is measured between the incident beam and the particular crystal planes under consideration, there is a possibility that this beam of X-ray will be diffracted under certain conditions. A diffracted beam is defined to be composed of a large number of scattered rays mutually reinforcing one another.

Diffraction is therefore essentially a scattering phenomenon and does not involve any new kind of interaction between X-ray and atoms. It's the atom that scatter incident X-rays in all directions and in some of these directions the scattered beam will be completely in phase, leading them to reinforce each other to form diffracted beams. Therefore, as illustrated in Figure 2(b), the only diffracted beam formed is that making an exit angle θ with respect to diffraction plane $1'$ equal to the angle of incidence. Demonstrated by one plane of atom and second for all the atoms making up the crystals (i.e. atoms scattering rays in plane 1, 2, and 3). For example considering rays 1 and 1a in the incident beams, they strike atoms K and P in the first plane of atoms and are scattered in all directions but only in $1'$ and $1a'$ these scattered beams are completely in phase and so capable of reinforcing one another because the difference in their length of path between the wave fronts XX' and YY' is equals to equation (6a) below;

$$QK - PR = PK \cos \theta - PK \cos \theta = 0 \quad (6a)$$

Similarly, the rays scattered by all the atoms in the. First plane in a direction parallel to $1'$ are in phase and add their contributions to the diffracted beam which is also true of all the plane separately. Additional example is for ray 1 and 2 which are scattered by atom K and L , and the path difference for rays $1K1'$ and $2L2'$ are given in equation (6b) below. That is the same path difference for the overlapping rays scattered by S and P in the shown direction since there is no path difference between rays scattered by S and L or P and K

$$ML + LN = d' \sin \theta + d' \sin \theta \quad (6b)$$

Scattered rays $1'$ and $2'$ will be completely in phase if this path difference is equal to a whole number n of wavelengths, as summed up by the Bragg's law (2c) below, which was first formulated by W. L. Bragg.

$$n\lambda = 2d' \sin \theta \quad (6c)$$

The law states the conditions that need to be met if diffraction is to occur; n is the order of diffraction and it may take on any integral value consistent with $\sin\theta$ not exceeding unity and is equal to the number of wavelengths in the path difference between rays scattered by adjacent planes. Therefore, for fixed values of λ and d' there may be several angles of incident θ_1 , θ_2 , and θ_3 at which diffraction may occur corresponding to $n = 1, 2$, and 3 [10].

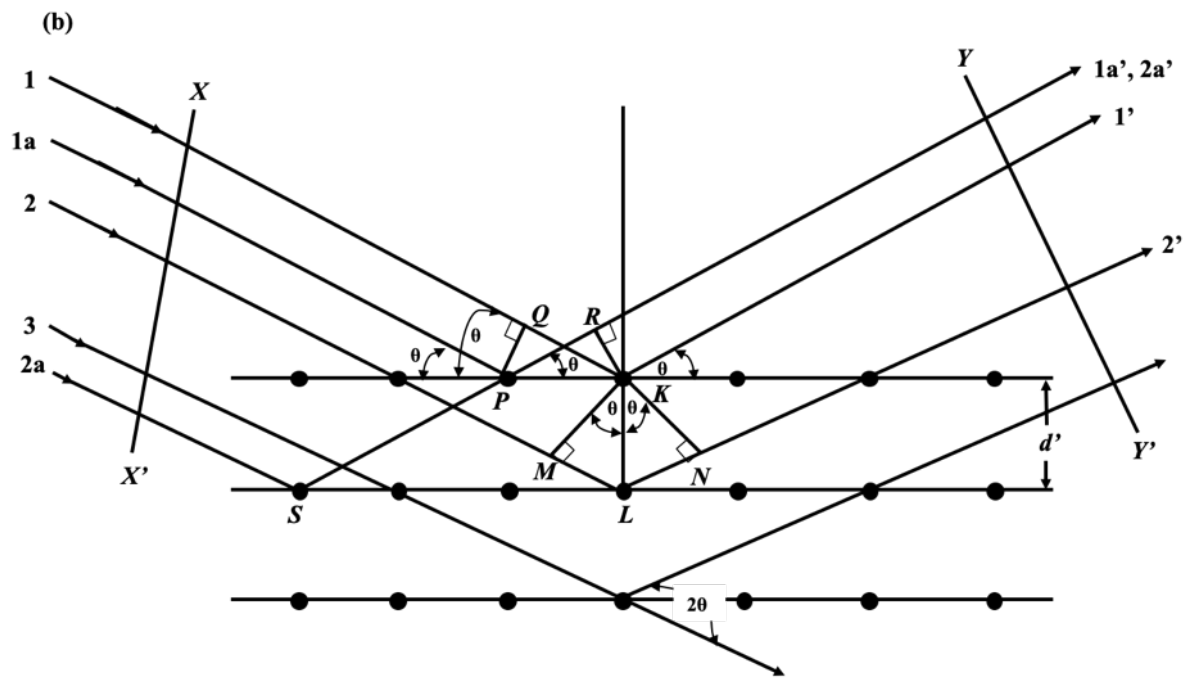


Figure 2. (b) Representation of the principle for diffraction of X-rays by a crystal [10].

Under this study XRD was used to characterize the crystallinity of the fabricated all thin films fabricated by MPM *via* spray coating of different spray solutions containing copper precursor at 180°C in air. The crystal phases of thin films were examined using a SmartLab X-Ray Diffractometer (XRD, Rigaku, Tokyo, Japan) with $\text{Cu-K}\alpha$ X-ray generated at 35 kV and 200 mA. The parallel beam optics was used at an incident angle of 0.3° in the 2θ range of $10\text{--}80^{\circ}$ with a scanning step width of 0.05° and speed of $5^{\circ}\text{ min}^{-1}$. The Debye-Scheerer and Hall method was used to calculate the averaged crystallite size of all thin films, using only the highest intensity peak at 2θ of 36.0° assignable to (111) phase of Cu_2O , based on the equation (6d).

$$D_{hkl} = \frac{\kappa\lambda}{\beta\cos\theta} \quad (6d)$$

Where; D_{hkl} , K , λ , β , and θ are defined as; the average crystallite size, Sherrer constant, X-ray wavelength, full width at half maxima (FWHM) of the diffraction peak and Bragg angle, respectively. A 0.9 value was used as the Sherrer constant, K [11].

2.4. Chemical characterization

2.4.1. Auger Electron Spectroscopy (AES)

AES is the most popular analysis technique for elemental analysis of surfaces. With a particular small depth resolution, it is well suited for study of solid surfaces or material exposed by sputter ion bombardment [12]. As a tool it was first demonstrated as a useful tool for surface analysis in 1967 and is receiving widespread application in the fields of surface physics, chemistry, metallurgy, thin films and electronic materials technology. In thin film technology it is well suited for the study of metals and semiconductors and plays an important role in research, development and production [12].

The instrumentation for Auger electron spectrometer is basic. Its components shown in Figure 3 consists of the (1) electron source and electron optical column, to form an electron probe onto the specimen surface (2) an ion optical column for cleaning the sample surface and/or sputtering for depth profiling (3) an electron energy analyzer (4) a secondary electron detector and a pulse counter (6) computer control and data display systems and acquisition [13]. The electronic optics and basic electronic for AES system also consist of an electron gun for excitation, analyzer, electron multiplier for amplification of the Auger electron signal, and a system for standard modulation and phase sensitive detection electronic [12]. The spectroscopy involves measurements of Auger electron's kinetic energies that are characteristic of the elements present in the sample, it is the energy analysis of the electron ejected from the solid material. This electron excited technique is initiated by bombarding the material with a beam of electrons. This analytical technique have two main attributes; thus, it is capable of quantitatively determining what elements are present and giving an indication of the quality of material present in a sample. The present elements in the sample material is identified from the individual Auger electron peaks by a comparison with tabulated values from standard handbook spectra while the elemental concentration of the identified present elements is determined from a respective characteristic Auger peak. Mostly, the sensitivity factors which refer to a certain Auger transition are conveniently replaced by relative sensitivity factors referring all standard values to that for a one reference Auger peak, thus the variation during the analysis need not be taken into account separately [14].

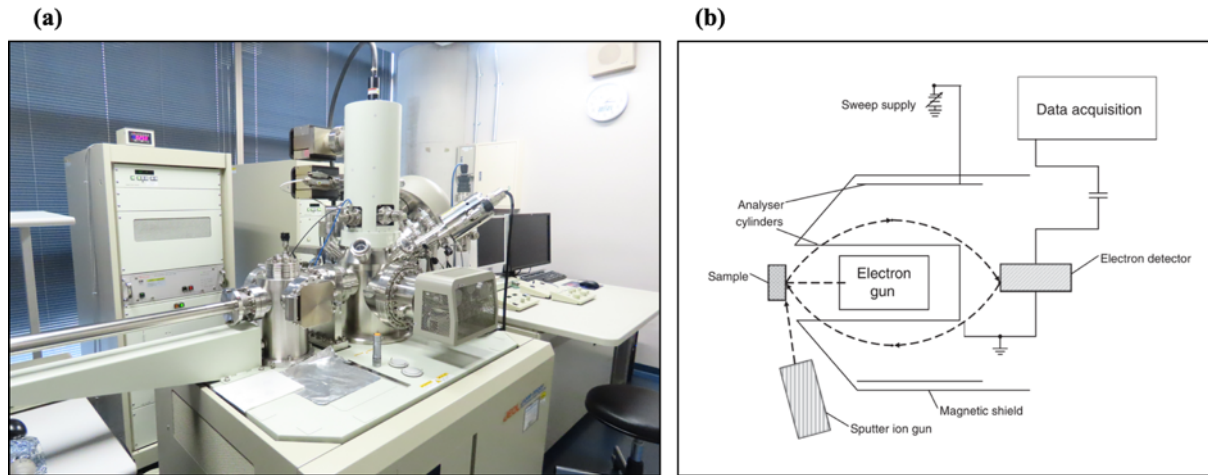


Figure 3. The schematic representation of (a) instrumentation of Auger electron spectroscopy and (b) its basic operational principle [14].

The first step in qualitative Auger analysis involves obtaining a survey spectrum with relatively modest resolution in a fairly short time, which are recorded at energies between 0 and 1000 eV as most elements have significant Auger transitions in such range [13]. The process is initiated by bombarding the material with a beam of electrons which can ionize one of the electron levels such as K level. The system then will return to equilibrium with an electron from M level dropping to fill the vacant K shell. It drives the system to give rise to emission of an X-ray photon. In addition, there is an alternative route which involves the transfer of energy through Auger radiation process to an electron such as one occupying the N level which can then have enough energy to be ejected from the solid sample material. This electron will have an energy related to the M and K level of the solid material, and the electrons ejected from the solid sample material are sorted according to their energy hence, providing the method of identifying the elements present in the solid sample material [12]. The process is described by its energy level diagram shown in Figure 3(c).

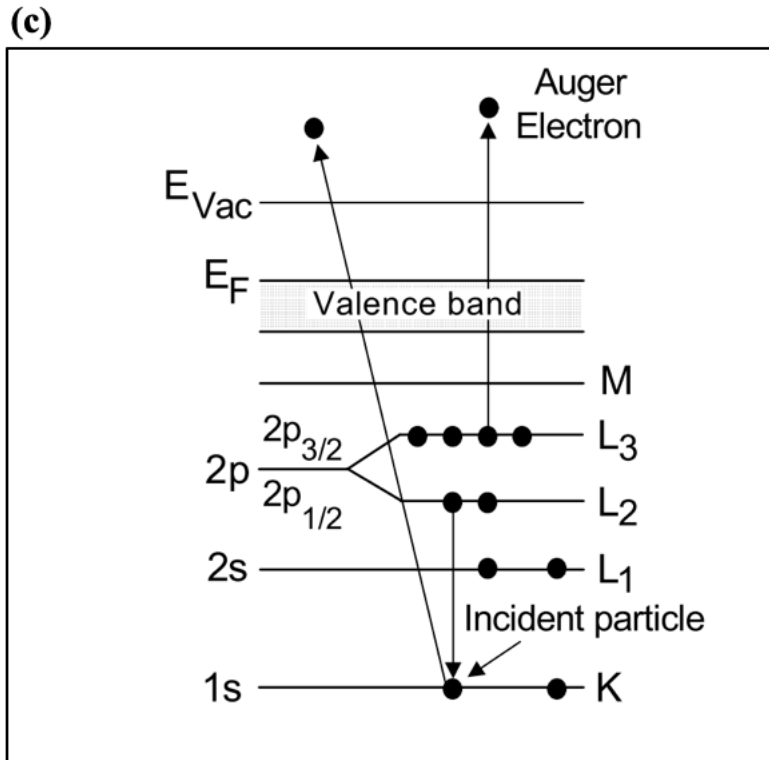


Figure 3. (c) The schematic representation of energy level diagrams describing the basic principle of process involved in Auger electron spectroscopy [12].

Under this study the chemical characterization of the fabricated thin films was done using AES. The analysis was done using a field emission Auger microprobe (JAMP-9500, JEOL, Tokyo, Japan), with 10 kV probe voltage and 10 nA current. Prior to each measurement, a 100 μm area of the film was etched with an Ar^+ beam of 2 kV and 10 nA for 10 s. The AES was able to provide information of the present elements in and their relative atomic ratio in the fabricated thin films.

2.4.2. Raman Spectroscopy

The Raman effect was observed in 1928 and was used to investigate the vibrational states of many molecules in the 1930s. Raman discovered that a small fraction of the scattered light was present at wavelength different from the incident one which is known as Raman shift and got the Nobel prize for his work in 1931 [15]. The non-destructive chemical analysis technique provides detailed information about chemical structure, phase and polymorphism, crystallinity, molecular interactions, contamination and impurity in solid chemical material. It is used for the identification of elemental bonding within the material and which is based upon interaction

of light with the chemical bonds within a material. Raman effect is a light scattering technique, whereby a molecule scatters incident light from a high intensity laser light source. Its electron excitation concept is similar to those of UV-Vis spectrophotometry described above. Most of the scattered light is at the same wavelength as the laser source (Rayleigh scatter) and does not provide useful information until a small amount of light is scattered at different wavelength which depends on the chemical structure of the analyte. The Raman spectrum features a number of peaks, showing the intensity of wavelength position of the Raman scattered light. Each peak corresponds to a specific molecular bond vibration, including individual bonds such as C–C, C=C, N–O, C–H and groups of bonds of benzene ring breathing mode, polymer chain vibration and lattice mode [15]. Because IR and Raman offer complementary technique in some cases Raman studies can be coupled with Infra-red for a more detailed vibrational energy mode evaluation of a material. The representation of a basic instrumentation consisting of monochromatic light source providing the laser irradiation onto the sample material, Raman scattering and Rayleigh scattering, that scatter the lights with a different and same wavelength, respectively and, spectra recording that saves the Raman shift are shown in Figure 4 [15].

Under this study the Raman spectra of quartz glass substrate and Cu₂O thin films was measured at room temperature under dark condition using a Raman spectrometer (LaBRAM HR800, Horiba, Kyoto, Japan) with a charge-coupled device detector. The Nd:YAG laser (532.028 nm) was used as the excitation source, with an intensity of 10 mW and exposure time of 180 s. The resolution used for all samples was approximately 1 cm⁻¹ with a laser spot-size of 100 μm². The observed Raman peaks were analyzed using calibration curves obtained from the peak area of Raman spectrum for Si wafer attached on a quartz glass substrate. Raman shift was observed in the analyzed thin films and provided the information about the type of vibrational energy mode within the bonding of elements in Cu₂O thin film. There was no necessity of coupling Raman with IR in this study as its use was only required for the identification of vibration mode of Cu₂O bonding which it could singularly provide.

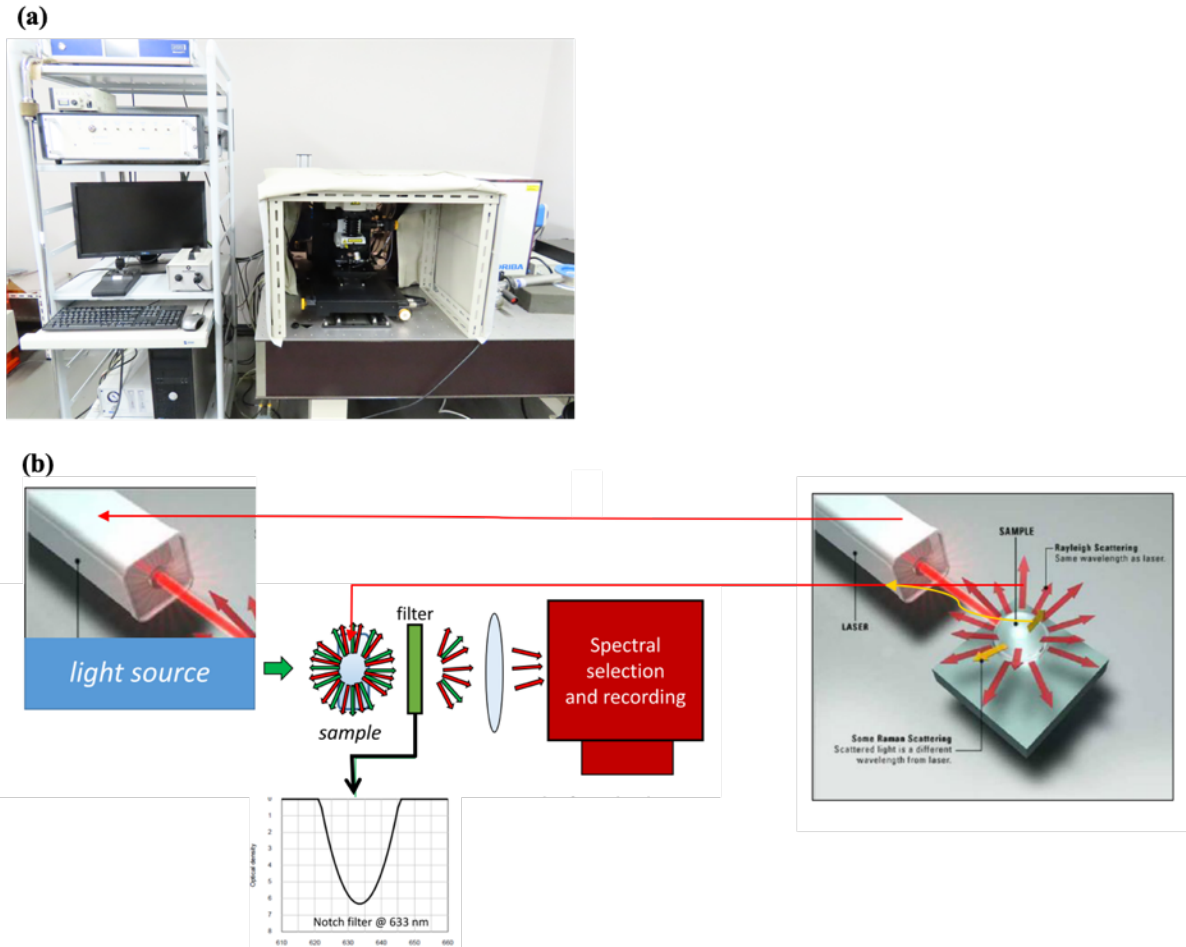


Figure 4. The representation of (a) Raman spectroscopy instrumentation and (b) its operational principle [15].

2.5. Morphology and thickness

The first electron microscope that accelerated electrons as a source instead of light was built by Max Knoll and Ernst Ruska in 1931 at the University of Berlin, Germany. Noteworthy, that the first scanning electron microscope (SEM) was built in 1938 to improve and challenge the difficulties of scanning the electrons through the sample. Field emission scanning electron microscope (FE-SEM) is a type of electron microscope that images the sample surface by scanning it with high energy beam of electrons in a raster scan pattern. The principle of electron microscope is identical to these of a light microscope but instead of using visible light as source of energy, it uses very energetic electrons. However, the resolution of the optical microscope is limited by its wavelength compared to accelerated electrons containing very short wavelength making it possible and convenient to see very small features under its analysis. The small wavelengths can be changed according to the applied high voltage [16].

When the electron beam interacts with the specimen, useful information about the sample is revealed, which includes; surface features, sizes and shape of the features, composition and crystalline structure of the sample material. The interaction of electron beam with the specimen can be achieved through series of steps; (i) If the incident electrons come close enough to the sample's atom, then these electrons will give some of their energy to specimen electron mainly in their *K* shell resulting in secondary electrons that changes their path and ionize the electron in the specimen atom instead. The ionized electrons escape the atoms as secondary electrons moving to the surface of specimen *via* elastic and inelastic collision. Due to their low energy which is sometimes caused by the level of conductivity of material, only the electrons close to the surface will escape and be detected by the detector that use it for imaging the topography of the specimen. (ii) Some electrons are backscattered or reflected electron when the incident electron directly hits the atoms. While different atoms will result in different rate of backscattered electrons, the contrast of the final image varies with the change in the atomic number of the specimen and these with high atomic number will appears brighter than these with lower atomic number. (iii) If the incident electrons pass through the specimen without any interaction with their atoms, these electrons are transmitted and used to get the image of the thin specimen. Also, through another scattering mechanism known as elastic scattered the electrons do not lose their energy and those are used to get information about orientation and arrangement of the atom in the sample material [16].

The components of SEM are shown by its basic instrumentation in Figure 5. The instrument contains an electron optical system that is located inside the microscope column and space surrounding the specimen and is kept at vacuum. The system consists of a specimen stage to place and support the specimen. The electron optical system also consists of an electron gun to produce electron beam, a condenser lens and an objective lens to focus the electron beam into electron probe, a scanning coil to scan the electron probe and other components. It also consists of a secondary-electron detector that detects secondary electrons emitted from specimen, whose output signals are amplified and transferred to image display. The scanning on the display unit is synchronized with the electron-probe scan, and brightness variation which depends on the number of the secondary electrons appears on the monitor screen of the display unit, thus forming a SEM image.

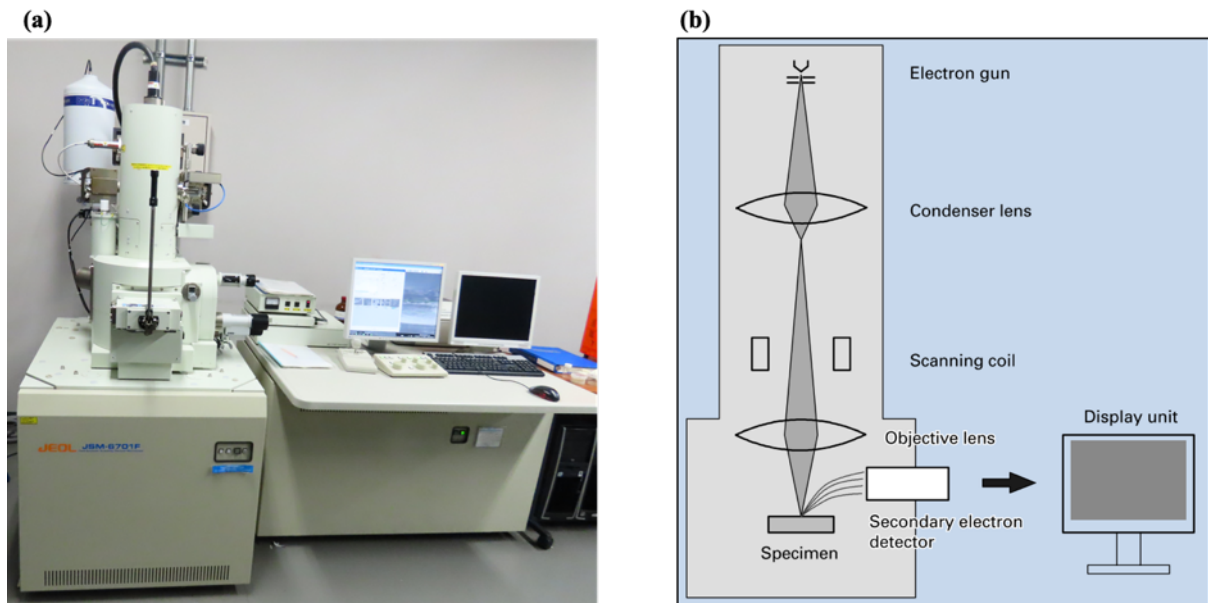


Figure 5. The basic instrumentation of the (a) outside, (b) inside and operational components of FE-SEM [16].

Under this study the surface morphology of all fabricated thin films was observed using a field emission scanning electron microscope (FE-SEM) (JSM-6701F, JEOL, Tokyo, Japan) at an accelerating voltage of 5 kV and 10 mA resultant current.

The thickness of each Cu_2O thin film was determined from a cross-sectional image measured using the identical instrument. The measured values at seven different positions across the cross-sectional image were arbitrarily collected to obtain the averaged film thickness. Measurement of cross-sectional images of some Cu_2O thin films provided additional information such as their porous structures due to their fabrication technique of spray coating. The porous structure of these films was related and linked to their photocatalytic activities. Thickness of some of the fabricated copper thin film was also calculated from their measured cross-sectional images.

2.6. Electrical Characterization

2.6.1. Hall effect measurement

The electrical properties in cuprous oxide is widely investigated due to their technical importance. Hall effect is a basic to solid state physics and an important diagnostic tool for the characterization of materials mainly semiconductors, which provides direct determination of both the sign of the charge carriers as electron or hole and their density. The basic representation of a laboratory set up Hall effect geometry [17] is shown in Figure 6. The set-

up display that the thin strip (thickness symbol) of the material under analysis is placed in a magnetic field B area oriented at right angle to the thin strip. The current I flow in response to applied electric field. At a microscopic scale, the generated current I is as a result of positive and negative charges moving in the direction or backwards of I , respectively. Regardless of the directional flow of current, the magnetic Lorentz force describe by equation (7a) causes the carries to curve upward.

$$qv \times B \quad (7a)$$

Since the charge cannot leave the top or bottom of the strip sample material a vertical charge builds up in the sample material. The charge imbalance produces a vertical electric field which counteracts the magnetic force, leading it to reach their steady state. The created vertical electric field can be measured as the transverse potential difference on the voltmeter. Supposedly, the charge carriers are electrons; i.e. $q = -e$, the negative charge accumulates on top position of the strip sample material causing the voltmeter to read a negative potential difference. Alternatively, if the charge carriers are holes; i.e. $q = +e$ a positive voltage is measured on the voltmeter [17].

The above described principle of Hall effect was used to evaluate the electrical properties of the fabricated Cu_2O thin films, under this study. The electrical resistivity, carrier mobility and concentration of Cu_2O thin films were evaluated from a Hall effect measurement using an HL5500 Hall system (Accent, London, UK). Each thin film sample was cut into four pieces of $10 \times 10 \times 1.6 \text{ mm}^3$ size and three pieces were used for measurement. The observed values from three different pieces were averaged to determine the electrical parameters of all thin films. The relationship between the electrical parameters of electrical resistivity (σ), carrier concentration (n), carrier mobility (μ), and elementary electric charge (e), is shown by the equation (7b) [11].

$$\sigma n \mu = 1/e \quad (7b)$$

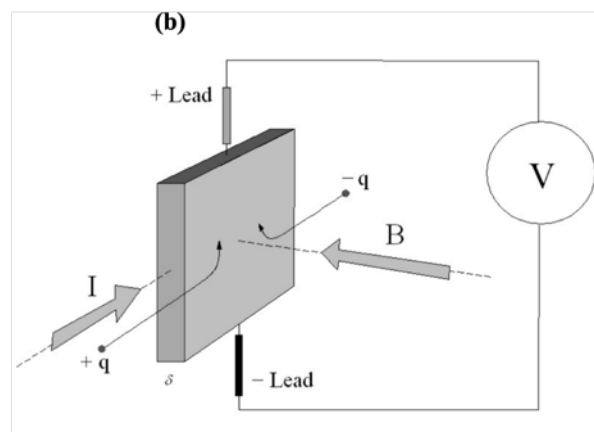
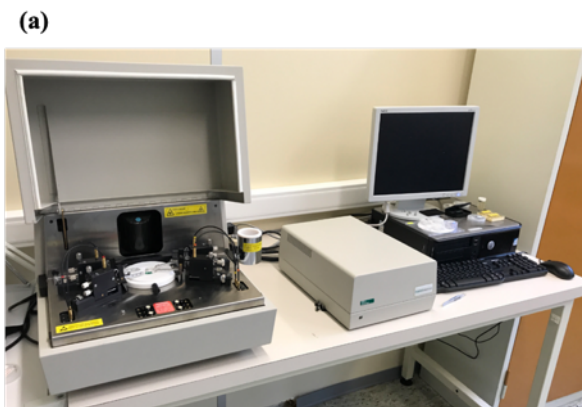


Figure 6. The representation of the (a) instrumentation of a laboratory set up Hall effect geometry and its (b) operational basic principle [17].

The measured electrical properties of the thin films provide an important information about their carrier charges and concentration which was related to their photocatalytic properties, optical properties, and morphologies under this study.

2.6.2 Four probe measurement

The four-probe method is one of the standards and most commonly used method for the measurement of resistivity, due to its practical advantages such as; overcoming problems of contact resistance, and permits accurate resistivity measurements in sample having wide variety of shapes. In single crystal material such as metallic copper and copper oxide thin films, the resistivity may vary smoothly from point to point. Hence, it is the evaluation of the amount of variation at some points where the resistivity is not constant.

Resistance of some metallic copper thin films fabricated under this study were evaluated using the four-probe method at room temperature. The instrument set up consisted of a regulated DC power supply (Model PAB32-1.2, Kikusui Electronic Corp., Kanagawa, Japan), two multimeters; (VOAC7512, Iwatsu Electric Co., Ltd., Tokyo, Japan) and (Model 2010, Keithley Electric Corp., Tokyo, Japan) used as a current source and voltmeter, respectively. The set-up also consisted of four Au-plated tungsten probes (FELL type, K&S, Tokyo Japan), placed at an interval of 1 mm with an added load of 0.1 kg. The simple schematic representation of four probe measurement for a copper thin film is shown in Figure 7. During measurement the sharp four probes are placed on a flat surface of the sample material, the current is passed through the two outer electrode probe 1 and 4 and the floating potential is measured across the inner pair electrode probe 2 and 3. To prevent minor carrier injection and make a sample surface-probe contacts must be mechanically lapped, which was assisted by a 0.1 kg load placed on top of the probes. Figure 7 shows the simple circuit used in the resistance measurement of thin films under this study.

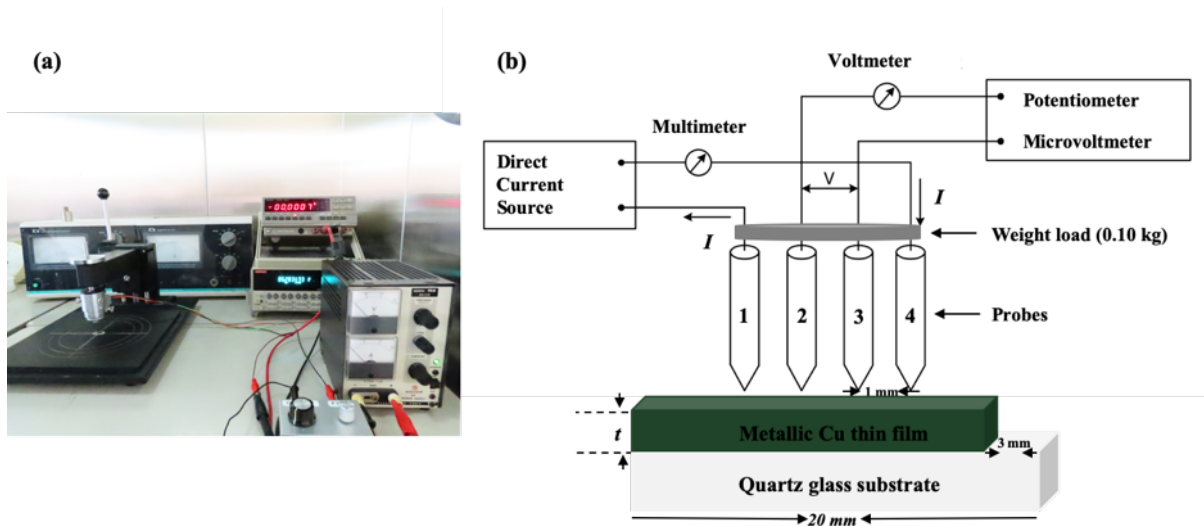


Figure 7. The representation of (a) instrumentation set up and (b) basic operational principle of four probe measurement for a copper thin film.

The electrical resistance (R) and resistivity (ρ) of the copper thin films was calculated according to the formula 1 and 2 below:

$$R = V/I \quad (1)$$

$$\rho = R \times t \times F_p \quad (2)$$

Where; R , V , I , ρ , t , and F_p are defined as electrical resistance, measured potential difference across inner pairs of probes, applied electric current through the outer pair of probes, electrical resistivity, measured film thickness by stylus profilometer, and resistivity correctional factor, respectively [18].

2.7. Physical Properties

2.7.1. Thickness of Cu thin films

The thickness of some fabricated metallic copper thin films was measured using stylus profilometer (DEKTAK-3, Sloan, California, USA). Before the films were fabricated, a portion of ca. 3 mm on the quartz glass substrate was masked with a heat resistant tape to keep uncoated substrate during the spray coating process. The thickness values were calculated as average of measured surface differences between the uncoated quartz glass substrate and the sprayed thin film.

2.7.2. Adhesion strength by scratch test

The adhesion strength of all thin film fabricated under this study onto the quartz glass substrate was evaluated using a scratch tester (HEIDON-22, Shinto Scientific, Tokyo, Japan) by applying a load of 1 kg and at the scratch speed of 53 mm min⁻¹.

2.8. Photocatalytic Properties

The photocatalytic activity of Cu₂O thin film was evaluated by the discoloration rate of MO solution, according to our previous method in which a different dye, methylene blue, was used as a model pollutant in water [19]. The MO concentration in test solution, whose pH value was adjusted to 7.0 by adding 1 or 2 drops of 1 mol L⁻¹ NaOH solution, was adjusted to 10 mg L⁻¹ by dissolving MO in deionized water. The pH value of MO solution was measured using the abovementioned pH meter. Each six samples of each thin film with an identical area of 20 × 20 mm² and/or 60 × 60 mm² were prepared for the discoloration test. The visible light from a fluorescent light, FS2015E-H (Hitachi, Tokyo, Japan) was illuminated on the thin film samples immersed in the MO solution at a vertical distance of 15 cm from the sample surface. The light intensity measured by a digital illuminometer M-101 (MonotaRO Co., Ltd., Amagasaki, Japan) was 0.45 mW cm⁻².

A portion of approximately 3 mL of the MO solution was transferred into a quartz cell (10 × 10 × 45 mm³) at an interval of 30 min. The absorption spectrum of each MO solution was recorded in the range of 200–700 nm by using a Hitachi U-2800 spectrophotometer in a double beam mode, and deionized water was used as a reference. Every measured portion was immediately returned back into the petri dish containing remained solution and thin film sample under visible-light irradiation and in dark condition, to continue the discoloration test up to 3 h and/or 4.5 h. The discoloration test was carried out three times for each thin film sample under visible-light irradiation and in dark condition. The schematic representation for the measurement of photocatalytic degradation test of MO by a Cu₂O thin film is shown in Figure 8.

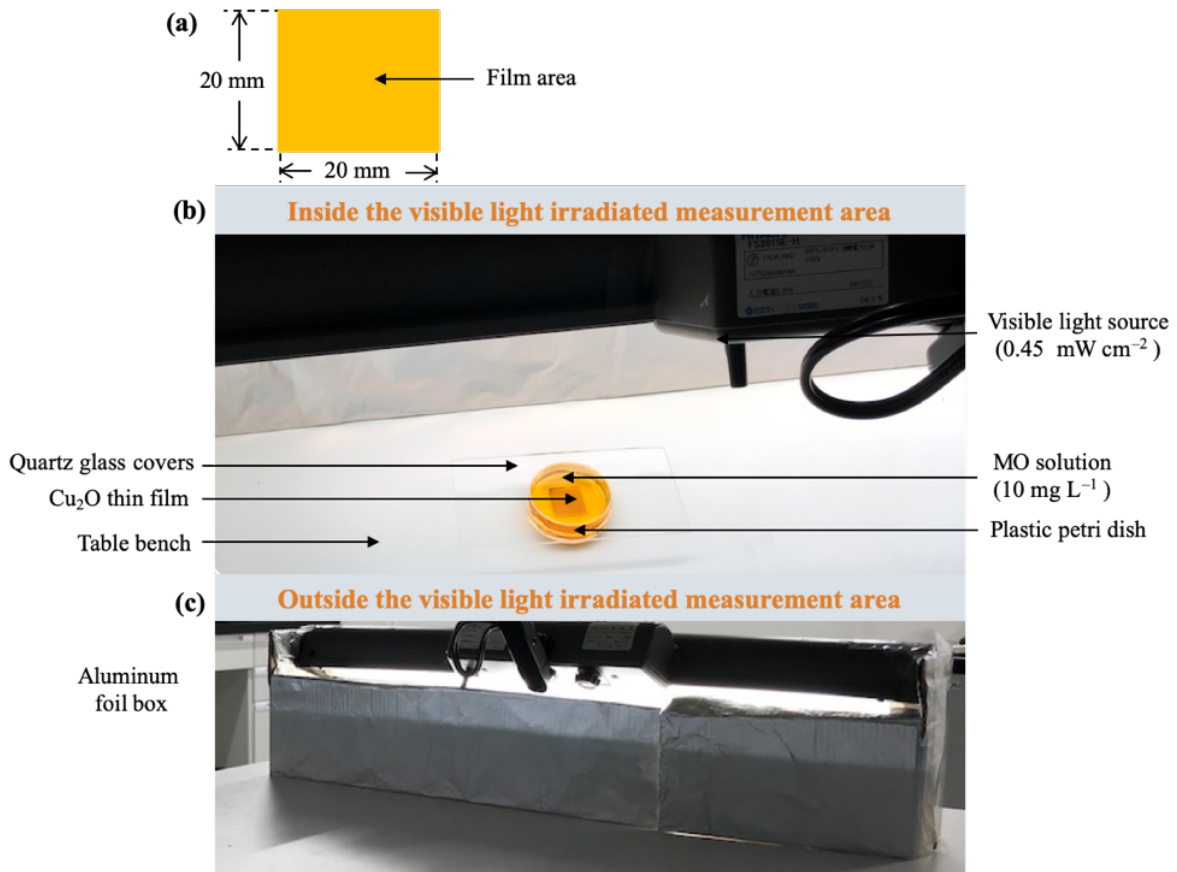


Figure 8. The schematic representation for the measurement of photocatalytic degradation test *via* discoloration of MO by (a) Cu₂O thin films (b) inside components and (c) outside the visible light irradiation measurement area.

An additional examination for some thin films in pure water was performed under abovementioned light irradiation to clarify the effect of MO onto the thin film at the neutral pH condition.

The discoloration efficiency ratio and rate constants of MO solution under visible light irradiation and in dark condition were calculated according to the pseudo-first order kinetic law described by the following equation (8) and (9) below.

$$C = (C_0 - C_t) / C_0 \times 100 \quad (8)$$

$$\ln(C/C_0) = kt \quad (9)$$

Where C , C_0 , C_t , and k are photocatalytic efficiency ratio, initial concentration of MO solution, concentration of MO solution at elapsed time t , and pseudo-first-order rate constant, respectively [19–22].

2.9 Summary

All the measuring instruments and equipment used in the characterization of the prepared precursor solutions and fabricated thin films were at full disposal at the Kogakuin University. The unknown concentration of Cu(II) in electrochemically prepared spray solution was determined by Beer Law plot from their measured absorption by UV-vis spectrophotometer, which was also used to measure the optical transmittance whose data was used to calculate the band gap of fabricated Cu₂O thin films. The structural and chemical information of the thin films was provided by X-ray diffractometer and Auger electron spectroscopy, respectively. The morphology of the thin films was measured by FE-SEM. The thickness of all the Cu₂O and some metallic copper thin films was calculated from their measured cross images of FE-SEM. Additionally, some of metallic copper thin films thickness was measured by stylus profilometer. The electrical properties of Cu₂O thin films was evaluated by means of Hall effect measurement, while these of metallic copper thin film by four probe measurement. The adhesion strength of thin films on quartz glass substrate was evaluated by means of scratch test. The tensile strength of metallic Cu thin films was measured and determined by Pull-stud method. The visible light photo-reactivity of the Cu₂O thin films was evaluated by photocatalytic test *via* the discoloration of MO which was used as a model pollutant dye.

References

- [1] Kyuzou, M.; Mori, W.; Tanaka, J. Electronic structure and spectra of cupric acetate mono-hydrate revisited. *Inorganica Chim. Acta.* **2010**, *363*, 930–934.
- [2] Sharma, S.; Rahman, N.; Najmul Hejaz Azmi, S.; et al. UV Spectrophotometric Determination of Cu(II) in Synthetic Mixture and Water Samples. *Journal of the Chinese Chemical Society.* **2010**, *57*, 622–631.
- [3] Sarker, K.C.; Ullaha, R. Determination of Trace Amount Of Copper (Cu) Using Uv-Vis. *International Journal of Scientific Research and Management.* **2013**, *1*, 33–44.
- [4] Kiran, K. Spectrophotometric Determination of Copper in Various Environmental Samples Using Green Reagent. *International Journal of Science Engineering and Technology.* **2014**, *02*, 20–31.
- [5] Ahmed, M.; Uddin, M. A Simple Spectrophotometric Method for the Determination of Cobalt in industrial, environmental, biological and soil samples Using bis(Salicylaldehyde)orthophenylenediamine. *Chemosphere.* 2007, *67*(10), 2020–2027.
- [6] Nagai, H.; Suzuki, T.; Hara, H.; et al. Chemical fabrication of p-type Cu₂O transparent thin film using molecular precursor method. *Mater. Chem. Phys.* **2012**, *137*, 252–257.

- [7] Zheng, W.; Chen, Y.; Peng, X.; et al. The phase evolution and physical properties of binary copper oxide thin films prepared by reactive magnetron sputtering. *Materials (Basel)*. **2018**, *10*, 1–13.
- [8] Mitsunaga, T. X-ray thin-film measurement techniques I. Overview. *The Rigaku Journal*. **2009**, *25*(1), 7–12.
- [9] Hishimone, P.; Nagai, H.; Morita, M.; et al. Highly-Conductive and Well-Adhered Cu Thin Film Fabricated on Quartz Glass by Heat Treatment of a Precursor Film Obtained Via Spray-Coating of an Aqueous Solution Involving Cu(II) Complexes. *Coatings*. **2018**, *8*(10), 1–10.
- [10] Cully B. D. and Stock S. R. *Elements of X-ray diffraction*. Pearson Publisher. 3rd edition, 2001; 1–664, I SBN 9780201610918.
- [11] Wu, H.; Tomiyama, N.; Nagai, H.; et al. Fabrication of a *p*-type Cu₂O thin- film via UV-irradiation of a patternable molecular-precursor film containing Cu(II) complexes. *Journal of Crystal Growth*. **2019**, *509*, 112–117.
- [12] Weber, R.E. Auger Electron Spectroscopy for Thin Film Analysis. *Journal of Crystal Growth*. **1972**, *17*, 342–353.
- [13] Gunawardane, R.P.; Arumainayagam, C.R. Chapter 10 *Auger Electron Spectroscopy*. *Handbook of Applied Solid State and Spectroscopy*. Springer. 2006; 451–483, ISBN 978-0-387-37590-8
- [14] Wucher, A. Surface and Thin Film Analysis with Electron and Mass Spectrometric Techniques. *Material Science Forum*. **1998**, *287*, 61–86. ISSN 1662-9752
- [15] Zhang, S.L. *Principles of Raman Spectroscopy and its Application in Nanostructures*. John Wiley and Sons Publisher. 1st Edition, 2012.
- [16] Alyamani, A.; Lemine, OM. *FE-SEM Characterization of Some Nanomaterial*. Scanning Electron Microscopy. Intech 2012; Doi: 10.5772/34361.
- [17] Bradley Armen, G.; Hall Effect Experiment. *Report, Tennessee copyright*. 2007
- [18] Yamashita, M. Related content Resistivity Correction Factor for the Four-Probe Method: Experiment I. *Japanese Journal of Applied Physics*. **1988**, *27*, 869–870.
- [19] Nagai, H.; Mochizuki, C.; Hara, H.; et al. Enhanced UV-sensitivity of vis-responsive anatase thin films fabricated by using precursor solutions involving Ti complexes. *Solar Energy Materials & Solar Cells*. **2008**, *92*, 1136–1144.
- [20] Tang, A.; Xiao, Y.; Ouyang, J.; et al. Preparation, photo-catalytic activity of cuprous oxide nano-crystallites with different sizes. *J. Alloys Compd*. **2008**, *457*, 447–451.

- [21] Gao, R.J.; Ding, T.; Duan, X.J. Kinetics Study on Photocatalytic Degradation of Methyl Orange Catalyzed by Sea Urchin-Like Cu₂O. *Journal of Material Science and Chemical Engineering*. **2016**, *4*, 35–40.
- [22] Dong, C.; Zhong, M.; Huang, T.; et al. Photodegradation of methyl orange under visible light by micro-nano hierarchical Cu₂O structure fabricated by hybrid laser processing and chemical dealloying. *ACS Appl. Mater. Interfaces*. **2011**, *3*, 4332–4338.

CHAPTER 3

Low Temperature Fabrication and Photocatalytic Activity of *p*-type Cu₂O Thin Films by Molecular Precursor Method

CHAPTER 3: Low Temperature Fabrication and Photocatalytic Activity of *p*-type Cu₂O Thin Films by Molecular Precursor Method

3.1. Introduction on *p*-type semiconductors

Cuprite also known as cuprous oxide has been a major ore of copper and is still mined in many places around the world. Among other copper ores, it provides the greatest yield of copper per molecule since there is only one oxygen atom to every two atoms of copper. The general crystal habits of Cu₂O includes the cube, octahedron, dodecahedron, and combinations of these forms [1]. Cuprous oxide poses a crystalline cubic structure with a lattice parameter of 4.2696 Å and a space group of Pn3m, forming an octahedral system. If oxygen atom is considered as the origin of the body centered cubic; bcc primitive cell, the four copper atoms are considered to be located in the diagonal position. The oxygen atoms are tetrahedrally coordinated by copper and the copper ones are linearly coordinated by the oxygen atoms. The bond distance between, Cu-O (a), O-O (b), and Cu-Cu (c) is 1.85, 3.68 and 3.02 Å, respectively creating a structure with a density of 6.10 g cm⁻³ and molar mass of 143.09 g mol⁻¹. While the concentration of copper and oxygen in the structure is 5.05×10 and 2.52×10 cm⁻³, respectively. The dichotomy characteristic of Cu₂O is explained by two (strong and light grey colors) identical interpenetration networks of Cu and O atoms inside the crystal lattice containing indirect chemical bond between them. The two types of atomic network are therefore only stable due to Van-der-Waal force [1, 2]. Figure 1 shows the crystal (a) and atomic (b) structures of the body centered cubic cell of Cu₂O material.

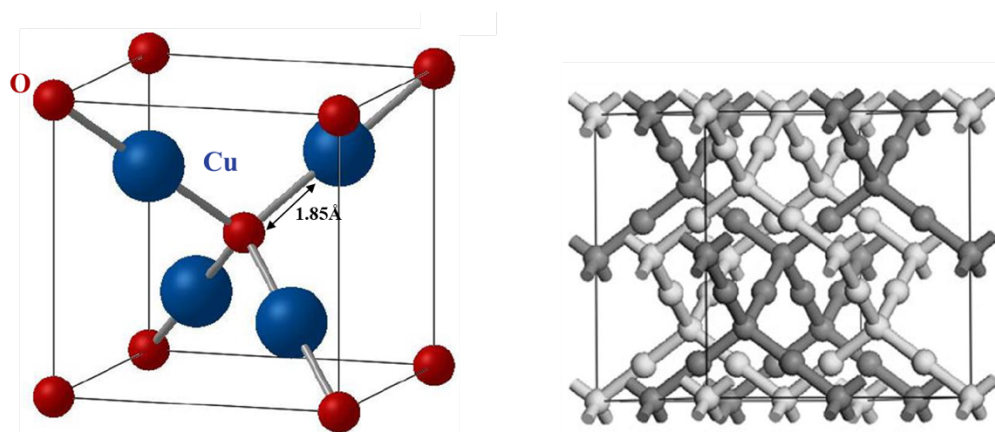


Figure 1. Crystallographic unit cell (a) and atomic (b) structures of the body centered cubic cell of Cu₂O [1, 2].

3.2. Properties and application of Cu₂O semiconductors

The applications of Cuprous oxide (Cu₂O) semiconductor are attributed to one of its important properties of narrow band gap. It is a promising semiconductor with a direct bandgap in the range of 1.91–2.3 eV [3–5]. It is used in solar energy conversion [6–9], as an electrode for lithium ion battery [10, 11], gas sensors [12] and photocatalytic degradation of organic pollutants and decomposition of water under visible light [13–15].

Over the last few decades, cuprous oxide (Cu₂O) nanoparticle powders have alarmingly emerged as one of the effective *p*-type semiconductors for photocatalytic degradation of Methyl Orange (MO) under visible light irradiation. The cuprous oxide nanoparticles with different nanosized structures and morphologies have been mostly prepared by a typical facile chemical synthesis. It has been used as a photocatalyst because of its several advantages that includes; firstly; it has low toxicity, inexpensive, good environmentally friendly, it is plentiful and readily available [3]. Secondly; the band gap of Cu₂O can be modified by factors such as particle size [16, 17]. Thirdly; it directly utilizes visible light as photocatalyst [18]. Fourthly; it has a powerful adsorption capacity for molecular O₂ which can harvest photoelectron to prevent the recombination of electrons and holes [15].

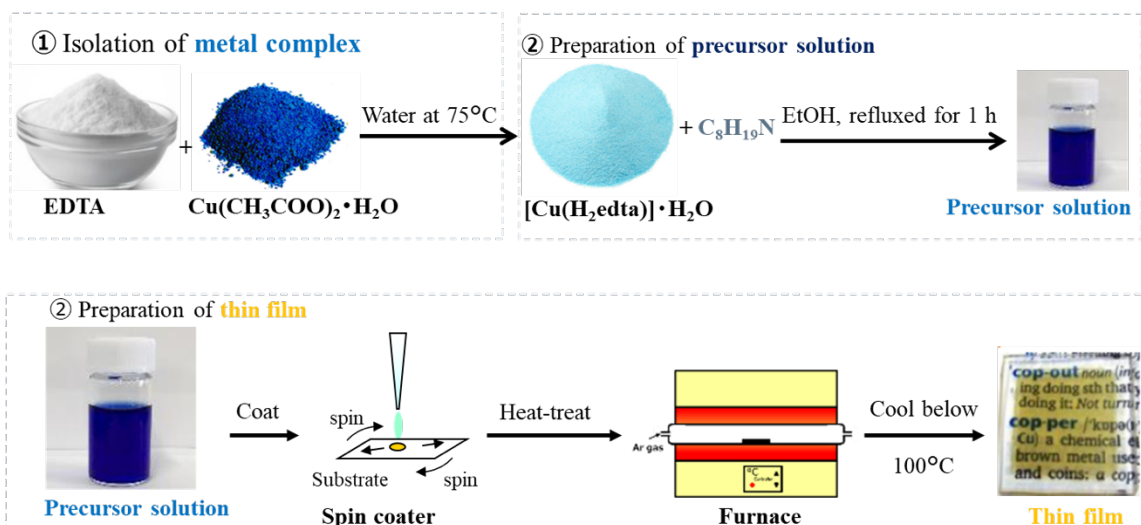
The visible light photocatalytic degradation of MO dye as model pollutant is one of the described applications of Cu₂O material that was tested under this study. Many researchers have already investigated photocatalytic properties and the optimization of experimental parameters including; type of Cu²⁺ reductants, synthetic temperature, type of copper salts as starting material, pH and reaction rate dependent of particle sizes and morphologies of Cu₂O nanoparticles. While Cu₂O nanoparticle prepared under good optimized conditions were found to exhibit high photocatalytic properties, these nanoparticles can be prepared by various methods such as liquid phase chemical synthesis [3, 19–22], electrodeposition method [23–26], chemical dealloying [27, 28], and irradiation process [29]. Even though single cubic Cu₂O nanoparticles can work as a photocatalyst on its own, the material can exude improved photocatalytic properties when doped with other materials. For example, Cu₂O nanocomposite of TiO₂ has found to have a better photocatalytic property toward methyl orange degradation than single phased Cu₂O, as coupling the Cu₂O and TiO₂ extend the absorption range to visible light region and promotes electron-hole pair separation [30–32].

3.3. Cu₂O thin films

Fabrication of a desired single phased CuO or Cu₂O is the key target in preparation of a copper oxide thin films. While the fabrication of a single phased copper oxide thin films can be challenging, few various fabrication methods had achieved it. However, Cu₂O thin films can be achieved by many deposition techniques, which includes; physical processes such as magnetic sputtering deposition [33, 34], pulse laser deposition [35]. As well as wet chemical processes such as; nebulizer spray technique [36], spray pyrolysis [37] and electrochemical deposition [38].

The molecular precursor method (MPM) is a wet process for thin film fabrication of various metal oxides and phosphate compounds, it is based on the design of metal complexes in coating solutions with many practical advantages such as excellent stability, homogeneity, miscibility, and coatability [39, 40]. Previously, an ethanol-based coating solution involving an isolated Cu(II) complex of ethylenediamine-*N, N, N', N'*-tetraacetic acid (EDTA) and dibutylamine was used to fabricate a *p*-type Cu₂O thin film with thickness of 50 nm *via* spin coating [41]. In our recent study, a precursor solution involving Cu(II) formate, propylamine and ethylenediamine dissolved in ethanol was used to also fabricate a *p*-type Cu₂O thin film with thickness of 90 nm, by ultraviolet (UV) irradiation and also *via* spin coating [42].

Volatile organic-solvent based precursor solutions are favorable for spin-coating method, because aqueous solutions are generally inadequate to spread onto various substrates due to high surface tension [40]. We have therefore developed the aqueous solutions useful to spray deposition in order to fabricate carbonate containing apatite films on Ti plate [43, 44]. The advantages of the spray coating method to deposit aqueous based precursor solutions on quartz glass substrate includes; it is simple and inexpensive instrumental set-up, reduced material loss and its adjustability for a large area deposition [45]. Figure 2 shows a schematic route of thin film fabrication by MPM [40].



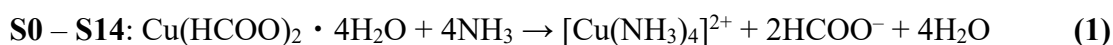
Scheme 1. Schematic route for the fabrication of Cu_2O thin films by MPM [48].

Under this study, the current chapter here report the *p*-type Cu_2O thin-film fabrication on a quartz glass substrate heated at 180°C in air directly by spraying aqueous precursor solutions, which were prepared by dissolving $\text{Cu}(\text{II})$ formate and ammonium formate, whose molar ratios to $\text{Cu}(\text{II})$ ion were 0, 2, 6 and 14, into aqueous ammonia solution. The photocatalytic discoloration of an aqueous solution involving MO as a model pollutant was evaluated at a neutral pH region by irradiating weak visible-light onto the *p*-type Cu_2O films immobilized on the quartz glass substrate. The electrical and optical properties of the resultant thin films were also evaluated and compared to those of Cu_2O films formed by other methods.

3.4. Preparations of $\text{Cu}(\text{II})$ in spray solution solutions with various ratio of HCOONH_4

Four spray solutions, **S0**, **S2**, **S6** and **S14** were prepared by adding different amounts of 28% NH_3 aqueous solution and HCOONH_4 into each aqueous solution involving 0.187 g (0.811 mmol) of $\text{Cu}(\text{HCOO})_2 \cdot 4\text{H}_2\text{O}$ in 25g of deionized water. The added amounts of 28% NH_3 aqueous solution and HCOONH_4 were as follows: **S0**; 28% NH_3 aqueous solution (1.775 g, 29.18 mmol), **S2**; 28% NH_3 aqueous solution (1.677 g, 27.57 mmol), and HCOONH_4 (0.108 g, 1.621 mmol), **S6**; 28% NH_3 aqueous solution (1.479 g, 24.23 mmol), and HCOONH_4 (0.323 g, 4.864 mmol), **S14**; 28% NH_3 aqueous solution (1.085 g, 17.84 mmol), and HCOONH_4 (0.753 g, 11.35 mmol). Each mixed solution was mechanically stirred for 1 h at room temperature. The obtained solutions, whose total concentration of Cu^{2+} was identical to 0.033 mmol g^{-1} , were used for spray-coating. The molar ratio of NH_3 to $\text{Cu}(\text{II})$ was adjusted to 36 in all solutions. The chemical reaction equation for the preparation of aqueous ammoniac spray

solutions; **S0**, **S2**, **S6** and **S14** containing Cu(II) formate and ammonium formate whose molar ratios to Cu(II) ion were 0, 2, 6 and 14, respectively is shown below:



3.5. Fabrication of Cu₂O thin films at 180°C in air by *via* spray coating

The experimental set up for spray coating in this present study was identical to those described in our previous study for Cu thin film deposition [45]. The spray coating procedures are as follows; an airbrush (Revolution HP-SAR; ANEST IWATA Co., Kanagawa, Japan) used as an atomizer of spray solution was vertically suspended adjacent to a hot plate. The pressure and solution inlets of the airbrush were connected to an air compressor set at 0.2 MPa and to a needle injected into the spray solution, respectively. A quartz glass substrate (20 × 20 × 1.6 mm³) was placed on the hot plate heated at 180°C. The distance between the tip of the atomizer and the substrate surface was adjusted to 30 cm. The substrate temperature was monitored by a chrome-alum type surface probe (A3-K-Q, TGK, Tokyo, Japan) fixed on top of the hot plate. Each 12 g of **S1**, **S2**, **S6**, and **S14** was independently sprayed onto the quartz glass substrate. Each solution was periodically sprayed for 5 s with a rate of 2.1 mL min⁻¹ at 20 s intervals. The obtained thin films are denoted as **F1**, **F2**, **F6**, and **F14**, respectively. Another thin film **F'2** was also obtained by spraying 16 g of **S'2** onto the quartz glass substrate under the identical conditions. Each eleven samples for each thin film were prepared by the identical procedures and used in the characterization.

3.6. UV-Vis absorption of spray solution

The absorption spectra of **S1**, **S2**, **S6**, and **S14** are shown in Figure 2. The maximum absorption position of a characteristic band in the visible region was observed at 610 and 605 nm for **S0** and **S2**, and at 604 nm for **S6**, and **S14**, respectively. The maximum absorption position of Cu(II) complex in spray solutions was observed to have a shifting pattern to a shorter wavelength with an increase ratio of ammonium formate to Cu²⁺ in aqueous spray solutions. This is due to the change in concentration of Cu(II) complex species in the respective aqueous spray solutions. The pH values of **S1**, **S2**, **S6**, and **S14** were 11.2, 10.6, 10.1, and 9.7, respectively, were also becoming more acidic with the increased ratio of ammonium formate. Table 1 shows the dependent of presence of Cu(II) complex species and pH on the added ratio of ammonium formate to Cu²⁺ in spray solutions.

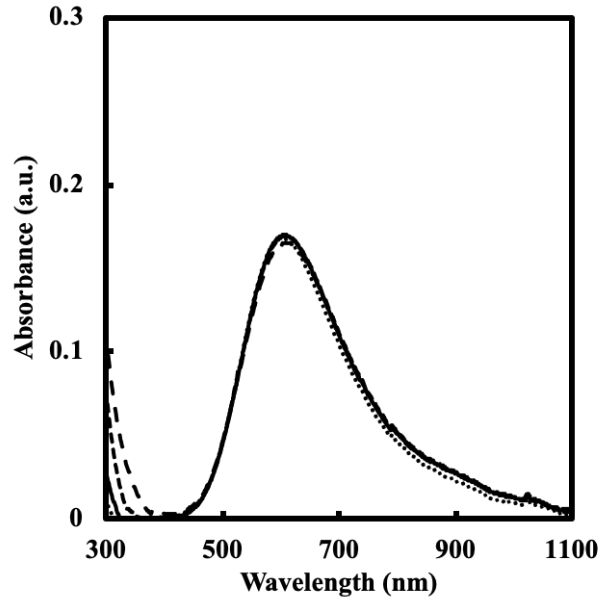


Figure 2. Absorption spectra of **S1**, **S2**, **S6**, and **S14** spray precursor solutions. The lines are labelled as; broken line: **S0**, long dotted line: **S2**, solid line: **S6**, and short dotted line: **S14**

3.7. Characterization of the fabricated thin films

The measurements techniques for the characterization of Cu_2O thin films are all explained in detail under the preceding chapter 2.

3.7.1. Crystal structure of the low temperature fabricated thin films

The XRD patterns of **F1**, **F2**, **F'2**, **F6**, and **F14**, are shown in figure 3 (a). Seven peaks found for all thin films at $2\theta = 29.7, 36.6, 42.5, 52.6, 61.6, 73.7$ and 77.4° are assignable to (110), (111), (200), (211), (220), (311) and (222) phases of cubic Cu_2O , respectively (ICDD card no. 01-071-3645). Only in the case of **F0**, six weak peaks were observed additionally at $2\theta = 32.5, 35.9, 38.8, 49.1, 66.3,$ and 68.0 which can be assigned to (110), (-111), (200), (-202), (310), and (220) phases of monoclinic CuO , respectively (ICDD card no. 01-080-1916). The average crystallite sizes of Cu_2O in the thin films are summarized in table 1.

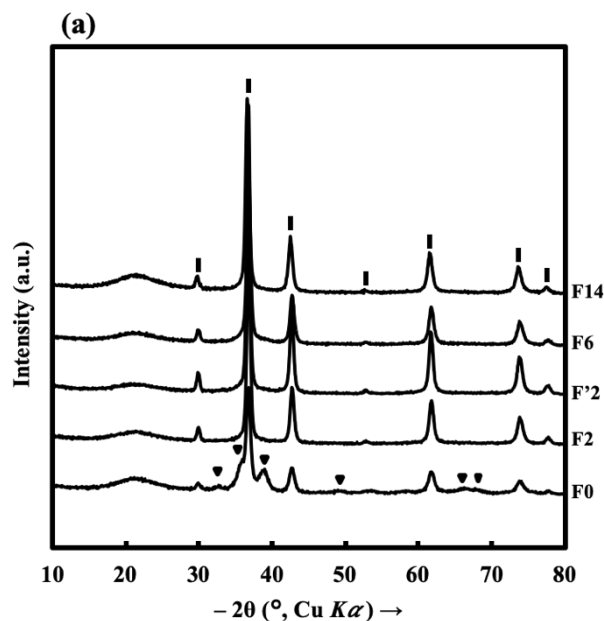


Figure 3. (a) XRD patterns of F1, F2, F'2, F6, and F14 via spray deposition of corresponding spray solutions onto quartz glass substrate at 180°C in air. The assignable peaks are denoted as follows; | : Cu₂O, ▼ : CuO.

Table 1. Crystallite sizes of F1, F2, F'2, F6, and F14 fabricated by spray deposition of corresponding spray solutions onto a quartz glass substrate at 180°C in air, respectively. The standard deviation is shown in parentheses.

Films	Crystallite size
	nm
F0	14.4(1)
F2	16.1(1)
F'2	16.9(1)
F6	17.1(1)
F14	16.6(1)

The XRD patterns of all thin films after discoloration test using MO solution under visible-light irradiation and in dark condition are presented in figure 3 (b) and 3 (c), respectively. In

the cases of **F0**, **F2**, and **F'2**, the patterns are all identical to those observed before the discoloration test. On the other hand, several small peaks appeared newly in the cases of **F6** and **F14** as follows: Four peaks at $2\theta = 32.2, 34.7, 38.2$ and 49.8° , which are assignable to (110), (-111), (200) and (-202) phases of monoclinic CuO respectively, appeared in the patterns after visible-light irradiation to **F6** and **F14**, and in those after keeping **F6** and **F14** in dark condition. In the pattern after keeping **F6** in dark condition, additional two peak at $2\theta = 66.5$ and 68.8° assignable to (310) and (-221) phases respectively of monoclinic CuO, were also observed. Further three small peaks at $2\theta = 13.2, 21.9$ and 26.6° , which can be assigned to (001), (110), and (002) phases respectively of triclinic $\text{Cu}(\text{OH})_2 \cdot \text{H}_2\text{O}$ (ICDD card no. 00-042-0638), appeared in the patterns after visible-light irradiation to **F6** and **F14** and in those after keeping **F14** in dark condition. While that at $2\theta = 17.2^\circ$, assignable to (020) phase of orthorhombic $\text{Cu}(\text{OH})_2$ (ICDD card no. 01-080-0656), appeared in the patterns after visible-light irradiation to **F6** and **F14** and in those after keeping **F14** in dark condition.

In figure 3 (d), the XRD patterns for **F6_x** and **F14_x** obtained after irradiating the identical visible-light in pure water. All the small peaks appeared in these patterns are good agreement with the abovementioned peaks assignable to the triclinic $\text{Cu}(\text{OH})_2 \cdot \text{H}_2\text{O}$ observed in the patterns after irradiating the visible-light onto **F6** and **F14** in the MO solution for discoloration test.

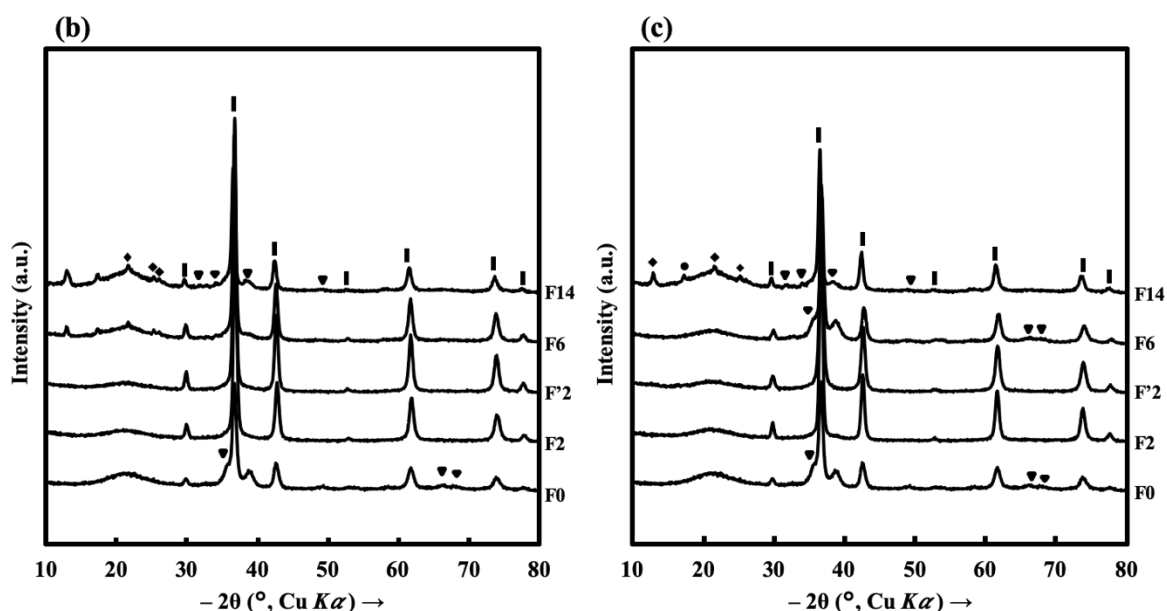


Figure 3. XRD patterns of **F1**, **F2**, **F'2**, **F6**, and **F14** after discoloration test of MO solution under (b) visible-light irradiation and (c) kept in dark condition. The assignable peaks are denoted as follows; | : Cu_2O , ▼ : CuO , ● : $\text{Cu}(\text{OH})_2 \cdot \text{H}_2\text{O}$, ◆ : unknown.

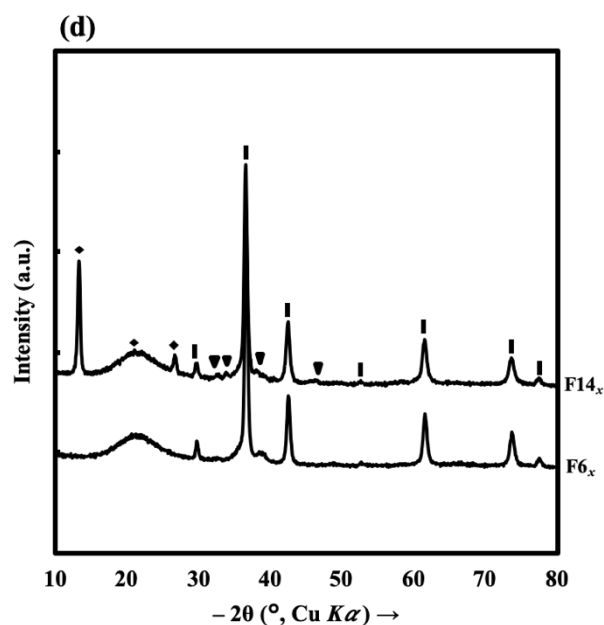


Figure 3. (d) XRD patterns after photodegradation test of **F6_x**, and **F14_x** using water solution under visible-light irradiation. The assignable peaks are denoted as follows; | : Cu₂O, ▼ : CuO, ● : Cu(OH)₂·H₂O, ◆ : unknown.

3.7.2 Morphologies and adhesion strength of the low temperature fabricated thin films

The surface morphology and cross-sectional images of **F1**, **F2**, **F'2**, **F6**, and **F14** are shown in figures 4. The spherical-shaped Cu₂O grains with different sizes agglomerate and distribute unevenly on the surface of each thin film as summarized in table 2. The thicknesses and critical load forces of the thin films on the quartz glass substrate are also shown in table 2. The adhesion strength of the resultant thin film decreased according to the increased amount of added ammonium formate into the spray solutions.

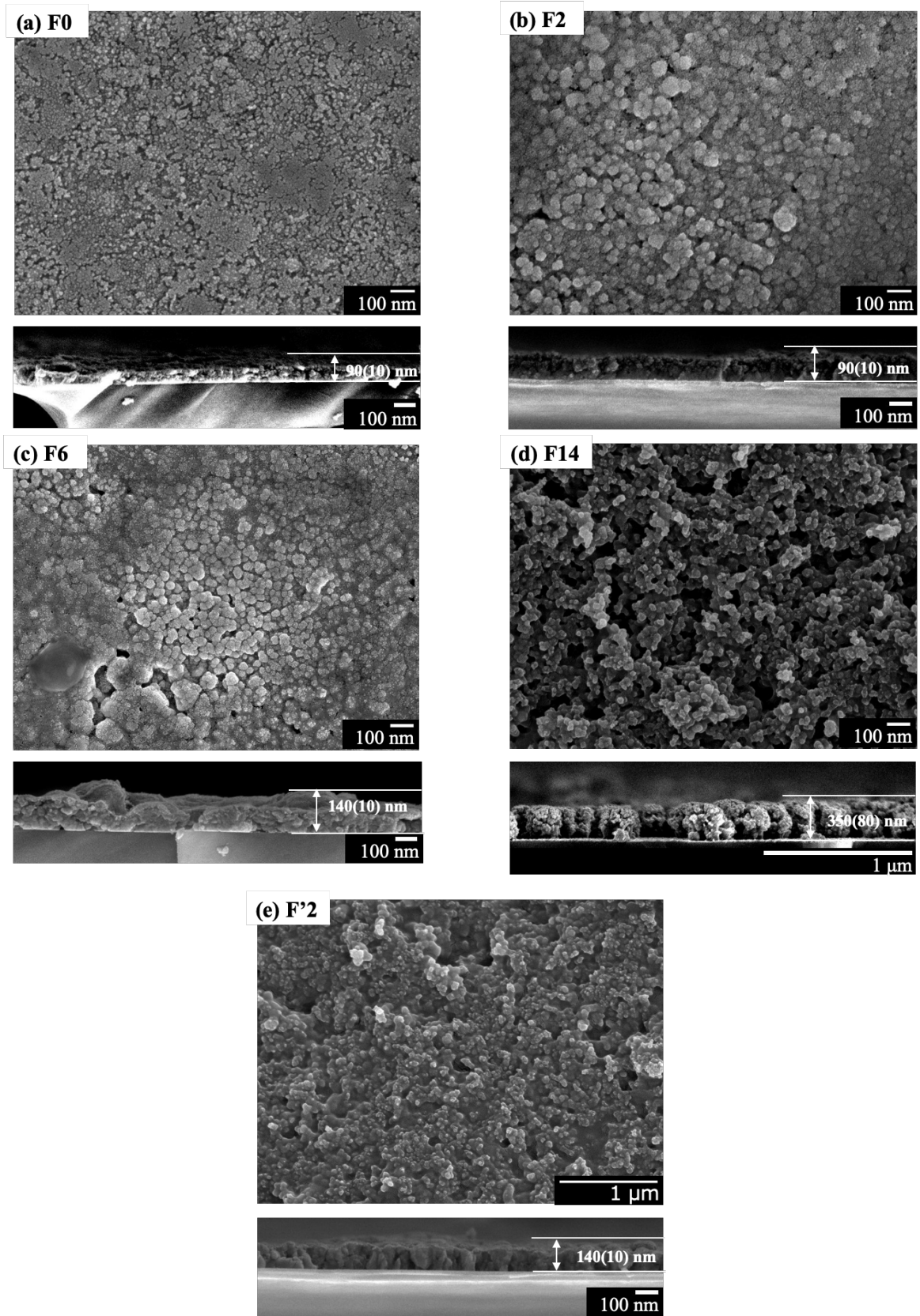


Figure 4. Surface morphologies and cross-sectional images of (a) F1, (b) F2, (c) F6, (d) F14, and (e) F'2 fabricated by deposition of corresponding spray solutions onto quartz glass substrate at 180°C in air.

Table 2. Film thickness, particle and crystallite sizes, and adhesion strength of **F0**, **F2**, **F'2**, **F6**, and **F14** fabricated by spray deposition of corresponding spray solutions onto a quartz glass substrate at 180°C in air, respectively. The standard deviations are shown in parentheses.

Films	Thickness nm	Particle size nm	Adhesion strength N
F0	90 ±10	40 ±20	8.7
F2	90 ±10	40 ±10	7.2
F'2	140 ±10	80 ±20	6.5
F6	140 ±20	80 ±20	6.7
F14	350 ±80	70 ±20	5.6

3.7.3. Electrical properties of the low temperature fabricated thin films

In table 3, the electrical properties and several fabrication conditions of **F0**, **F2**, **F'2**, **F6**, and **F14** are summarized, along with those of the Cu₂O films formed previously by other wet chemical processes. The carrier density of each thin film is all positive as indicated in table 3. Because the major charge carrier is positive, it was clarified that the resultant thin films are all *p*-type semiconductor. The carrier concentration of all thin films is in good agreement with those of previously fabricated films by the MPM [41, 42].

Table 3. Electrical properties of **F0**, **F2**, **F'2**, **F6**, and **F14** fabricated by spray deposition of corresponding spray solutions onto a quartz glass substrate pre-heated at 180°C in air, respectively. The standard deviation is shown in parentheses.

Films	Carrier mobility $\text{cm}^2 \text{v}^{-1} \text{s}^{-1}$	Carrier concentration cm^{-3}	Resistivity $\Omega \text{ cm}$
F0	0.64(1)	$5.84(1) \times 10^{16}$	240(50)
F2	0.70(1)	$2.80(3) \times 10^{17}$	40(4)
F'2	0.51(1)	$1.25(1) \times 10^{17}$	139(6)
F6	0.77(1)	$1.97(1) \times 10^{17}$	66(28)
F14	0.56(2)	$3.00(1) \times 10^{16}$	480(20)

3.7.4. Chemical composition of the low temperature fabricated thin films

Figure 5 shows the Auger spectra of **F0**, **F2**, **F'2**, **F6**, and **F14**. Broad peaks observed at 264 eV for carbon, 509 eV for oxygen, and 764, 835 and 914 eV for copper atoms in the wide scan spectra are in agreement with those of Cu_2O film previously fabricated at 350°C by MPM *via* spin coating [41]. The atomic ratio of Cu to O was determined to be 1.5 in all thin films, indicating the Cu atom deficiency.

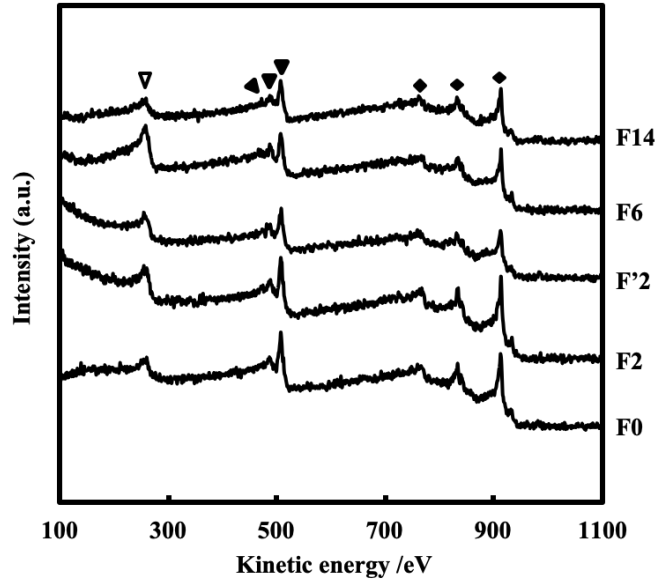


Figure 5. Auger spectra of **F0**, **F2**, **F'2**, **F6**, and **F14**. The peaks are denoted as follows; ∇ : C, \blacktriangledown : O, \blacklozenge : Cu.

3.7.5. Raman spectra of the low temperature fabricated thin films

Figure 6 shows the Raman spectra of **F0**, **F2**, **F'2**, **F6**, and **F14**. Only in the spectra of **F_C** and **F_D**, the shoulder peak corresponding to $2\Gamma_{12}$ photon vibration mode of O-deficient Cu_2O was observed at 148 cm^{-1} [46]. A strong peak corresponding to Γ_{15} photon vibrational mode of Cu_2O was observed at 217 cm^{-1} in the spectra of **F'2**, and **F6**, and at 219 cm^{-1} in those of **F2** and **F14**, respectively, which agree with the position at 218 cm^{-1} in several reports [46-49]. No peak assignable to this Γ_{15} mode was however observed in the spectrum of **F0**. The peaks assignable to $2\Gamma_{12} + \Gamma_{25}$ photon vibration mode of Cu_2O were observed at 293 cm^{-1} for **F0** and **F2** and at 291 cm^{-1} for **F6** and **F14**, respectively. These values are observed in low energy region from that at 295 cm^{-1} reported in a literature [50]. The corresponding peak to Γ_{15} photon vibration mode of Cu_2O were observed at 610 cm^{-1} for **F0** and **F2**, and at 615 , 622 and 624 cm^{-1} for **F'2**, **F6**, and **F14**, respectively. These positions are comparable to the reported values, around 615 cm^{-1} [29] and $620\text{--}624\text{ cm}^{-1}$ [49, 51, 52], respectively. The peaks observed at 145 , 204 , $325\text{--}327$ and 499 cm^{-1} in the spectra of all thin films corresponds to SiO_2 [49, 53, 54]. The presence of O-deficient Cu_2O which his observed 148 cm^{-1} in fabricated films is clearly shown in Figs. 7(a)–7(e) when the peaks around $145\text{--}148\text{ cm}^{-1}$ were separated and theoretically fitted assuming Gaussian distribution.

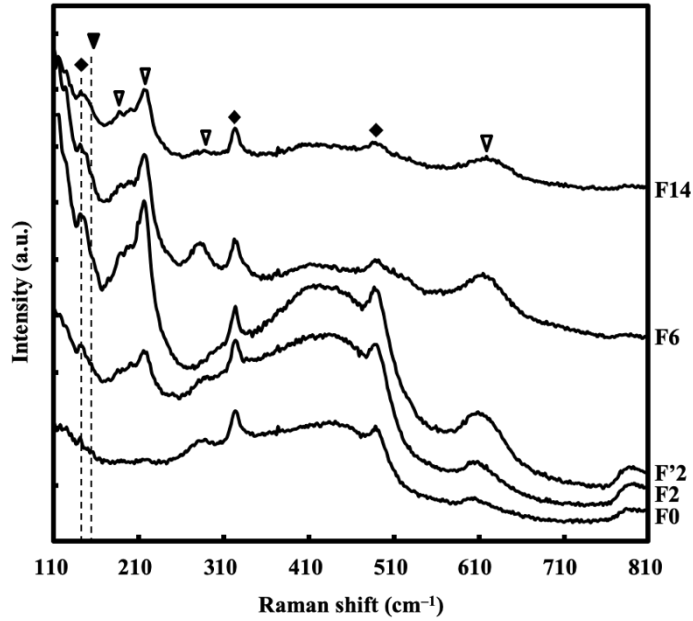


Figure 6. Raman spectra of F0, F2, F'2, F6, and F14 fabricated *via* spray deposition of corresponding spray solutions onto quartz glass substrate at 180°C in air, before photodegradation test. The peak is denoted as follow; ▼: Cu₂O with oxygen deficiency, ∇: other Cu₂O, and ◆: Si

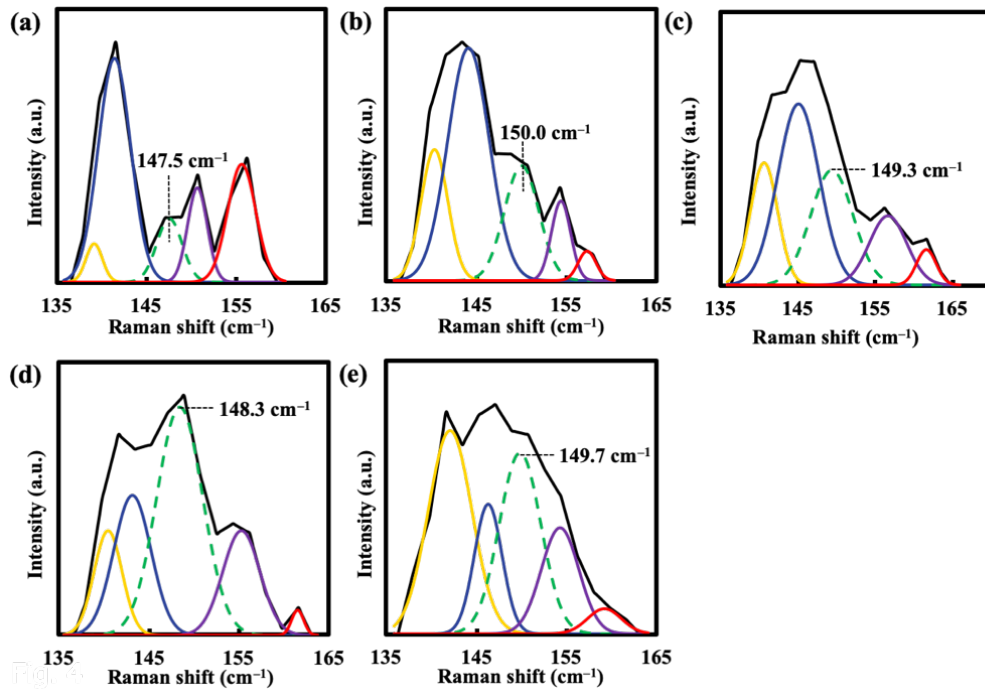


Figure 7. Separated O-defect site of Raman spectra of (a) F1, (b) F2, (c) F'2, (d) F6, and (e) F14. The peaks are labelled as; solid black line: original data of Raman peak (145 - 148 cm⁻¹), broken solid coloured lines: theoretically fitted curve by assuming Gaussian distribution

3.7.6. Optical and photocatalytic of the low temperature fabricated thin films

Figure 8(a) shows the transmittance spectra of **F0**, **F2**, **F'2**, **F6**, and **F14**, showing the characteristics of Cu_2O thin films in the visible and far infra-red regions [36]. The optical band gaps of **F0**, **F2**, **F'2**, **F6**, and **F14** shown in Figure 8(b) were determined as 2.41, 2.51, 2.50, 2.41 and 2.15 eV, respectively, assuming direct transition semiconductor.

The relationship between $\ln(C/C_0)$ and elapsed time t under visible-light irradiation and in dark condition are shown in Figs. 9(a) and 9(b), respectively. In the cases of **F0**, **F2**, and **F'2**, it was revealed that the time-dependence of MO concentration is quite small both under visible-light irradiation and in dark condition. It was contrarily clear that the MO concentration decrease efficiently in the cases of **F6** and **F14**.

In every case, the time-dependence of MO concentration can be approximated by the straight line, indicating that the discoloration reaction by the present Cu_2O thin films can be assumed to obey the pseudo-first-order kinetics. Based on the assumption, the discoloration rate constants of MO solution by **F0**, **F2**, **F'2**, **F6**, and **F14** under the visible-light irradiation are determined to be in the following order of 0.004, 0.004, 0.003, 0.042 and 0.087 min^{-1} , respectively. From the time-dependence of MO concentration in dark condition, the rate constant of MO adsorption onto the thin films and substrates could be also determined as 0.002, 0.002, 0.001, 0.002 and 0.056 min^{-1} , respectively for **F0**, **F2**, **F'2**, **F6**, and **F14**. It was thus revealed that only **F14** has the effective ability of MO adsorption.

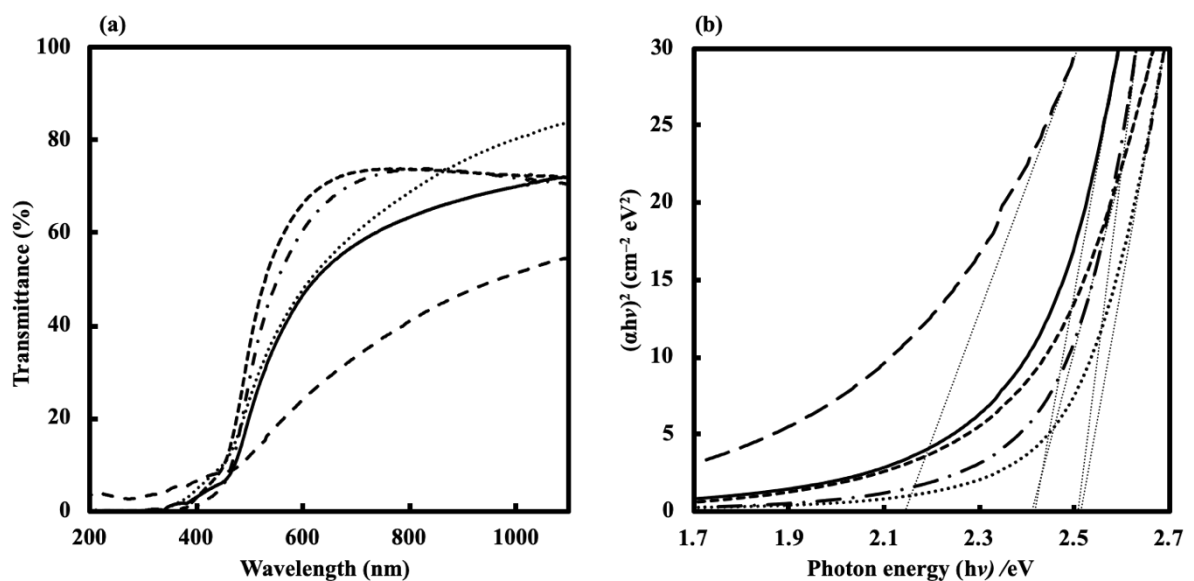


Figure 8. (a) Transmittance spectra of **F0**, **F2**, **F'2**, **F6**, and **F14** fabricated *via* spray deposition of **S0**, **S2**, **S6**, and **S14** onto quartz glass substrate at 180 °C in air. The lines are labelled as;

⋯: F0, - - -: F2, — —: F'2, —: F6, and - - -: F14. (b) The tauc plots of F0, F2, F'2, F6, and F14 fabricated *via* spray deposition of S0, S2, S6, and S14 onto quartz glass substrate at 180°C in air and determined as 2.41, 2.51, 2.50, 2.41 and 2.15 eV, respectively assuming direct transition semiconductor. The lines are labelled as; ⋯: F0, - - -: F2, — —: F'2, —: F6, and - - -: F14.

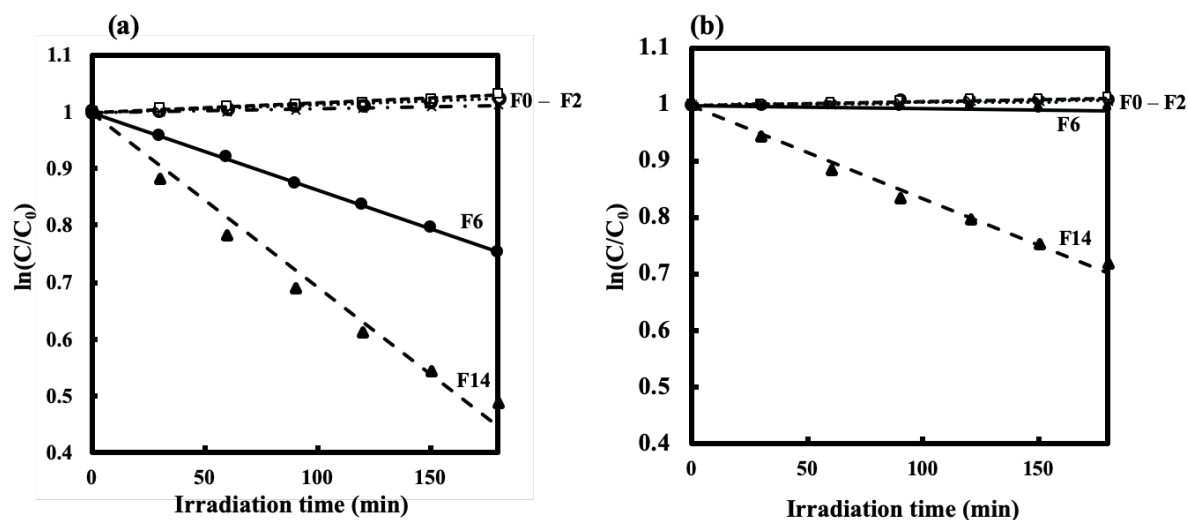


Figure 9. The relationship between $\ln(C/C_0)$ of methyl orange solution and elapsed time for discoloration test, under (a) visible light and (b) dark condition, where C_0 and C indicate the initial concentration of methyl orange and concentration after elapsed time (min). The approximated lines are labelled as follows; \circ : F0, \square : F2, \times : F'2, \bullet : F6 and \blacktriangle : F14.

The proposed reaction mechanism for discoloration of MO by Cu_2O is shown in Figure 10.

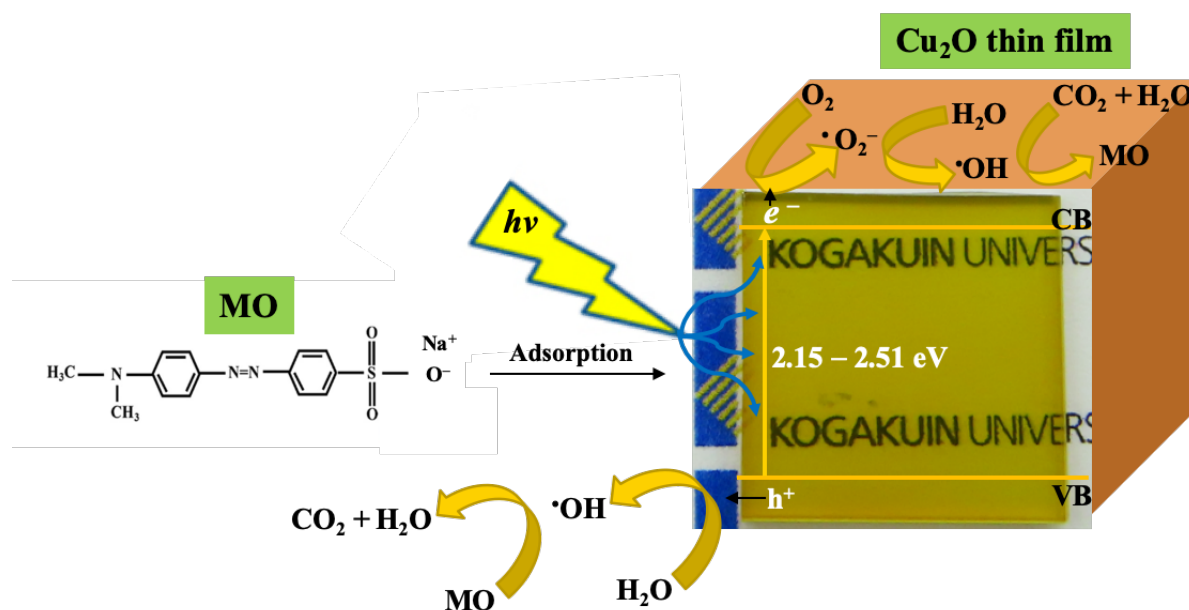


Figure 10. Schematic diagram of adsorption and photodegradation of Cu_2O thin film by MO.

3.8. Results and discussions

3.8.1. Spray precursor solutions

The spray solutions **S0**, **S2**, **S6** and **S14** of stable and blue color could be facily prepared by dissolving Cu(II) formate and ammonium formate into aqueous ammonia solution. The amount ratios of added ammonium formate to Cu(II) ion were adjusted to 0 and $2^n - 2$ ($n = 1-4$), in order to examine the effect of ammonium formate. In addition, the total amount of ammonia and ammonium ion in four spray solutions were regulated to be almost identical by controlling both the added ammonia solution and ammonium formate. Thus, the molar ratio of ammonia to Cu(II) was adjusted to a constant value of approximately 36, which is expected to be enough to form $[\text{Cu}(\text{NH}_3)_4]^{2+}$ ion in these solutions. As a result, the pH values of the solutions are in the range from 11.2 to 9.7.

Bjerrum *et al.* discussed the structure of the ammine complexes of Cu(II) on the basis of their visible absorption spectra using ligand field theory [54], and it is well known that the absorption peak position, at 590 nm, of $[\text{Cu}(\text{NH}_3)_4]^{2+}$ complex shifts to longer wavelength region by replacing NH_3 to H_2O or coordinating with ligands through oxygen atoms. The maximum absorption bands of the present spray solutions were observed in the wavelength range of 610 – 605 nm (Figure 2), and the shift depends on the pH value of each solution. These results suggest that the OH^- ions were incorporated into the originally formed $[\text{Cu}(\text{NH}_3)_4]^{2+}$ complexes, under a chemical equilibrium depending on the corresponding pH value.

3.8.2. Fabrication and purity of the low temperature fabricated thin films

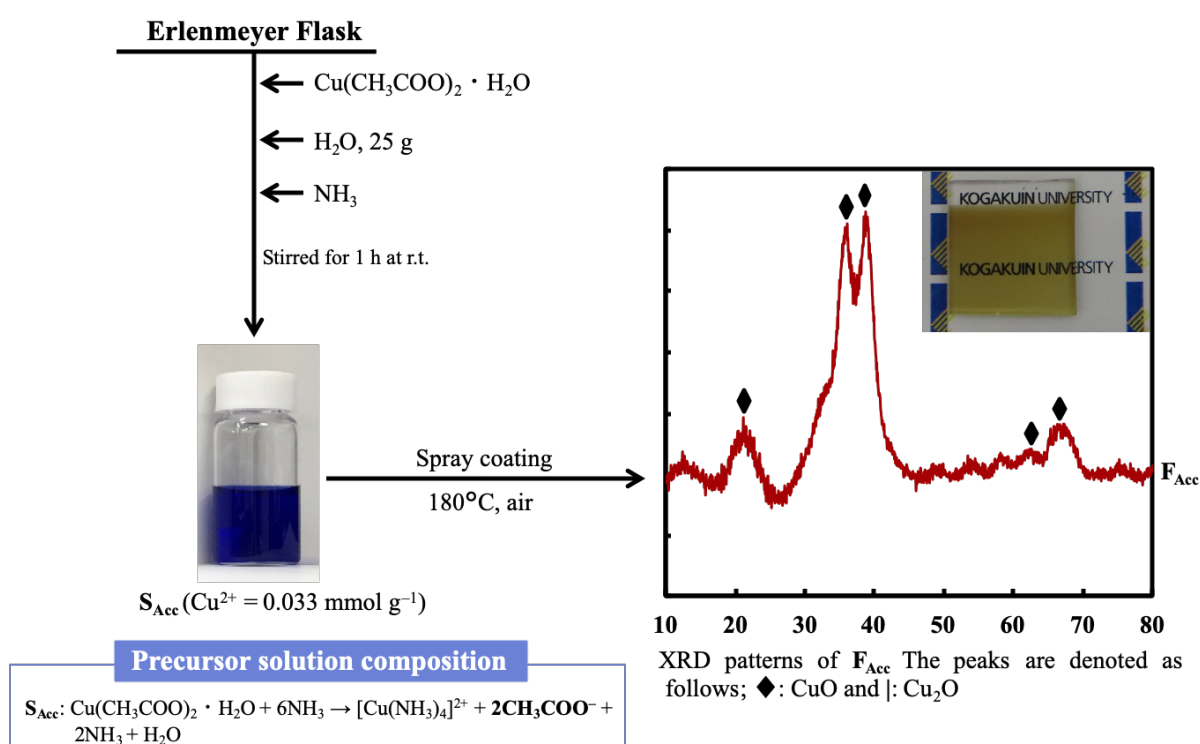
It is noteworthy that the Cu_2O thin films could be fabricated by spray coating of the present solutions onto the quartz glass substrate pre-heated at 180°C in air, with no further heat treatment (Figure 3(a)). It was furthermore indicated that the addition of ammonium formate into the spray solution is quite useful to obtain crystalline Cu_2O well-adhered on the substrate at low temperature, because the small amount of over-oxidized CuO was formed as a minor by-product only in the case of **F0** which was obtained by spraying **S0** with no added ammonium formate.

Rivera *et al.* fabricated a single phased Cu_2O by spray coating at 330°C using a solution involving Cu(II) nitrate, glucose as a reducing agent, and a deionized water/2-propanol mixture as the solvent. They reported that the intermediate Cu phase appears in the temperature range from 270 to 310°C due to insufficient thermal energy to promote the complete formation of crystalline Cu_2O [37]. However, there is no evidence of metallic Cu formation in the present study using ammonium formate as a reductant. In addition, the AES results show that the

carbon concentration in all thin films is less than 15 atomic% (Figure 5). The organic residues derived from formate ion could be thus removed during the spray onto the substrate preheated at 180°C in air. It is therefore supposed that the reduction of Cu(II) ion in the original complex to Cu(I) one occurred simultaneously with removal of excess amounts of ammonia and formate ion and then Cu-deficient Cu₂O crystallized, when the fine droplets of the precursor solution reach the substrate.

The formation of Cu(OH)₂·H₂O as a minor product was also observed when **F6** and **F14** were immersed in water both under visible-light irradiation and in dark condition. The XRD patterns for **F6_x** and **F14_x** obtained after irradiating the identical visible-light in pure water was also analyzed. All the small peaks appeared in these patterns are in good agreement with the abovementioned peaks assignable to the triclinic Cu(OH)₂·H₂O observed in the patterns after irradiating the visible-light onto **F6** and **F14** in the MO solution for discoloration test. It was thus revealed that a part of the obtained Cu₂O react with water molecules spontaneously under these conditions.

It is noteworthy that changing the type reductant from HCOONH₄ to acetate results in the formation of CuO thin film. Hence ammonium formate was very important as reductant for the formation of Cu₂O single phase. Scheme 3 shows the formation of CuO single phase using precursor solution prepared using copper acetate with no addition of HCOONH₄.



Scheme 2. Formation of single CuO thin film at 180°C in air

3.8.3. Crystal growth of Cu₂O, morphology and adhesion strength of thin films

The average particle sizes of Cu₂O in **F'2** and **F6** are approximately 2 times larger than those in **F0** and **F2**, and the increasing particle size is consistent to the increasing film thickness, as shown in Table 2. The gradual increase of crystallite sizes was also observed depending on the increased amount of added ammonium formate into spray solution, with the exception of **F14**. These results may be related to the heating-time difference in each spray procedure which requires the interval for temperature recovery to 180°C, even if the total amount of each solution was identical when the amounts of added ammonium formate were different. In fact, the needed time for temperature recovery prolonged by spraying the increased amount of the added ammonium formate into the solution. Thus, the primary and secondary crystals of produced Cu₂O were grown by the increased amount of the added ammonium formate into the spray solution.

In the case of **F14**, the film thickness is extraordinarily large and the abovementioned tendency on the particle and crystallite sizes cannot be observed (Table 2). It is important to note that the surface morphology of **F14** is also different from others and indicates a porous structure with many voids and surface roughness (Figure 4(e)). It can be concluded that the thin film structure of the crystalline Cu₂O in **F14** was strongly affected by large amount of evolved gases, which were produced by decomposition of 14 times molar amount of HCOONH₄ against Cu(II) ion, during spray onto the substrate which was pre-heated at 180°C. As a result, the film was fabricated so thick that the adhesion strength of the film became weak. From the view point of surface area, it is assumed that **F14** has the largest amongst the present thin films

3.8.4. Electrical and optical properties of Cu₂O thin films

As shown in Table 3, the electrical resistivity of **F0**, **F2**, **F'2**, **F6** and **F14** are lower than that formed at 300°C by Prabu *et al.* [36], and in the identical order of magnitude as that deposited at 340°C by Rivera *et al.* [37]. The carrier mobility and concentration of all thin films are in comparable range to those fabricated by the usual MPM with spin-coating procedure [42].

The optical bandgaps of **F0**, **F2**, **F'2**, **F6** and **F14** distribute from 2.5 to 2.2, though previously reported values of crystalline Cu₂O are in the range of 1.9–2.3 eV [3–5]. It is generally known that the bandgap becomes wider when a semiconductor is amorphous. As has been stated in the previous section, the required time for temperature recovery during spray

elongated depending on the increased amount of the added HCOONH_4 into the solution. Therefore, it is supposed that the bandgap of produced Cu_2O depends approximately on the crystallinity determined by the heating time at 180°C .

3.8.5. Application of Cu_2O thin films in photocatalytic degradation of MO under visible light

By the discoloration test of MO solution at neutral pH region, it was clarified that **F6** and **F14** show the high pseudo-first-order rate constant, 0.042 and 0.087 min^{-1} respectively, under visible-light irradiation (Figure 9(a)). Contrarily the photocatalytic activity of **F0**, **F2**, and **F'2** are negligibly small. It can be assumed that the film thickness is independent on the photocatalytic activity, because **F2** and **F'2** were formed by using an identical solution and the film thickness of **F'2** is identical to that of **F6**. Thus, the photocatalytic activity of the present Cu-deficient Cu_2O thin films can be attributed to the O-defect site, because the Raman spectra of only **F6** and **F14** indicate the presence of O-defect site at 148 cm^{-1} as the shoulder peak (Figure 6–7) [46]. The discoloration rate constant in dark condition is 0.056 min^{-1} under the presence of **F14**, though those in the cases of other four thin films are smaller than 0.002 min^{-1} . Therefore, it was indicated that only **F14** has an effective adsorption ability amongst these thin films. These results are consistent to the porous structure which is characteristics to only **F14**, as has been shown by the FE-SEM observation (Figure 4). In the case of **F14**, the deviations from the straight lines assuming the pseudo-first-order kinetics can be observed both under light irradiation and in dark condition (Figure 9). It is suggested that the deviations are owing to the strong adsorption ability of **F14**, because such deviations do not appear in the case of **F6**. From this point of view, it can be accepted that the rate constant evaluated by using **F6** demonstrates the net photo-degradation degree of MO in an aqueous solution at neutral pH region.

It is noteworthy that the thin films are not stable in aqueous MO solution (Figs. 2(b)–2(d) and pure water 2(c)) at neutral pH, as they were oxidized to CuO and some unknown crystal phases appeared in both cases.

3.9. Summary

The Cu_2O thin films could be facilely fabricated on a quartz glass plate at 180°C by spraying aqueous precursor solutions. The spray solutions were prepared by dissolving Cu(II) formate in co-presence of ammonium formate whose molar ratios against Cu(II) ion were 0, 2, 6, and 14 times in aqueous ammonia solution. It is noteworthy that this present procedure with simple

instrumentation needs no further heat-treatment of the sprayed thin films to obtain crystalline Cu_2O . In addition, these immobilized thin films whose adhesion strength to the quartz glass substrate was larger than 5.6 N, and this minimum value was observed for the thickest thin film of 350 nm in the case of the molar ratio at 14.

It is interesting that the photocatalytic activity of the obtained Cu_2O thin film depends on the amount of added ammonium formate into the spray solutions. The 6 times molar ratio of added ammonium formate against Cu(II) ion is a threshold to provide the photocatalytic activity to the resultant Cu -deficient Cu_2O thin films, whose chemical components were determined by AES. The O-defect site in the photocatalytic Cu_2O thin films was characterized by using Raman spectroscopy. In addition, FE-SEM of the thin films provided the important information on the morphology directly relevant to the adsorption ability. The optical and electrical properties of the thin films were also examined in detail. It was however clarified that these properties of the Cu_2O thin films are not significantly related to their photocatalytic activity.

The Cu_2O nanoparticles are widely studied to exhibit special property of adsorption, of which a high adsorption ability of the nanoparticle has led to their high photocatalytic activity [3–8]. It was clearly demonstrated by this present study that both the O-defect site and porous structure are important factors to fabricate a highly photocatalytic Cu_2O thin film having high adsorption ability. The immobilized Cu_2O thin films facilely fabricated at low temperature on the glass substrate can be used to remove organic pollutants as a convenient photocatalyst under visible light irradiation. Images of the Cu_2O thin films are shown in Figure 11.

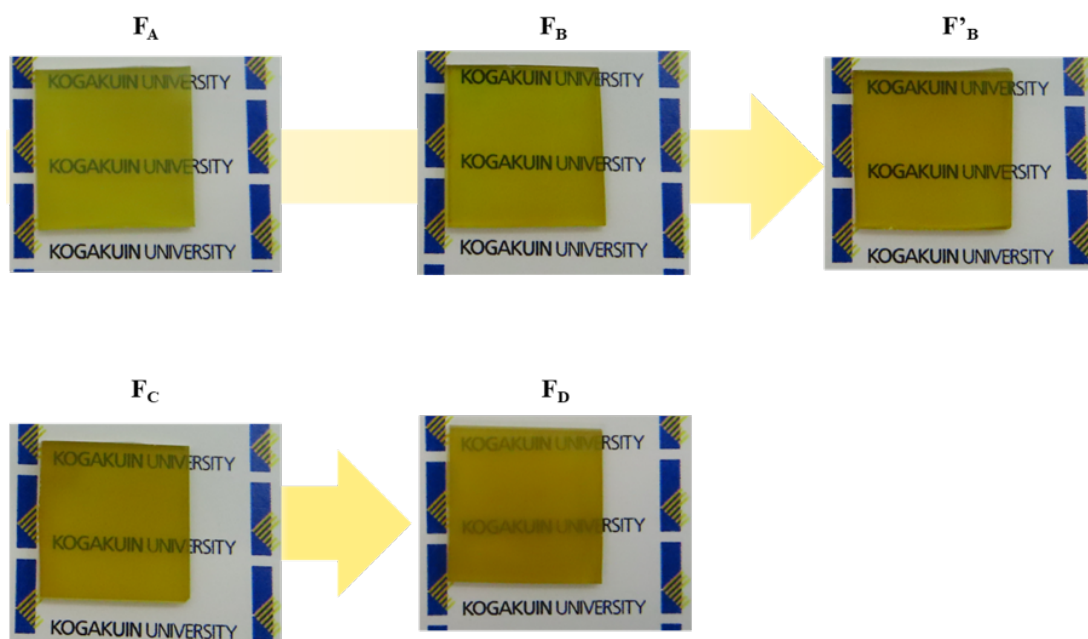


Figure 11. Images of the fabricated Cu_2O thin films.

References

- [1] Korzhavyi, P.A. Literature Review on the properties of cuprous oxide Cu_2O and the process of copper oxidation. Technical Report: SKB TR-11-08, 2011. ISSN 1404-0344.
- [2] Resende, J.A. Copper-based *p*-type semiconducting oxides : from material to device. Report, 2018. NNT 2017GREI072.
- [3] Huang, L.; Peng, F.; Yu, H.; et al. Preparation of cuprous oxides with different sizes and their behaviors of adsorption , visible-light driven photocatalysis and photocorrosion. *Solid State Sci.* **2009**, *11*, 129–138.
- [4] Hara, M. Cu_2O as a photocatalyst for overall water splitting under visible light irradiation. *Chem. Commun.* **1998**, *2*, 357–358.
- [5] Yang, Y.; Xu, D.; Wu, Q.; et al. $\text{Cu}_2\text{O}/\text{CuO}$ bilayered composite as a high-efficiency photocathode for photoelectrochemical hydrogen evolution reaction. *Sci. Rep.* **2016**, *6*, 1–13.
- [6] Katayama, J.; Ito, K.; Matsuoka, M.; et al. Performance of $\text{Cu}_2\text{O}/\text{ZnO}$ solar cell prepared by two-step electrodeposition. *J. Appl. Electrochem.* **2004**, *34*, 687–692.
- [7] Fernando, C.A.N.; Bandara, T.M.W.J.; Wethasingha, S.K. H_2 evolution from a photoelectrochemical cell with n- Cu_2O photoelectrode under visible light irradiation. *Sol. Energy Mater. Sol. Cells.* **2001**, *70*, 121–129.
- [8] Zhu, Q.; Zhang, Y.; Wang, J.; et al. Microwave Synthesis of Cuprous Oxide Micro-/Nanocrystals with Different Morphologies and Photocatalytic Activities. *J. Mater. Sci. Technol.* **2011**, *27*, 289–295.
- [9] Hung, B.L.; Tsung, C.; Huang, W.; et al. Room-temperature Formation of Hollow Cu_2O Nanoparticles. *Communication.* *0*, 1–17.
- [10] Hasan, M.; Chowdhury, T.; Rohan, J.F. Nanotubes of Core/Shell $\text{Cu}/\text{Cu}_2\text{O}$ as Anode Materials for Li-Ion Rechargeable Batteries. *J. Electrochem. Soc.* **2010**, *157*, A682–A688.
- [11] Chen, R.; Wang, Y.; Nuli, Y.; et al. Cu_2O nanowires as anode materials for Li-ion rechargeable batteries. *Sci. China Technol. Sci.* **2014**, *57*, 1073–1076.
- [12] Zhang, J.; Liu, J.; Peng, Q.; et al. Nearly Monodisperse Cu_2O and CuO Nanospheres: Preparation and Applications for Sensitive Gas Sensors . *Chem. Mater.* **2006**, *18*, 867–871.
- [13] Pan, L.; Kim, J.H.; Mayer, M.T.; et al. Boosting the performance of Cu_2O photocathodes

- for unassisted solar water splitting devices. *Nat. Catal.* **2018**, *1*, 412–420.
- [14] Paracchino, A.; Laporte, V.; Sivula, K.; et al. Highly active oxide photocathode for photoelectrochemical water reduction. *Nat. Mater.* **2011**, *10*, 456–461.
- [15] Xu, H.; Wang, W.; Zhu, W. Shape evolution and size-controllable synthesis of Cu₂O octahedra and their morphology-dependent photocatalytic properties. *J. Phys. Chem. B.* **2006**, *110*, 13829–13834.
- [16] Schä, P.; Van Der Veen, M.A.; Domke, K.F. Unraveling a two-step oxidation mechanism in electrochemical Cu-MOF synthesis. *Chem. Commun.* **2016**, 4722, 4722–4725.
- [17] Chang, Y.; Teo, J.J.; Zeng, H.C. Formation of colloidal CuO nanocrystallites and their spherical aggregation and reductive transformation to hollow Cu₂O nanospheres. *Langmuir.* **2005**, *21*, 1074–1079.
- [18] Feng, L.; Zhang, C.; Gao, G.; et al. Facile synthesis of hollow Cu₂O octahedral and spherical nanocrystals and their morphology-dependent photocatalytic properties. *Nanoscale Res. Lett.* **2012**, *7*, 1–10.
- [19] Wang, Y.; Huang, D.; Zhu, X.; et al. Surfactant-free synthesis of Cu₂O hollow spheres and their wavelength-dependent visible photocatalytic activities using LED lamps as cold light sources. *Nanoscale Research Letters.* **2014**, *9*, 36–38.
- [20] Gao, R.J.; Ding, T.; Duan, X.J. Kinetics Study on Photocatalytic Degradation of Methyl Orange Catalyzed by Sea Urchin-Like Cu₂O. *Journal of Material Science and Chemical Engineering.* **2016**, *4*, 35–40.
- [21] Sun, W.; Sun, W.; Zhuo, Y.; et al. Facile synthesis of Cu₂O nanocube/polycarbazole composites and their high visible-light photocatalytic properties. *J. Solid State Chem.* **2011**, *184*, 1638–1643.
- [22] Zhang, X.; Song, J.; Jiao, J.; et al. Preparation and photocatalytic activity of cuprous oxides. *Solid State Sci.* **2010**, *12*, 1215–1219.
- [23] Tang, A.; Xiao, Y.; Ouyang, J.; et al. Preparation, photo-catalytic activity of cuprous oxide nano-crystallites with different sizes. *J. Alloys Compd.* **2008**, *457*, 447–451.
- [24] Khattar, H.K.; Jouda, A.M.; Alsaady, F. Preparation of Cu₂O Nanoparticles as a Catalyst in Photocatalyst Activity Using a Simple Electrodeposition. *Nano Biomed Eng.* **2018**, *10*, 406–416.
- [25] Singh, D.P.; Singh, J.A.I.; Mishra, P.R.; et al. Synthesis , characterization and application of semiconducting oxide (Cu₂O and ZnO) nanostructures. *Bull. Mater. Sci.* **2008**, *31*, 319–325.

- [26] Saini, K.; Pandey, R.S. Concentration-dependent electrochemical synthesis of quantum dot and nanoparticles of copper and shape-dependent degradation of methyl orange. *Advanced Materials Letters*. **2017**, *8*, 1080–1088.
- [27] Dong, C.; Zhong, M.; Huang, T.; et al. Photodegradation of methyl orange under visible light by micro-nano hierarchical Cu₂O structure fabricated by hybrid laser processing and chemical dealloying. *ACS Appl. Mater. Interfaces*. **2011**, *3*, 4332–4338.
- [28] Dan, Z.; Yang, Y.; Qin, F.; Wang, H.; Chang, H. Facile Fabrication of Cu₂O Nanobelts in Ethanol on Nanoporous Cu and their Photodegradation of Methyl Orange. *Material*. **2018**, *11*, 1–14.
- [29] Xiangfeng; L.I.N.; Ruimin, Z.; Xiaohai, S.; et al. Cu₂O nanoparticles : Radiation synthesis , and photocatalytic activity. *Nuclear Science and Techniques*. **2010**, *21*, 146–151.
- [30] Zhang D. Synergetic effects of Cu₂O photocatalyst with titania and enhanced photoactivity under visible irradiation. *Acta Chimica Slovaca*. **2013**, *6*, 141–149.
- [31] Jaber, S.H. Synthesis of TiO₂ and Cu₂O nanoparticles and TiO₂/Cu₂O nanocomposite and study the ability to remove pollutants from aqueous solution. *Scientific Conference*. **2017**, *3*, 137-146.
- [32] Janczarek, M.; Kowalska E. On the Origin of Enhanced Photocatalytic Activity of Copper-Modified Titania in the Oxidative. *Catalyst*. **2017**, *7*, 1 – 26.
- [33] Hojabri, A.; Hajakbari, F.; Moazzen, M.; Kadkhodaei S. Effect of Thickness on Properties of Copper Thin Films Growth on Glass by DC Planar Magnetron Sputtering. *Sid.Ir*. **2012**, *2*, 107–112.
- [34] Mistry, S.; Cropper, M.; Valizadeh, R.; Jones, L.B.; Middleman, K.J.; Hannah, Milityn, B.L.; Noakes, T.C.Q. A comparison of surface properties of metallic thin film photocathodes. *IPAC 2016 - Proc. 7th Int. Part. Accel. Conf*. **2016**, 3691–3694.
- [35] Aadim, K.A.; Hussain, A.A.K.; Abdulameer, M.R. Effect of Laser Pulse Energy on the Optical Properties of Cu₂O Films by Pulsed Laser Deposition. *Acta Phys. Pol*. **2015**, *128*, 419–422.
- [36] Prabu, R.D. Studies on copper oxide thin films prepared by simple nebulizer spray technique. *J. Mater. Sci. Mater. Electron*. **2017**, *28*, 1–9.
- [37] Osorio-Rivera, D.; Torres-Delgado, G.; Márquez-Marín, J.; et al. Cuprous oxide thin films obtained by spray-pyrolysis technique. *J. Mater. Sci. Mater. Electron*. **2018**, *29*, 851–857.
- [38] Norziehana, N.; Isa, C. Electrodeposition and Characterization of Copper Coating on

- Stainless Steel Substrate from Alkaline Copper Solution Containing Ethylenediaminetetraacetate (EDTA). *J. Mech. Eng.* **2017**, *2*, 127–138.
- [39] Nagai, H.; Sato, M. Heat Treatment in Molecular Precursor Method for Fabricating Metal Oxide Thin Films. *Heat Treat. – Conv. Nov. Appl.* Intech 2012.
- [40] Nagai, H.; Sato, M. Molecular Precursor Method for Fabricating *p*-Type Cu₂O and Metallic Cu Thin Films. *Mod. Technol. Creat. Thin-film Syst. Coatings.* 2017.
- [41] Nagai, H.; Suzuki, T.; Hara, H.; et al. Chemical fabrication of *p*-type Cu₂O transparent thin film using molecular precursor method. *Mater. Chem. Phys.* **2012**, *137*, 252–257.
- [42] Wu, H.; Tomiyama, N.; Nagai, H.; et al. Fabrication of a *p*-type Cu₂O thin- film via UV-irradiation of a patternable molecular-precursor film containing Cu(II) complexes. *Journal of Crystal Growth.* **2019**, *509*, 112–117.
- [43] Mochizuki, C.; Hara, H.; Takano, I.; et al. Application of carbonated apatite coating on a Ti substrate by aqueous spray method. *Mater. Sci. Eng. C.* **2013**, *33*, 951–958.
- [44] Mochizuki, C.; Hara, H.; Oya, K.; et al. Behaviors of MC3T3-E1 cells on carbonated apatite films, with a characteristic network structure, fabricated on a titanium plate by aqueous spray coating. *Mater. Sci. Eng. C.* **2014**, *39*, 245–252.
- [45] Hishimone, P.; Nagai, H.; Morita, M.; et al. Highly-Conductive and Well-Adhered Cu Thin Film Fabricated on Quartz Glass by Heat Treatment of a Precursor Film Obtained Via Spray-Coating of an Aqueous Solution Involving Cu(II) Complexes. *Coatings.* **2018**, *8*(10), 1–10.
- [46] Singh, M.; Jampaiah, D.; Kandjani, A.E.; et al. Oxygen-deficient photostable Cu₂O for enhanced visible light photocatalytic activity. *Nanoscale.* **2018**, *10*, 6039–6050.
- [47] Deng, Y.; Handoko, A.D.; Du, Y.; et al. In Situ Raman Spectroscopy of Copper and Copper Oxide Surfaces during Electrochemical Oxygen Evolution Reaction: Identification of Cu(III) Oxides as Catalytically Active Species. *ACS Catal.* **2016**, *6*, 2473–2481.
- [48] Itoh, H.; Suzuki, Y.; Sekino, T.; et al. Electrospray deposition and characterization of Cu₂O thin films with ring-shaped 2-D network structure. *J. Ceram. Soc. Japan.* **2014**, *122*, 361–366.
- [49] Swarnkar, R.K.; Singh, S.C.; Gopal, R. Effect of aging on copper nanoparticles synthesized by pulsed laser ablation in water: Structural and optical characterizations. *Bull. Mater. Sci.* **2011**, *34*, 1363–1369.
- [50] Gong, Y.S.; Lee, C.; Yang, C.K. Atomic force microscopy and Raman spectroscopy studies on the oxidation of Cu thin films. *J. Appl. Phys.* **1995**, *77*, 5422–5425.

- [51] Devaraj, M.; Saravanan, R.; Deivasigamani, R.; et al. Fabrication of novel shape Cu and Cu/Cu₂O nanoparticles modified electrode for the determination of dopamine and paracetamol. *J. Mol. Liq.* **2016**, *221*, 930–941.
- [52] Kobayashi, T.; Hirajima, T.; Hiroi, Y.; et al. Determination of SiO₂ raman spectrum indicating the transformation from coesite to quartz in Gföhl migmatitic gneisses in the Moldanubian Zone, Czech Republic. *J. Mineral. Petrol. Sci.* **2008**, *103*, 105–111.
- [53] Krishnamurti, D. Raman T. the Spectrum of Quartz and. *Memoir; Raman Research Institute*, 1958, *108* 276–277.
- [54] Bejerrum, J.; Agarwala, B.V. Metal Amine Formation in Solution. XIX. On the Formation of Tetraamminedi- μ -hydroxodicopper(II) and Hydroxotetra-ammine Complexes in Ammoniacal Copper(II) Solutions. *Acta Chemica. Scandivanica A.* **1980**, *34*, 475–481.

CHAPTER 4

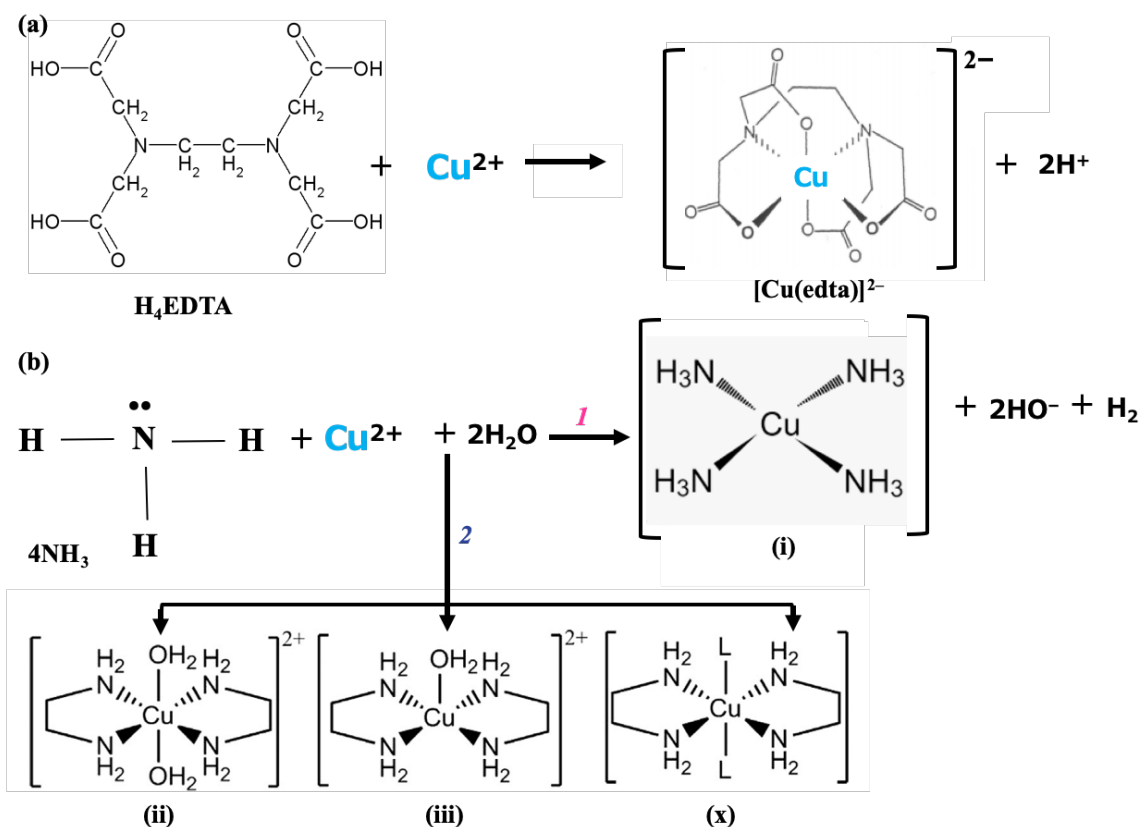
Preparation of aqueous Cu₂O precursor solution using electrochemical method

CHAPTER 4: Preparation of aqueous Cu₂O precursor solution using electrochemical method

4.1. INTRODUCTION

4.1.1. Introduction on copper(II) metal complexes

The coordination chemistry of ethylenediamine-*N, N, N', N'*-tetraacetic acid (EDTA) with Cu(II) ion has been widely studied and characterized. The structure and formation of Cu(II) complex of EDTA by chemical convention has also been extensively studied in previous reports including; reaction between acidic aqua solution of CuCl₂·2H₂O, HNO₃ and H₄edta [1], CuSO₄·5H₂O and Na₂H₂EDTA [2], CuSO₄, Na₂H₂EDTA and H₂SO₄ and/ NaOH [3], Cu(CH₃COO)₂, EDTA, ammonia and acetic acid [4]. The EDTA ligand is preferable to use because it is a powerful complexing agent with high affinity for many heavy metal ions including Cu²⁺ due to its abundant functional group (carboxyl and amino) [4], inexpensive compared to other chelates [5] and maintains long term stability of Cu ions in solution over wide range of pH [6]. There is a possibility that copper (II) ion forms four relatively strong complexes with NH₃ through coordination geometries of square-planar, square pyramidal, octahedral and octahedral with Jahn-Teller distorted structures [7]. Among other advantages such excellent stability and ionic dispersion in aqueous solution at room temperature, NH₃ ligand is preferable to use as ligand because it can easily link to Cu²⁺ ions due to its high formation stability constant of 12.5, in second to that of Cu-EDTA complex which is 18.1 [8]. As a result, when both ligands existed in one aqueous solution, Cu-EDTA is preferably formed than copper ammine complex. Figure 1 shows the metal ligand coordination structure of Cu²⁺ with EDTA (a) and NH₃ (b) ligands, respectively.



Scheme 1. Chemical structure of Cu(II) complexes of (a) EDTA and (b) NH_3 in different coordination geometry (i) square planar (ii) ionic (cis/trans) octahedral, (iii) ionic (cis/trans) square pyramidal, and (x) neutral (cis/trans) octahedral [9].

4.1.2. Fundamental principle of electrochemical process for the coating applications and preparation of metal complexes

Electrochemical process is mainly known for deposition or plating of various metals from their dissolved ions in solution by using applied potential energy. A thin and tightly adherent desired coating of metal oxide, or salt can be deposited onto the surface of conductive substrates by simple electrolysis of solution containing the desired metal ion or its chemical complex. The electroplating system consists of an electrolytic cell, electrodes, electrolyte and a power supply. The electrolyte contains dissolved metal ions forming electrolytic solution that serves as a conductive medium and complete the electrical circuit for electrochemical reactions known as electrolysis. In electrolysis process the metal electrodes such as copper plates are connected to external energy or current source and immersed into electrolytic solution.

When current flow through the electrolyte, the cations and anions are attracted to the cathode and anode, respectively. A charge transfer reaction occurs in the electrodes whereby anions lose their electrons to the anode and cations get the deficient electrons from the cathode.

Therefore, deposition occurs, creating a flow of electrons through external energy source and exchanging the atoms and charges by utilizing the energy from the external source. As replenishment for the deposited ions, the metal from the anode is dissolved and transferred into the solution to balance the ionic potential of the electrolyte. The amount of the metal deposited onto cathode is equal to those dissolved at the anode. The deposition area is easily controlled by the electrical resistance of cathode surface that determines the number of available electrons for deposition [10, 11]. The typical electrolysis requires both electrodes to be in the same electrolytic bath cell in order to achieve their plating. Figure 1(a) shows the schematic representation of copper electroplating *via* electrolysis of copper electrodes in a one electrolytic bath of copper sulphate [10] and Figure 1(b) indicates the electrochemical synthesis of solid Cu(II) complex of stearic acid in a one compartment cell.

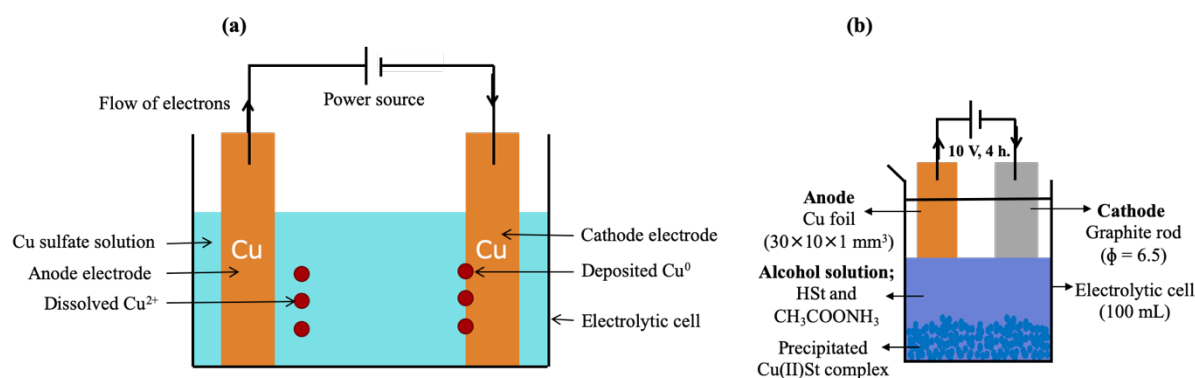


Figure 1. Schematic representation of (a) copper electroplating unit [10] and (b) electrochemical synthesis of Cu(II) complexes [25] in a one electrolytic compartment .

Electrolysis can deposit many materials including metals, metal alloys, conducting polymer and semiconductors [12], the process known as electrodeposition or plating. In thin film fabrication, the parameters of electrochemical deposition technique can be varied to control the morphologies such as; structure, size and shapes of the resultant material, thus presenting a simple, gentle and economical method for the preparation of large area film [13]. The method is widely used because it allows the precise control of film thickness in materials such as semiconductors whose properties and applications strongly depends on and its relatively inexpensive [14, 15]. Various Cu₂O thin films has been prepared by electrochemical deposition approach [13, 16, 17].

Beside electroplating, electrochemical process can also be used to synthesis metal complexes and salts, whose solid precipitates can suspend at the bottom of the electrolytic cell or dissolved in the electrolyte solution. Electrochemical technique is used in industrial and

laboratory scales to prepare Cu(II) complexes, [18, 19] and other metal complexes and salts, such as magnesium, [20], silver [21, 22], Zinc [23] and Vanadium [24], in various solvents. Previously, a Cu(II) salt was prepared using electrochemical technique based on the reaction between Cu^{2+} ions from the electrochemical oxidation of Cu anode with palm-based stearic acid [25, 26]. Electrochemical technique offers several advantages in inorganic synthesis of metal complexes and salts which includes: the ability to achieve oxidizing or reducing power that cannot be equaled by any ordinary chemical reagent, production of uncontaminated solution of metal complex salts, optimization of applied electrode potential to influence the selectivity of the reaction and allowing the preparation of many substances that cannot be prepared using conversional method [25, 27]. Much work has been done on processes involving electrochemical synthesis reactions of Cu(II) complexes of EDTA using solid Cu metal [28] and salts [29] as starting materials.

4.1.3. Electrochemical process for preparation of coating solution containing Cu(II) complexes in MPM

In our laboratory and research team, the preparation of coating solutions has been achieved by molecular precursor method only from metal complexes or salts prepared by chemical conversion method. MPM which is previously discussed in chapter 3, section 3.3 is an emerging chemical technique used for thin film fabrication of metal oxides and phosphate and it is based on the molecular design of metal complex in a solvent [30, 31]. The method produce exceptional quality coating solution and corresponding excellent precursor film due to its molecular design of Cu (II) complex in the solvent with high stability, homogeneity and miscibility, which can be used for various coating methods, hence becoming its boosting practical advantages, in contrast to conventional sol-gel method, mainly known for thin film processing *via* dip coating [31–34]. This wet chemical method has reported the fabrication of Cu_2O and Cu thin films using coating precursor solutions prepared from reaction of (1) $[\text{Cu}(\text{H}_2\text{edta})]\cdot 0.5\text{H}_2\text{O}$ with dibutylamine in ethanol [30], (2) dibutylamine salt of Cu(II) complex with EDTA mixed with copper formate in propylamine [35] and (3) $[\text{Cu}(\text{H}_2\text{edta})]\cdot \text{H}_2\text{O}$ in NH_4OH with copper formate in deionized water [36]. However, its only from a well-designed metal complexes in a stable coating solution this chemical method can achieve the fabrication of thin films of various metals and oxides with good properties that validates their various applications. Therefore, it is very important for the method to prepare an excellent coating solution. For copper thin film fabrication, MPM has previously utilized as two steps for the preparation of coating solution involving copper precursor. The first step is

the isolation of copper(II) complexes of EDTA and the second one is the dissolution of the isolated solid Cu(II) complex of EDTA in alcohol [30] or aqueous [36] solvent solutions. The $[\text{Cu}(\text{H}_2\text{edta})]\cdot\text{H}_2\text{O}$ salt used in MPM is usually prepared by reaction between EDTA, copper (II) acetate monohydrate and deionized water at 75°C [30]. The Cu(II) complexes of EDTA used in the previous studies were synthesized from Cu(II) salts as sources of Cu^{2+} ions.

However, Cu^{2+} ions can also be generated by electrochemical dissolution of metallic Cu anode. For example, as stated earlier Nordin *et al.*, reported the preparation of a Cu(II) salt from electrochemical oxidation of metallic Cu anode in $\text{CH}_2\text{COONH}_4$ with palm-based stearic acid [25] (Figure 1(b)) and oleic acid [26]. electrolytes. The electrosynthesis of Cu(II) complexes with ammonia ligand by electrochemical process involving oxidation of copper metal for application in MPM as coating solution is still not reported. In this chapter we attempted the novel synthetic route that provides a single step and direct preparation of the Cu(II) complex with ammonia ligand and ammonium counter ions in solution from metallic copper instead of Cu(II) salts. In order to prepare the aqueous precursor solution, two copper plates in an electrolytic solution involving HCOONH_4 and ammonia were used as reactive electrode. The precursor solution has a potential in application for fabrication of p-type Cu_2O thin films.

4.2. EXPERIMENTAL

4.2.1. Preparation of electrolytic solutions; ES

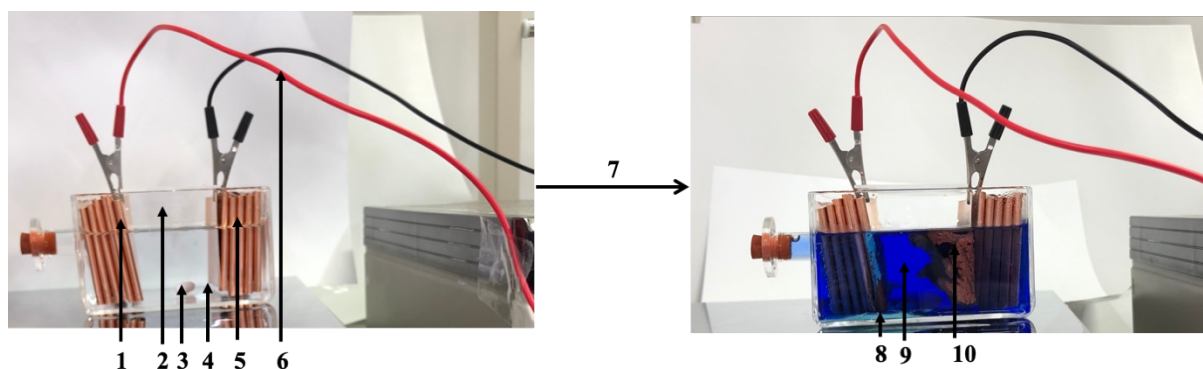
The aqueous solution of 28% NH_3 (4.321 g, 71.04 mmol) and HCOONH_4 (3.541 g, 56.16 mmol) were added into 300 g of deionized water. The mixed solution was mechanically stirred for 1 h at room temperature and used as the electrolytic solution. The pH of ES was measured using a pH meter (GST-2729C) (DKK-TOA Corporation).

4.2.2. Electrochemical preparation of precursor solution in a single electrolytic compartment

The schematic route for the electrochemical preparation of the aqueous precursor solution in a single cell electrolytic at ambient temperature compartment is shown in Scheme 2. The abovementioned electrolytic solution (300 mL) was separately transferred into a single electrolytic compartment. Two pre-weighted (123.4 g) sheets of Cu plates ($900 \times 37 \times 0.3$

mm³) as anode and cathode were separately immersed into the electrolytic solution contained in an electrolytic compartment. The closest plate-to-plate distance was adjusted to 50 mm. Various constant potential of 1, 5, 15 and 18 V and limited current of 2 A was applied to the Cu electrodes, from a constant-voltage and constant-current direct current (CVCC-DC) power supply (PMC18-2, Kikusui Co., Ltd, Tokyo, Japan). Electrolysis was performed for a period of 20–30 min at ambient temperature with mechanical stirring on a magnetic stirrer to obtain precursor solutions; **S**_{1v}, **S**_{5v}, **S**_{10v}, **S**_{15v}, and **S**_{18v}. The total concentration of Cu²⁺ complex in resulted precursor solution; **S**_{5v}, **S**_{10v}, **S**_{15v}, and **S**_{18v} were estimated as 0.0179, 0.0282, 0.0375 and 0.0329 mmol g⁻¹, respectively by the anode weight dissolution after electrolysis. The Cu²⁺ ion concentration in **S**_{5v}, **S**_{10v}, **S**_{15v}, and **S**_{18v} were determined by UV-Vis spectrophotometry as 0.0238, 0.0411, 0.0482 and 0.0398 mmol g⁻¹, respectively.

Each 1 mL of the electrolyzed solution was extracted from the electrolytic cell after every 10 min, for UV-Vis spectrophotometry analysis. Each resultant electrolyzed solution was filtered using microfilters (0.8 μm) and its pH was measured using a pH meter.



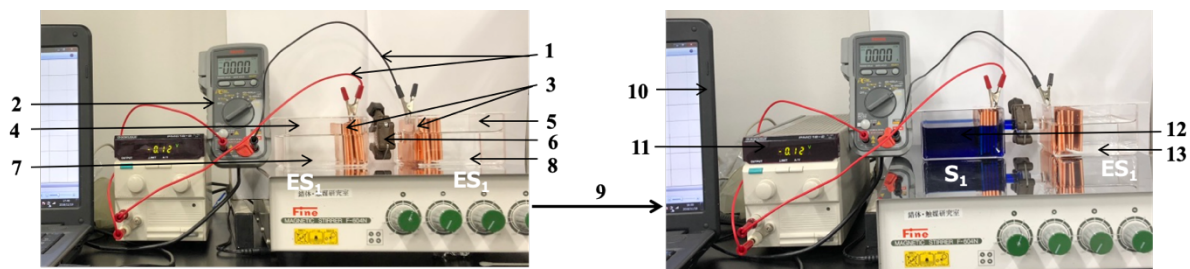
Scheme 2. Schematic representation for a simple **single** electrolytic compartment for preparation of, aqueous precursor solutions; **S**_{5v}, **S**_{10v}, **S**_{15v}, and **S**_{18v}. 1. Anode copper plate, 2. Electrolytic cell, 3. Magnet, 4. Electrolytic solution; **ES**₁ 5. Cathode copper plate, 6. Connecting wire, 7. Electrolysis process; 5, 10, 15 and 18 V, 20–30 min, r.t., 8. Precipitates, 9. Electrolyzed solution; **S**_{5v}, **S**_{10v}, **S**_{15v}, or **S**_{18v}, and 10. Electroplated Cu⁰.

4.2.3. Electrochemical preparation of Cu(II) complexes containing EDTA in a two electrolytic compartments

The schematic route for the electrochemical preparation of aqueous precursor solution in two electrolytic compartments at ambient temperature is shown in Scheme 3. The abovementioned electrolytic solution (300 mL) was separately transferred into each

compartment, linked together through the cellulose semipermeable membrane. Two pre-weighed (122.4 g) sheets of Cu plates ($900 \times 37 \times 0.3 \text{ mm}^3$) as anode and cathode were immersed separately into the electrolytic solution of each compartment. The closest plate-to-plate distance was adjusted to 70 mm across the cellulose membrane in the center of two compartments, which were covered individually with a $20 \times 20 \times 1.6 \text{ mm}^3$ quartz glass plate to prevent it from evaporation of electrolytic solution.

The constant potential of 18 V and limited current of 2 A was applied to the Cu electrodes, from an identical power supply as that used for a one electrolytic compartment. Electrolysis was performed for various period of 1, 2, 3 and 4 hours at ambient temperature with mechanical stirring on a magnetic stirrer to obtain precursor solutions; S_1 , S_2 , S_3 , and S_4 . The total concentration of Cu^{2+} complex in resulted precursor solution; S_1 , S_2 , S_3 , and S_4 were estimated as 0.0101, 0.0338, 0.0664, and 0.0800 mmol g^{-1} , by the anode weight dissolution after electrolysis. The Cu^{2+} ion concentration in S_1 , S_2 , S_3 , and S_4 were determined as 0.0109, 0.0350, 0.0656, and 0.0715 mmol g^{-1} by UV-Vis spectrophotometry. UV-Vis spectrophotometry analysis was done for each resultant aqueous precursor solution after their respective electrolysis.



Scheme 3. Schematic representation for a simple **two** electrolytic compartments for preparation of aqueous precursor solutions; S_{1h} , S_{2h} , S_{3h} , or S_{4h} . 1. Connecting wire, 2. Digital multimeter, 3. Cu plate anode and cathode electrodes, 4. Anode electrolytic cell, 5. Cathode electrolytic cell, 6. Semi-permeable cellulose membrane 7. Anolyte; ES_1 , 8. Catholyte; ES_1 , 9. Electrolysis process; 18 V, 1, 2, 3, and 4 h, r.t., 10. Computer, 11. Direct current supplier 12. Anolyte after electrolysis; S_{1h} , S_{2h} , S_{3h} , or S_{4h} , and 13. Catholyte after electrolysis; ES_1 .

4.2.4. Preparation of reference solutions; S_r

The reference solution; S_r was prepared by the reaction of copper formate (0.24 g, 1.05 mmol) and NH_3 (0.26 g, 4.20 mmol) in 10 g of deionized water at ambient temperature. The mixed blue solution was stirred using a magnetic stirrer for 1 h at room temperature, filtered through microfilters (0.8 μm) and used with no further modification. The total concentration

of Cu^{2+} in the obtained S_r was 0.1 mmol g^{-1} . The UV-Vis absorbance spectra of reference solution were used to determine the concentration of electrochemically prepared aqueous solution.

4.3. Results

4.3.1. UV-Vis spectra, pH and determination of concentration of Cu^{2+} in aqueous precursor solutions

4.3.1.1. One compartment electrolysis system

The concentration of Cu^{2+} in S_{5v} , S_{10v} , S_{15v} , and S_{18v} were determined from weight difference of anode and confirmed by UV-Vis spectrophotometry. The UV-Vis absorption spectra of reference and electrolyzed solutions containing Cu(II) complexes, was obtained at 10 minutes interval of electrolysis. The absorbance spectra evaluated the dependency of copper dissolution on electrolytic time as shown in Figure 2(a) along with these of reference solution. The reference solution was prepared in equivalent reagent amount of corresponding electrolytic solution in order to confirm the identity of Cu(II) complex contained in the electrolyzed solution by comparing their absorption peak position in the visible region. Both electrolyzed and reference solution absorption peak position were identified to be in close agreement. The dissolution of copper in electrolyte solution strongly depends on electrolytic time as indicated by the increasing absorbance intensity after every 10 min (Fig. 2(b)). The amount of dissolved Cu^{2+} in aqueous solution was also found to depend on applied voltage, as shown in Fig. 2(c). The pH of colorless electrolyte solution was different from that of dark blue resultant aqueous precursor solution. The pH and concentration of Cu^{2+} dissolved in aqueous precursor solutions contained in a one electrolytic compartment are shown in Table 1.

The identities and concentration of the electro-synthesized Cu(II) complexes were determined by the UV-Vis spectrophotometry. After electrolysis of ES in a single compartment system using various applied voltage of 5, 10, 15, and 18 V for 20–30min at r. t., the 10 min interval spectra of S_{5v} , S_{10v} , S_{15v} , and S_{18v} solutions containing Cu(II) complex species, forms a broad absorption band in the visible region of 601(0) nm (Figure 3(a)). In agreement to the absorbance of reference solution; S_r absorbed at the same position of the visible region.

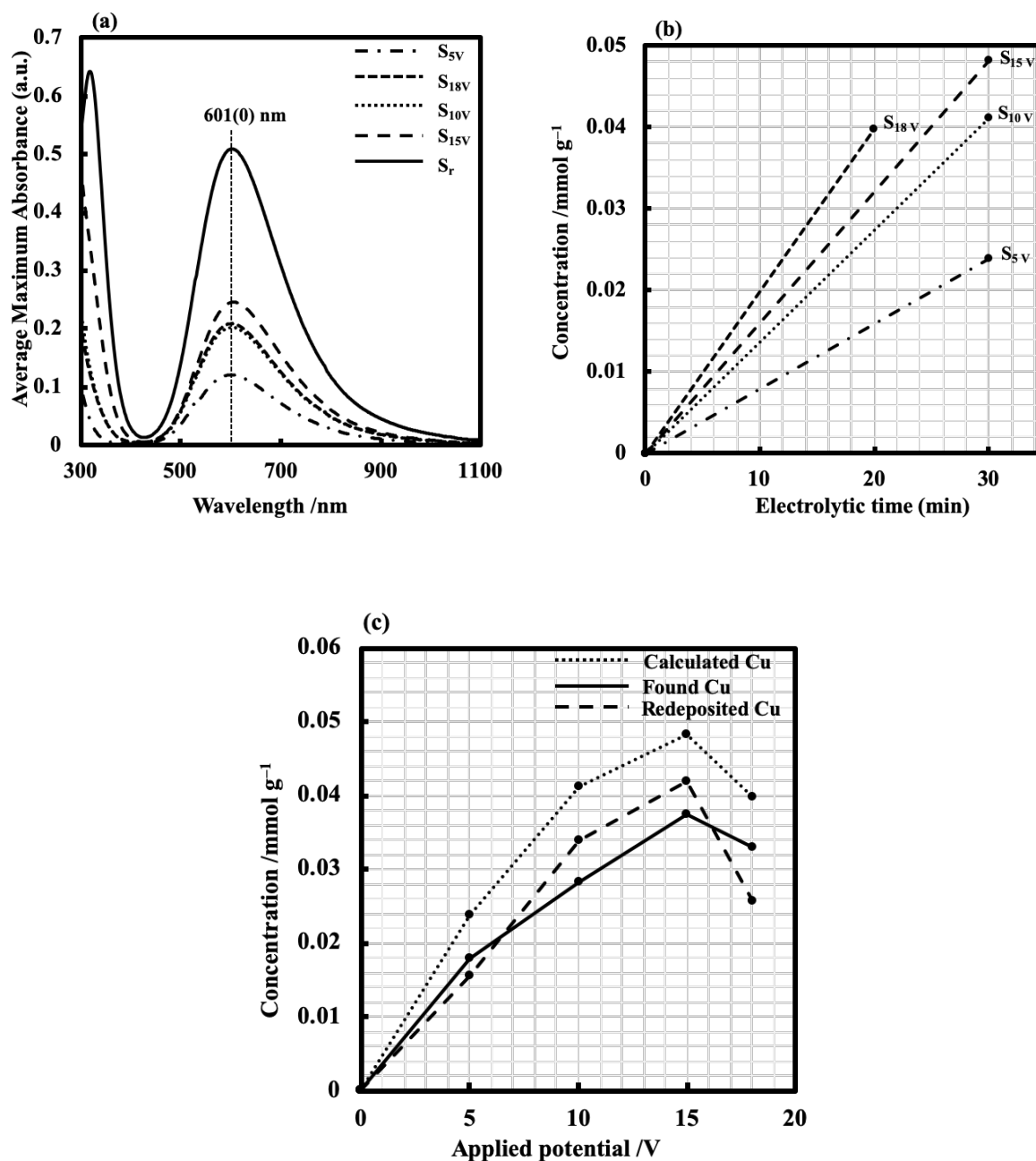


Figure 2. (a) UV-Vis absorption spectra and (b) rate of copper dissolution in S_{5v} , S_{10v} , S_{15v} , and S_{18v} electro-synthesized aqueous precursor solutions in a **one** electrolytic compartment using various applied voltage for 20–30 minutes at ambient temperature. (c) The dependency of dissolved Cu^{2+} on applied voltage for S_{5v} , S_{10v} , S_{15v} , and S_{18v} electro-synthesized aqueous precursor solutions in a **one** electrolytic compartment using various applied voltage for 20–30 minutes at ambient temperature.

Table 1. pH and resultant concentration of Cu^{2+} in in $\text{S}_{5\text{V}}$, $\text{S}_{10\text{V}}$, $\text{S}_{15\text{V}}$, and $\text{S}_{18\text{V}}$ electro-synthesized aqueous precursor solutions in a **one** electrolytic compartment using various applied voltage for 20–30 minutes at ambient temperature.

Precursor solutions	pH		Concentration of Cu /mmol g ⁻¹				Applied potential /V
	initial	final	*found			calculated	
			bulk Sol.	electrode	total		
$\text{S}_{5\text{V}}$	9.45	9.39	0.0179	0.0156	0.0335	0.0238	5
$\text{S}_{10\text{V}}$	9.45	9.31	0.0282	0.0339	0.0621	0.0411	10
$\text{S}_{15\text{V}}$	9.44	9.24	0.0375	0.0419	0.0794	0.0482	15
$\text{S}_{18\text{V}}$	9.45	9.15	0.0329	0.0257	0.0586	0.0398	18

*The found $[\text{Cu}^{2+}]$ was determined from the Cu plates anodic electrode mass difference and UV-Vis spectrophotometry calculated the $[\text{Cu}^{2+}]$ in $\text{S}_{5\text{V}}$, $\text{S}_{10\text{V}}$, $\text{S}_{15\text{V}}$, and $\text{S}_{18\text{V}}$.

4.3.1.2 Two compartments electrolysis system.

The identities and concentration of the electro synthesized Cu(II) complexes in S_1 , S_2 , S_3 , and S_4 were also determined by the UV-Vis spectrophotometry. The absorbance spectra of S_1 , S_2 , S_3 , and S_4 along with these of reference solution; S_r are shown in Figure 3. The S_r used for resultant precursor solution by both electrolysis systems was identical and its absorbance spectra was in close agreement to these of S_1 , S_2 , S_3 , and S_4 along the visible region. The dependency of amount of Cu^{2+} dissolved in aqueous solutions contained in an anode cell of a two electrolytic compartment is summarized in Table 2.

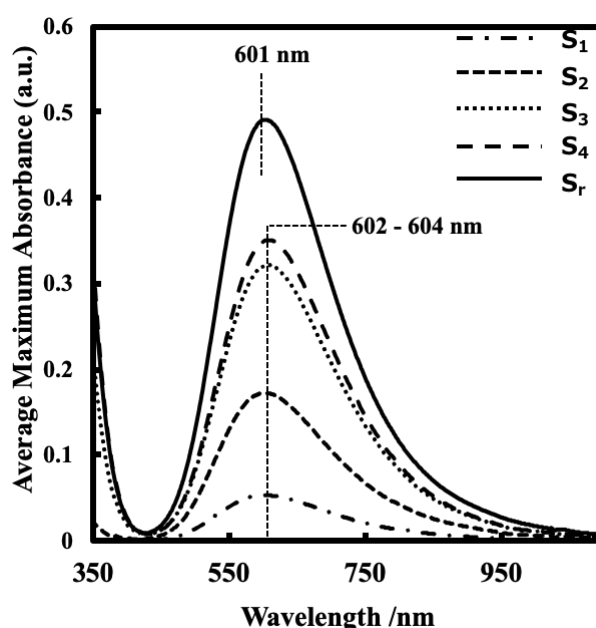


Figure 3. UV-Vis absorption spectra of **S₁**, **S₂**, **S₃**, and **S₄** electro-synthesized aqueous precursor solutions in a **two** electrolytic compartment using 18 V for various electrolytic time at ambient temperature.

Various electrolytic time of 1, 2, 3, and 4 hours were in an attempt to electro-synthesize the aqueous precursor solution in a two-cell electrolytic compartment using ES as that used for a one cell electrolysis system. Unlike for a one cell system the resultant dark blue aqueous precursor solutions; **S₁**, **S₂**, **S₃**, and **S₄** with different pH from those of their initial respective colorless ES, were only obtained in anode cell. The cathode cell retained identical ES with identical initial and final pH. The pH of the ES and **S₁**, **S₂**, **S₃**, and **S₄** precursor solutions are shown in Table 2.

Table 2. pH and resultant concentration of Cu²⁺ in **S₁**, **S₂**, **S₃**, and **S₄** electro-synthesized aqueous precursor solutions in a **two** electrolytic compartment using 18 V for various electrolytic time at ambient temperature.

Precursor solutions	Electrolytic time	pH		Mass of dissolved electrode Cu /g				*[Cu ²⁺] /mmol g ⁻¹	
		initial	final	Anode		Cathode		found	calculated
				initial	final	initial	final		
S₁	1	9.42	9.33	118.1	116.9	115.6	115.6	0.0101	0.0109
S₂	2	9.45	9.37	120.3	119.6	122.1	122.1	0.0338	0.0350
S₃	3	9.42	9.29	118.1	116.9	115.6	115.6	0.0664	0.0656
S₄	4	9.45	9.19	121.8	120.3	122.1	122.1	0.0800	0.0715

*The found [Cu²⁺] was determined from the Cu plates anodic electrode mass difference and UV-Vis spectrophotometry calculated the [Cu²⁺] in **S₁**, **S₂**, **S₃**, and **S₄**.

4.4. Discussion

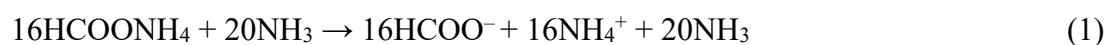
4.4.1. Aqueous solutions of Cu²⁺ complex involving NH₃ and HCOO⁻ counter ions

4.4.1.1. One compartment electrolysis system

A one electrolytic compartment (Scheme 1) involving Cu plate electrodes in the same cell, was initial attempted for the electro-synthesis of Cu²⁺ complex in aqueous electrolyte. The compartment lacks separation of electrolyte by cellulose semipermeable membrane. However, contains identical electrolyte bath, experimental design and conditions as these of two electrolytic compartments. The system was associated with precipitation of copper hydroxide and heavy cathode plating in the electrolyte bath and cathode electrode, respectively. The reaction mechanism for the formation of Cu(II) complexes in aqueous solution by a one

electrolytic compartment system is described below:

Anolyte/catholyte before electrolysis; ES



Anode:



Net anode:



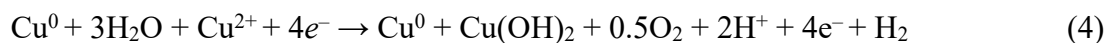
Cathode:



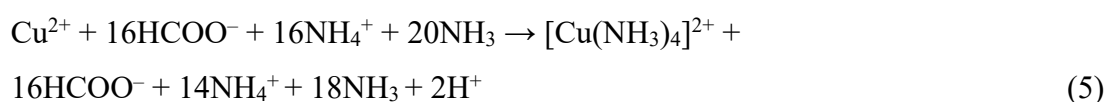
Net cathode:



Net electrodes reaction:



Bulk solution reaction



The electrolytic compartment system for the electro-synthesis of Cu(II) complex was previously described by Nordin *et al.* [25], who discusses the identical redox electrode reactions in an exemption of reduction reaction of Cu^{2+} at cathode electrode. The above electrode reactions are also discussed in several electrochemical studies associated with copper anode dissolution in aqueous electrolytes, these studies includes; (i) electro-winning of copper powder from copper sulphate solution in presences of glycerol and sulfuric acid using copper anode and gold electrode [29], (ii) electrodeposition of copper powder from copper sulphate solution in presence of glycerol and sulfuric acid using copper plates as both electrodes, which involves the dissolution of anode Cu electrode in electrolyte solution that does not include copper sulphate [37], (iii) dissolution of copper electrode in sulfuric acid at polarization by industrial alternating current [28].

4.4.1.2. Two-compartment electrolysis system

A precursor solution involving Cu^{2+} complex of NH_3 and HCOO^- counter ion was achieved via electrolysis process incorporating a two-compartment system (Scheme 2). Based on the electrolytic solution color changes from colorless to blue in anode cell of the two-cell electrolysis system, it indicates the ionic coordination of NH_4^+ to Cu^{2+} in presence of HCOO^- counter ions. According to the UV-Vis spectrum of **S₁**, **S₂**, **S₃**, and **S₄**, the maximum absorbance of Cu^{2+} complex at ca. 601–604 nm implies the formation of preferable $[\text{Cu}(\text{NH}_3)_4]^{2+}$ complex with HCOO^- counter ions, which is also confirmed by its presence in **S_r** that is absorbed in the near position (601 nm), within the visible region of the spectrum. The mass change of anode was therefore used to determine the concentration of Cu^{2+} in **S₁**, **S₂**, **S₃**, and **S₄** aqueous precursor solution to be 0.0101, 0.0338, 0.0664, and 0.0800 mmol g^{-1} (Table 2). Each concentration could be facily calculated by using the mass decrease of the electrolyzed anode because no mass change of cathode occurred before and after electrolysis with the two-compartment apparatus. The electro-synthesized $[\text{Cu}(\text{NH}_3)_4]^{2+}$ complex in **S₁**, **S₂**, **S₃**, and **S₄** and **S_r** aqueous precursor solutions is comparable to that of already prepared complexes with peak position between 600–640 nm, as described in literature [38, 39, 40]. The shift of the peak to a shorter wavelength in electro-synthesized $[\text{Cu}(\text{NH}_3)_4]^{2+}$ complex under this study could be due to presences of excess HCOO^- counter ions whose molar ration to copper was 1/16.

The reaction mechanism for the electro-synthesized $[\text{Cu}(\text{NH}_3)_4]^{2+}$ with HCOO^- counter ions in aqueous precursor solution; **S₁**, **S₂**, **S₃**, and **S₄** is described by the reaction equations below. Before electrolysis, the composition of electrolyte bath in both electrodes cells is identical to that used in a one electrolytic compartment as shown by equation 1. During electrolysis the oxidation of Cu^0 to Cu^{2+} at anode occurs simultaneously with hydrogen evolution reaction *via* H_2O splitting at cathode's electrode surface. The net electrode reaction is described in equation 4. The Cu^{2+} ions originally from oxidation of anode Cu reacts with NH_3 in presences of HCOO^- counter ions to form $[\text{Cu}(\text{NH}_3)_4]^{2+}$. A shown in Scheme 1 cathode copper plate electrode remained undissolved in cathode electrode cell after electrolysis, due to semi-permeable cellulose membrane between the electrode cells. The small sized (0.8 diameter) porous membrane kept the two-electrolyte bath separated and unmixed which also prevented the migration of Cu^{2+} across the two electrolytic cells. The reaction mechanism for the formation of Cu(II) in a two electrolytic compartments is shown below:

Anode:



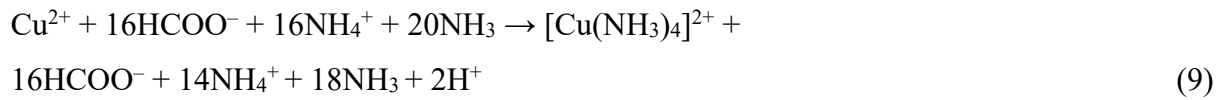
Cathode:



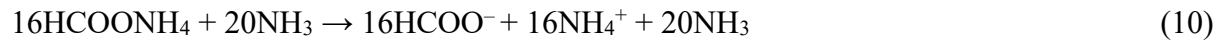
Net electrode reactions:



Anode solution reaction:



Cathode solution reaction:



4.5. Summary

An aqueous precursor solution was directly prepared from Cu plates as a source of Cu^{2+} ion in an electrolytic solution involving ammonia and HCOONH_4 . A novel apparatus with two compartments separated by a semi-permeable cellulose membrane was contrived to efficiently obtain the aqueous precursor solution. It can be concluded that a useful precursor solution for spray-coating to fabricate Cu_2O single-phase thin film was obtained after the solution was electrolyzed for 2 h at an applied voltage of 18 V. The concentration of Cu in final electrolyzed solutions by both electrolytic compartment systems was found to strongly depend on the constant applied voltage, distance between electrodes, detected current, reaction time, different complexes' reaction mechanisms and pH. Despite a typical and traditional usage of a one electrolytic compartment in electrochemical processes [25, 26], it is hereof demonstrated that the electrochemical preparation of Cu(II) complexes in aqueous solution can efficiently be achieved by using two electrolytic compartments connected together by a cellulose semi permeable membrane. A one electrolytic compartment system failed to efficiently keep all the total amount of oxidized anodic Cu^{2+} in the electrolyte solution that are required for the formation of complex. Thus, re-depositing half of its amount from the electrolytes onto cathode electrode. On the other hand, the two electrolytic compartments system allowed maximum utilization of all the anodized Cu into the electrolyte solution, in the formation of Cu(II) complex. In contrast to a typical one electrolytic compartment system, the cellulose semipermeable membrane fixed between electrodes of a two electrolytic compartments system

resolved the re-deposition of Cu onto surface of cathode electrode. As a result, a two electrolytic compartments system was found to have a high current efficiency that drove its accelerated formation of Cu(II) complex than in a one electrolytic compartment. Hence, this study established and indicated two electrolytic compartments system to be more effective for preparing stable precursor solution, than its counterpart under this study. A two electrolytic compartments system will provide a solution to heavy cathode plating during electrochemical preparation of other than Cu various metal complexes in aqueous solution. Hence, it will greatly contribute to the electrochemical industries involved in preparation of various metal complexes in solution for different applications. The electrochemically prepared Cu(II) complex involving NH_3 ligand is a potential candidate for the fabrication of functional and conductive Cu thin films by MPM *via* spray coating method. The fabrication of such thin films using the electrochemically prepared aqueous solution of Cu precursor by a two electrolytic compartments system is fully discussed in the next chapter 5.

Reference:

- [1] Wang, C.; Yang, C.; Lee, C.; et al. Hydrothermal Synthesis and Structural Characterization of a Two-Dimensional Polymeric Copper(II) Complex Containing an Unusual Bridged $\text{H}_2\text{edta}^{2-}$ Ligand. **2002**, *41*, 429–432.
- [2] Wu, P.; Zhou, J.; Wang, X.; et al. Adsorption of Cu-EDTA complexes from aqueous solutions by polymeric Fe/Zr pillared montmorillonite: Behaviours and mechanisms. *Desalination*. **2011**, *277*, 288–295.
- [3] Gyliene, O.; Aikaite, J.; Nivinskiene, O. Recovery of EDTA from complex solution using Cu(II) as precipitant and Cu(II) subsequent removal by electrolysis. *J. Hazard. Mater.* **2004**, *116*, 119–124.
- [4] Thuy, T.T.; Herman, G.; Lommens, P.; et al. Complexation behaviour in aqueous edta sol-gel systems for the synthesis of $\text{YBa}_2\text{Cu}_3\text{O}_{7-x}$ high-temperature superconductors. *J. Braz. Chem. Soc.* **2012**, *23*, 1289–1297.
- [5] Pocięcha, M.; Lestan, D. EDTA leaching of Cu contaminated soil using electrochemical treatment of the washing solution. *J. Hazard. Mater.* **2009**, *165*, 533–539.
- [6] Norziehana, N.; Isa, C. Electrodeposition and Characterization of Copper Coating on Stainless Steel Substrate from Alkaline Copper Solution Containing Ethylenediaminetetraacetate (EDTA). *J. Mech. Eng.* **2017**, *2*, 127–138.
- [7] Nilsson, K.B.; Eriksson, L.; Kessler, V.G.; et al. The coordination chemistry of the copper(II), zinc(II) and cadmium(II) ions in liquid and aqueous ammonia solution, and

- the crystal structures of hexaamminecopper(II) perchlorate and chloride, and hexaamminecadmium(II)chloride. *J. Mol. Liq.* **2007**, *131–132*, 113–120.
- [8] Inoue, F.; Philipsen, H.; Radisic, A.; et al. Electroless Copper Bath Stability Monitoring with UV-VIS Spectroscopy, pH, and Mixed Potential Measurements. *J. Electrochem. Soc.* **2012**, *159*, D437–D441.
- [9] Sharma, R.P.; Saini, A.; Kumar, S.; et al. Diaquabis(ethylenediamine)copper(II) vs. monoquabis(ethylenediamine)copper(II): Synthesis, characterization, single crystal X-ray structure determination, theoretical calculations and antimicrobial activities of $[\text{Cu}(\text{en})_2(\text{H}_2\text{O})_2](2\text{-phenoxybenzoate})2\text{H}_2\text{O}$. *A Polyhedron.* **2017**, *123*, 430–440.
- [10] Sundaram, M.; Swain, A.; Arunachalam, R. Preparation of Coated Micro Tools for Micromachining Applications. Report. 2009;
- [11] Landolt, D.; Chauvy, P.F.; Zinger, O. Electrochemical micromachining, polishing and surface structuring of metals: Fundamental aspects and new developments. *Electrochim. Acta.* **2003**, *48*, 3185–3201.
- [12] El-Giar, E.M.; Said, R.A.; Bridges, G.E.; et al. Localized electrochemical deposition of copper microstructures. *J. Electrochem. Soc.* **2000**, *147*, 586–591.
- [13] Xue, J.; Shen, Q.; Liang, W.; et al. Preparation and formation mechanism of smooth and uniform Cu_2O thin films by electrodeposition method. *Surf. Coatings Technol.* **2013**, *216*, 166–171.
- [14] Katayama, J.; Ito, K.; Matsuoka, M.; et al. Performance of $\text{Cu}_2\text{O}/\text{ZnO}$ solar cell prepared by two-step electrodeposition. *J. Appl. Electrochem.* **2004**, *34*, 687–692.
- [15] Isa, N.N.C.; Mohd, Y.; Zaki, M.H.M.; et al. Characterization of copper coating electrodeposited on stainless steel substrate. *Int. J. Electrochem. Sci.* **2017**, *12*, 6010–6021.
- [16] Yu, X.; Huang, L.; Wei, Y.; et al. Controllable preparation, characterization and performance of Cu_2O thin film and photocatalytic degradation of methylene blue using response surface methodology. *Mater. Res. Bull.* 2015, *64*, 410–417.
- [17] Ravichandiran, C.; Sakthivelu, A.; Davidprabu, R.; et al. Microelectronic Engineering In-depth study on structural, optical, photoluminescence and electrical properties of electrodeposited Cu_2O thin films for optoelectronics: An effect of solution pH. *Microelectron. Eng.* **2019**, *210*, 27–34.
- [18] José, É.; Herrmann, A.B.; Olkuszewski, J.L.; et al. Determination of Trace Metals in Electrolytic Copper by ICP OES and ICP-MS. *Brazilian Archives of Biology and Technology.* **2005**, *48*, 681–687.

- [19] Shaikh, A.A.; Badrunnessa, M.; Firdaws, J.; et al. A cyclic voltammetric study of the influence of supporting electrolytes on the redox behaviour of Cu(II) in aqueous medium. *J. Bangladesh Chem. Soc.* **2012**, *24*, 158–164.
- [20] Ono, S.; Moronuki, S.; Mori, Y.; et al. Electrochimica Acta Effect of Electrolyte Concentration on the Structure and Corrosion Resistance of Anodic Films Formed on Magnesium through Plasma Electrolytic Oxidation. *Electrochim. Acta.* **2017**, *240*, 415–423.
- [21] Parr, J.M.P.; Kim, Y. Electrochemical silver dissolution and recovery as a potential method to disinfect drinking water for underprivileged societies. *Environ. Sci. Water Res. Technol.* **2016**, *2*, 304–311.
- [22] Rodri, L.; Rodríguez-Sánchez, L.; Blanco, M.C.; et al. Electrochemical Synthesis of Silver Nanoparticles. *J. Phys. Chem. B.* **2000**, *104*, 9683–9688.
- [23] Stanojevic, D.; Toskovic, D.; Rajkovic, M.B. Intensification of zinc dissolution process in sulphuric acid. *J. Min. Metall. Sect. B Metall.* **2005**, *41*, 47–66.
- [24] Hecht, M.; Fawcett, W.R. Electrochemistry of [V(III)EDTA]- in Ethylene Glycol–Water Mixtures. 1. Thermodynamic and Transport Properties: Solvation of the Reactant and Product. *J. Phys. Chem.* **1996**, *100*, 14240–14247.
- [25] Nordin, N.; Hasan, S.Z.; Zakaria, Z.; et al. Effect of applied voltage on slow-release of Cu(II) ions on the synthesis of Copper(II) stearate complex by electrochemical technique. *J. Braz. Chem. Soc.* **2015**, *26*, 1115–1123.
- [26] Kuprum, P.; Karboksilat, I.I.; Berasaskan, O.; et al. Synthesis and Characterization of Copper(II) Carboxylate with Palm-Based Oleic Acid by Electrochemical Technique. *Malaysian Journal of Analytical Science.* **2015**, *19*, 236–243.
- [27] Othman, M.R. Electrosynthesis and Characterization of Cu (OH)₂ Nanoparticle using Cu and Cu-PVC Electrodes in Alkaline Solution. *Int. J. Electrochem. Sci.*, **2015**, *10*, 4911–4921.
- [28] Baeshov, A.B.; Kadirbayeva, A.S.; Jurinov, M.J. Dissolution of a copper electrode in sulfuric acid at polarization by an industrial alternating current. *Int. J. Chem. Sci.* **2014**, *12*, 1009–1014.
- [29] Viswanath, S.G.; Jachak, M.M.J. Electrodeposition of Copper powder from Copper Sulphate Solution in Presence of Glycerol and Sulphuric Acid. *Assoc. Metall. Eng. Serbia.* **2012**, *19(2)*, 119–135.
- [30] Nagai, H.; Suzuki, T.; Hara, H.; et al. Chemical fabrication of p-type Cu₂O transparent thin film using molecular precursor method. *Mater. Chem. Phys.* **2012**, *137*, 252–257.

- [31] Nagai, H.; Sato, M. Molecular Precursor Method for Fabricating *p*-Type Cu₂O and Metallic Cu Thin Films. *Mod. Technol. Creat. Thin-film Syst. Coatings*. 2017.
- [32] Armelao, L.; Barreca, D.; Bertapelle, M.; et al. A sol–gel approach to nanophasic copper oxide thin films. *Thin Solid Film*. **2003**, *442*, 48–52.
- [33] Götzendörfer, S.; Polenzky, C.; Ulrich, S.; et al. Preparation of CuAlO₂ and CuCrO₂ thin films by sol–gel processing. *Thin Solid Film*. **2009**, *518*, 1153–1156.
- [34] Ding, J.; Sui, Y.; Fu, W.; et al. Applied Surface Science Synthesis and photoelectric characterization of delafossite conducting oxides CuAlO₂ laminar crystal thin films via sol–gel method. *Appl. Surf. Sci.* 2010, *256*, 6441–6446.
- [35] Nagai, H.; Mita, S.; Takano, I.; et al. Conductive and semi-transparent Cu thin film fabricated using molecular precursor solutions. *Mater. Lett.* **2015**, *141*, 235–237.
- [36] Hishimone, P.; Nagai, H.; Morita, M.; et al. Highly-Conductive and Well-Adhered Cu Thin Film Fabricated on Quartz Glass by Heat Treatment of a Precursor Film Obtained Via Spray-Coating of an Aqueous Solution Involving Cu(II) Complexes. *Coatings*. **2018**, *8*(10), 1–10.
- [37] Viswanath, S.G.; George, S. Electrowinning of copper powder from copper sulphate solution in presence of glycerol and sulphuric acid. *Indian J. Chem. Technol.* **2011**, *18*, 37–44.
- [38] Bejerrum, J.; Agarwala, B.V. Metal Amine Formation in Solution. XIX. On the Formation of Tetraamminedi- μ -hydroxodicopper(II) and Hydroxotetra-ammine Complexes in Ammoniacal Copper(II) Solutions. *Acta Chemica. Scandivanica A*. **1980**, *34*, 475–481
- [39] Haram, S.K.; Mahadeshwar, A.R.; Dixit, S.G. Synthesis and characterization of copper sulphide nanoparticles in aqueous surfactant solutions. *Adsorpt. Sci. Technol.*, **1998**, *16*, 667–677.
- [40] Trouillet, L.; Toupance, T.; Villain, F.; et al. In situ characterization of the coordination sphere of Cu(II) complexes supported on silica during the preparation of Cu/SiO₂ catalysts by cation exchange. *Phys. Chem. Chem. Phys.*, **2000**, *2*, 2005–2014.

CHAPTER 5

Selective Low Temperature Fabrication of Cu and Cu₂O Thin Films by Spray Application of Aqueous Solution Prepared by Electrochemical Method

CHAPTER 5: Selective Low Temperature Fabrication of Cu and Cu₂O Thin Films by Spray Application of Aqueous Solution Prepared by Electrochemical Method

5.1. Introduction

5.1.1. Introduction on metallic copper thin films

Conductive copper thin film is a suitable material for its applications in electrodes or conductive patterns in multilayered electronic parts, printed circuit boards and the hybrid integrated circuit in electronic industries [1, 2]. Our environment is full of radio frequencies (RF) and electromagnetic radiation due to rapid wireless communication technologies which have many applications such as base station of mobile communication network and wireless internet antenna [3] which can interfere with other electrical and electronic devices causing malfunctioning of other sensitive electronic devices in environment [4]. Hence Cu thin films are potential candidates for effectiveness of electromagnetic interference shielding (EMI) [4, 5]. Copper nanosized materials also exhibit superior magnetic and thermal properties [6]. They have attracted much attention for over a decade because of their photocatalytic and optical properties, high electrical and thermal conductivity [1] which contribute attractive prospects in the design of many new devices requiring such functionalities. In addition, copper nanosized material's various application makes a good substitute for conductive and expensive noble metals like gold and silver in the chemical and metallurgical process [7, 8].

However, the attractive properties of copper nanomaterial and thin films owes it to these of bulk copper such as its abundant availability, less toxicity, versatility, malleability and resistance to corrosion and good electrical and thermal conductivity [9, 10]. The physical and chemical properties of copper nanomaterials are also different from these of bulk copper material due the high surface area to volume ratio [11].

5.1.2. Fabrication methods of Cu thin film and their simple advantages

Physical and wet chemical processes are known methods mainly used for the fabrication of copper thin film. Physical processes such as magnetic sputtering deposition [12] and pulsed laser deposition [13] are expensive and requires complicated experimental set ups. Figure 1 shows the example of pulsed laser deposition process. Whereby strong pulsed laser beam is used to induce and translate target raw material into a gas phase. The vaporized materials then react with the substrate in high vacuum of reduced atmospheric pressure, which is necessary to form desirable thin film. The substrate is mainly positioned in adjacent direction to the ablated target material and the reduced atmospheric pressure varies with nature of target

material. Metallic copper thin films can be fabricated using 99.99% bulk Cu as target material at vacuum pressure of 6×10^{-6} mbar [12].

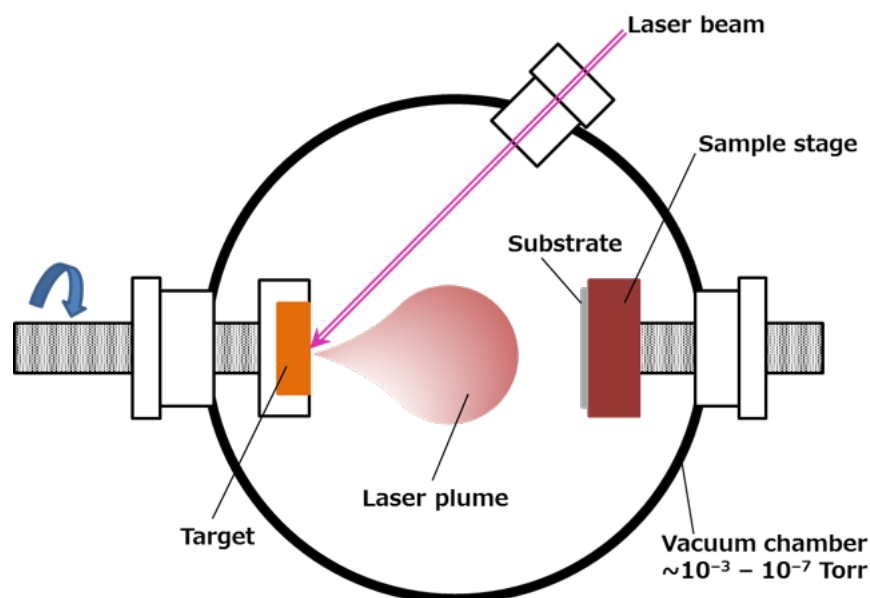


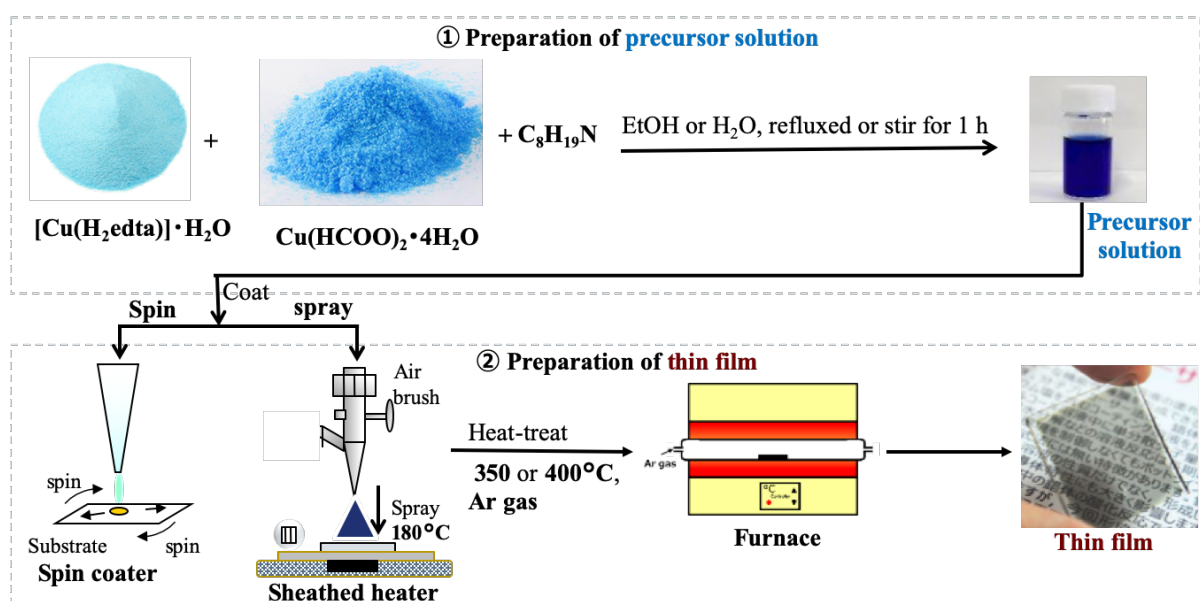
Figure 1. Schematic representation of dry process of a **PLD** set-up [43].

While wet chemical processes such as; electrochemical deposition [14, 15] and molecular precursor method (MPM) [16, 17] are considered to require less fabrication time and low energy cost. Also, the methods do not require high vacuum to form thin films as, however the deposition of precursor materials in the solution require high temperature during deposition to transform into precursor film onto the substrate.

5.1.3. Molecular precursor method employing alcohol and aqueous solvents

The MPM is a wet process for the formation of thin films of various metal oxides and phosphate compounds. It is based on the design of metal complexes in coating solutions with excellent stability, homogeneity, miscibility, coatability, amongst its other many practical advantages [18]. The procedure is well known for fabrication of both copper oxides semiconductors Cu_2O [18–20] and metallic Cu [16, 17] thin films by utilizing Cu(II) complex dissolved in coating solutions initially derived from metal complexes and salts such as $[\text{Cu}(\text{H}_2\text{edta})] \cdot \text{H}_2\text{O}$ and $\text{Cu}(\text{HCOO})_2 \cdot 4\text{H}_2\text{O}$. The type of coating solution favors different deposition technique. For example, when fabricating these thin films by spin coating, volatile organic compounds (VOCs) are generally used as solvents because aqueous solutions are

generally inadequate to spread onto various substrate due to their high surface tension [18]. However, industrially, VOCs free solvents are desired because they are less ignition able, cheap and have reduced risk on human health and environment [17]. The typical procedures involve mixing of appropriate amount of copper salts in alcohol [16, 18–20] or aqueous solvent [17] at ambient temperature to result in stable coating precursor solution. The resultant precursor solution is spin [16] or spray [17] coated onto substrate to obtain a precursor film, of which is further subjected to high temperature under inert gas flow to obtain a desirable thin film (Scheme 1). In addition the fabrication of copper oxides films can also be achieved using $\text{Cu}(\text{CH}_3\text{COO})\cdot\text{H}_2\text{O}$ salts as a starting compound, by a wet process of sol-gel method [21]. Until now, the wet chemical procedure has only fabricated the desired thin films using high temperature of up to 400°C under Ar gas. Scheme 1 shows the outline for fabrication of thin films by wet chemical processes of MPM *via* spin or spray coating.



Scheme 1. Schematic route for high temperature fabrication of metallic copper thin films by wet chemical process of MPM *via* spin [16] and spray [17].

In the previous chapter 3, a highly photo-reactivity *p*-type Cu_2O thin-film was fabricated on a quartz glass substrate heated at 180°C in air directly by spraying precursor aqueous solutions, which were prepared by dissolving Cu(II) formate and ammonium formate, whose molar ratios to Cu(II) ion was 14, into aqueous ammonia solution. However, it is also possible to fabricate a metallic Cu thin film by adding EDTA in the previously prepared **S14** spray solution that initially fabricated Cu_2O thin films. Hence, this chapter fully discusses the

selective fabrication of both *p*-type Cu₂O and metallic Cu thin films by reductant of HCOONH₄ or EDTA *via* spraying at a minimum temperature of only 180°C in atmospheric air.

5.1.4. Application of electrochemically prepared Cu₂O precursor solution

The preparation of aqueous spray solutions of copper precursor can also easily be achieved in a one-step route by electrochemical process. As describe in previous chapter 4 the electrosynthesis of Cu(II) complexes of EDTA and amine can be achieved using solid copper plate instead of various Cu(II) salts as sources of Cu²⁺ ions used in typical MPM. Instead of a starting materials of Cu(HCOO)₂·4H₂O, to be a source of Cu(II) complexes in coating solution, as per our previous studies. The Cu²⁺ ions are generated by electrochemical oxidation of anode copper electrodes. This chapter highlights the fabrication of thin films by spray coating using electrochemically prepared Cu₂O precursor aqueous solution by one step-route and in a two electrolytic compartment which was newly contrived in chapter 4. The aqueous spray solution containing Cu(II) complex species was electro-synthesized by electrochemical oxidation of anode metallic copper electrode in an aqueous electrolytic solution containing ammonium formate and ammonia at room temperature, with no isolation of solid Cu(II) complexes or salts at room temperature. Under this chapter, the goal is to change the reductant of precursor in electrochemically prepared spray solution by addition of EDTA into it, and spray-coated onto a quartz glass substrate at 180°C in air to result in a conductive Cu thin film *via* MPM. The electrical conductivity and chemical composition of the resultant Cu thin film will be evaluated and compared to those of Cu thin films previously formed by MPM at high temperature of 400°C under Ar gas.

5.2. Experimental

5.2.1. Preparation of electrolytic solutions

Two electrolytic solutions, into which EDTA is added or not, were prepared according to the following procedures. **ES₁** was prepared by adding 4.321 g (71.04 mmol) of 28% NH₃ aqueous solution and 3.541 g (56.16 mmol) of HCOONH₄ into 300 g of deionized H₂O. **ES₁** contains identical electrolyte composition to that prepared in previous chapter 4. **ES₂** was prepared by adding 1.02 g (3.48 mmol) of EDTA, 4.321 g (71.04 mmol) of 28% NH₃ aqueous solution and 3.541 g (56.16 mmol) of HCOONH₄ into 300 g of deionized H₂O. Each mixed solution was mechanically stirred for 1 h at room temperature.

5.2.2. Electrochemical preparation of precursor aqueous solutions

Each 300 g of ES_1 and ES_2 were respectively transferred into each electrolytic compartment, linked together through a cellulose membrane in the center of two separated compartments. Two pre-weighted sheets of Cu plates positioned 70 mm apart, were immersed in the electrolytic solution of each compartment as anode and cathode, respectively. A constant potential of 18 V and a limited current of 2 A, was applied from CVCC–DC power supply. Electrolysis was performed for 2 h, at ambient temperature with constant magnetic stirring to obtain spray precursor solutions; S_1 and S_2 , respectively. S_1 contains identical electrolyte and precursor compositions to that prepared in previous chapter 4 by electrolysis for minimum of 2 h in a two electrolytic compartments system. Another spray solution S'_1 was also prepared by adding 1.02 g (3.48 mmol) of EDTA into S_1 and stirred for 1 h at room temperature. Scheme 2 shows two ways of electrochemical preparation of precursor aqueous solutions.



Scheme 2. Two ways of electrochemical preparation of precursor aqueous solutions.

5.2.3. Fabrication of thin films

The experimental setup and condition for spray coating used in this chapter were identical to those described in previous chapter 3. The spraying conditions were also identical to these used in chapter 3. Whereby; an airbrush (Revolution HP-SAR; ANEST IWATA Co., Kanagawa, Japan) used as an atomizer of spray solution was vertically suspended adjacent to

a hot plate. The pressure and solution inlets of the airbrush were connected to an air compressor set at 0.2 MPa and to a needle injected into the spray solution, respectively. The distance between the tip of the atomizer and the substrate surface was adjusted to 30 cm. A quartz glass substrate was placed on the hot plate heated at 180°C. The substrate temperature was monitored by a chrome-alum type surface probe (A3-K-Q, TKG, Tokyo, Japan) fixed on top of the hot plate. Each 12 g of S_1 , S'_1 , and S_2 was independently sprayed onto the pre-heated quartz glass substrate. Each solution was periodically sprayed for 5 s with a rate of 1.64 mL min⁻¹ at 20 s intervals. The obtained thin films are denoted as F_1 , F'_1 , and F_2 , respectively.

The resultant sprayed films; F'_1 and F_2 were subsequently placed on the surface of a quartz glass (30 × 30 × 1.6 mm³) holder and the set was inserted in a quartz glass tube (40 mm diameter and 650 mm length) protruding through the inside of the tubular furnace (EPKRO-12K, Isuzu, Toyota, Japan). Prior to heat treatment, the tube was filled with constant Ar gas flow maintained at a rate of 1.5 L min⁻¹ for a period of 10 minutes. The furnace was heated from 25°C to 350°C at constant temperature raising rate of 14°C, kept at 350°C for a period of 50 minutes, followed by its cooling to room temperature. The resultant film from heat treatment are denoted as treated film; TF_2 and TF'_1 , respectively by heat treated from F_2 and F'_1 , respectively. Additional films were fabricated by placing a same sized quartz glass substrate on top layer of the resultant heat-treated film; TF_2 and TF'_1 in the tubular furnace and post annealed at 400°C for 50 minutes under Ar gas flow of 1.5 L min⁻¹. The resultant additional post annealed films are represented as PF_2 and PF'_1 . Further heat treatment of sprayed film; F_2 and F'_1 was optional in order to compare their properties with these of previously fabricated metallic Cu thin films under identical high treatment conditions.

5.3. Results and their discussion

5.3.1. Direct preparation of aqueous solutions involving Cu(II) complexes by electrochemical process

The electrochemical process using Cu electrodes was examined to simplify the preparation of coating solutions involving Cu(II) complex species into a single step. A newly contrived electrolytic apparatus with two compartments having a junction through semi-permeable cellulose membrane between them was developed in chapter 4. Because it was shown that usual electrolysis using Cu electrodes in one cell was too inefficient to obtain the desired species with enough concentration by several preliminary examination. Such inefficiency of

electrolysis using one cell to obtain Cu(II) complexes had been also reported by other research groups [22, 23].

Consequently, the spray solutions S_1 and S_2 , whose total concentrations of Cu^{2+} are 0.033 and 0.018 mmol g^{-1} respectively, could be obtained directly by electrolysis of Cu plates in the electrolytic solutions ES_1 and ES_2 for 2 h, respectively. According to evidences established in chapter 4, each concentration could be facilely calculated by using the mass decrease of the electrolyzed anode, because no mass change of cathode occurred before and after electrolysis with the two-compartment apparatus. In fact, the dissolution of Cu anode and H_2 generation on Cu cathode occurred with neither Cu plating on the cathode nor precipitation of colloidal copper hydroxide during preparation of S_2 by electrolysis using this two-compartment apparatus, which were observed in the case of one cell.

As another spray solution S'_1 was prepared by adding EDTA into S_1 , the total concentration of Cu^{2+} was of course identical to that of S_1 , 0.033 mmol g^{-1} .

5.3.2. Absorption spectra and pH values of spray solutions

The absorption spectra of S_1 , S'_1 , and S_2 are shown in Figure 2. The maximum absorption position of a characteristic band in the visible region was observed at 601, 608 and 619 nm for S_1 , S'_1 , and S_2 , respectively. The pH values of S_1 , S'_1 , and S_2 were almost identical, as has been obtained as 9.44, 9.42, and 9.46, respectively.

The formation of $[Cu(NH_3)_4]^{2+}$ complex with $HCOO^-$ counter ions in S_1 can be assumed from its maximum absorption position of identical complexes; $[Cu(NH_3)_4]^{2+}(H_2O)$, and $[Cu(NH_3)_4]^+(HO)$, at 590 and 597 nm [24] and $[Cu(NH_3)_4]^{2+}$, at 630 nm [25] and 640 nm [26, 27], respectively. On the other hand, the maximum absorption position of S_2 appeared at longer wavelength, indicating its nearly formation of $[Cu(edta)]^{2-}$ complex at 730 – 734 nm [27] and 725 nm [28]. In the case of S'_1 , the corresponding value is between S_1 and S_2 , showing the mixture of both complex species.

The absence of EDTA ligand in ES_1 allowed the dissolution of Cu plate at accelerated reaction rate, resulting in higher concentration of total Cu(II) ion in S_1 , in comparison to the slower reaction observed when using ES_2 in which EDTA is originally added. Therefore, it was useful to add EDTA into S_1 already involving sufficient concentration of total Cu(II) ion to yield S'_1 . It was thus revealed that the presence of EDTA in the electrolytic solution affects the dissolution rate of Cu anode.

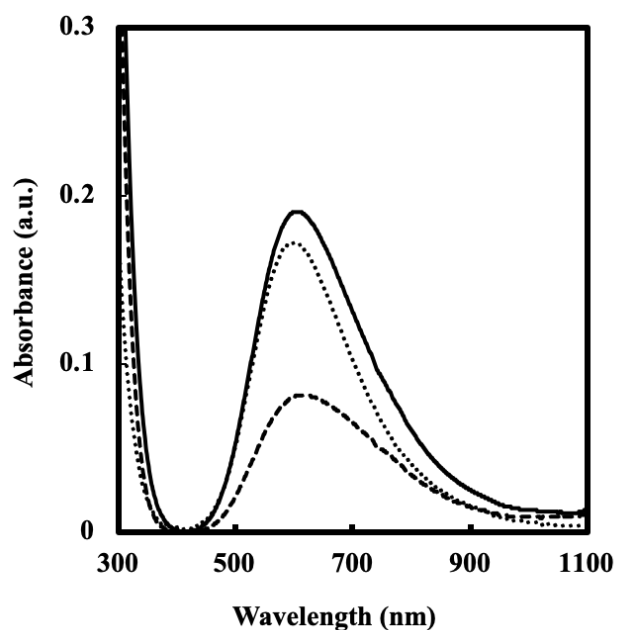


Figure 2. Absorption spectra of S_1 , S'_1 , and S_2 spray precursor solutions. The lines are labelled as; dotted line: S_1 , solid line: S'_1 , and long broken line: S_2 .

5.3.3. The role of EDTA in selective formation of Cu_2O , Cu or composite Cu/ Cu_2O thin films by spray deposition

The XRD patterns of F_1 , F'_1 , and F_2 are shown in Figure 3. Seven peaks observed for F_1 , at $2\theta = 29.8, 36.7, 42.6, 52.7, 61.6, 73.8$ and 77.6° are assignable to (110), (111), (200), (211), (220), (311) and (222) phase of cubic Cu_2O , respectively (ICDD card no. 01-071-3645). The electrical conductivity of F_1 was $3.38(1) \times 10^2 \Omega \text{ cm}$ which is comparable to that of the Cu_2O thin film; F_{14} obtained in chapter 3. It was thus clarified that the spray solution S_1 is useful to form pure Cu_2O thin film at 180°C in air by one-electron reduction of Cu(II) complex of ammine ligand. In contrast, only three peaks found for both F'_1 and F_2 at $2\theta = 43.3, 50.4,$ and 74.1 are assignable to (111), (200), and (220) crystal phase of metallic Cu, respectively (ICDD card no. 00-004-0836). Therefore, it was clearly revealed that the Cu thin film can be fabricated by the spray solutions, S'_1 and S_2 just involving EDTA whose molar ratios to NH_3 and $HCOONH_3$ are approximately 1/20 and 1/16, respectively.

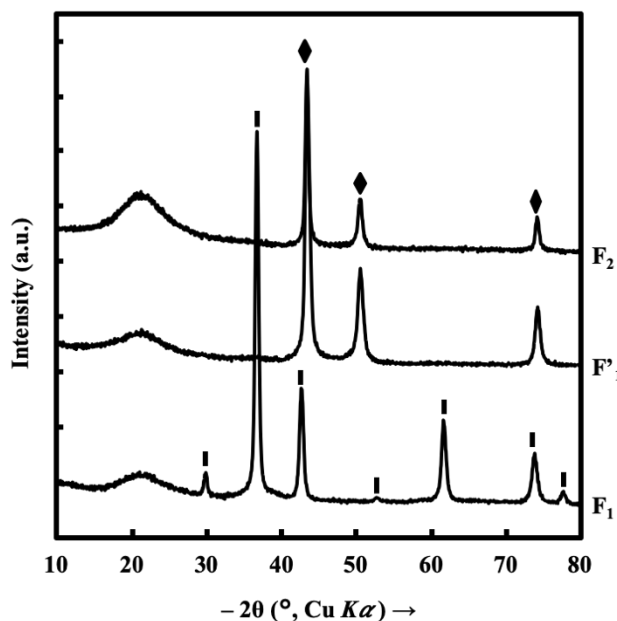


Figure 3. XRD patterns of F_1 , F'_1 , and F_2 fabricated by MPM *via* spray deposition of corresponding electrochemically prepared solutions onto quartz glass substrate at 180°C in air. The peaks are denoted as follows; \blacklozenge : Cu and $|$: Cu_2O .

In our previous study, the fabrication of Cu thin film was achieved by the MPM using heat-treatment of spin-coated precursor film involving an EDTA complex of Cu(II) ion under Ar gas at 350°C [16]. It is thus noteworthy that the low-temperature formation of Cu_2O or Cu thin film can be selected by the absence or presence of EDTA in the spray solution, respectively.

The current results demonstrated that keeping the concentration of Cu^{2+} as 0.03 mmol g^{-1} while reducing that of EDTA from 0.006 to 0.003 mmol g^{-1} consequently result in the formation of composite Cu/ Cu_2O thin films denoted as F'_{1x} . This highlights the significant of the amount of EDTA required for the fabrication of conductive Cu single phase at 180°C in air. Figure 4 shows the phase transition in XRD patterns of F'_1 and F'_{1x} thin films fabricated by spray coating S'_1 containing 0.006 and 0.003 mmol g^{-1} concentration of EDTA, respectively onto quartz glass substrate at 180°C in air.

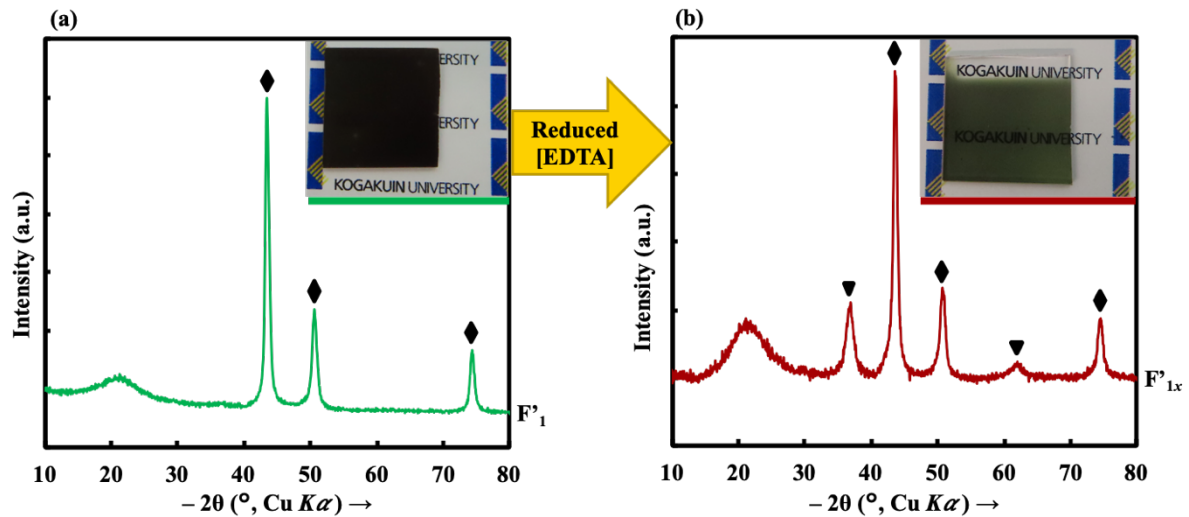


Figure 4. XRD patterns of (a) F'_{1} , and (b) F'_{1x} fabricated by MPM *via* spray deposition of electrochemically prepared S'_1 containing different concentration of EDTA onto quartz glass substrate at 180°C in air. The peaks are denoted as follows; \blacklozenge : Cu and \blacktriangledown : Cu_2O .

Also, the F'_{1x} composite Cu/ Cu_2O is much thinner and with an improved electrical resistivity in contrast to Cu single phase F'_1 . The improved conductivity of the F'_{1x} is attributed to the reduced amount of carbon in the film by lowering the concentration of EDTA in its corresponding S'_1 spray solution. Table 1 shows the comparison of thickness and electrical resistivity of F'_1 and F'_{1x} thin films fabricated by spray coating S'_1 containing 0.006 and 0.003 mmol g^{-1} concentration of EDTA, respectively onto quartz glass substrate at 180°C in air.

Table 1. Comparison of averaged thickness and electrical resistivity of F'_1 and F'_{1x} thin films fabricated using spray solution S'_1 containing 0.006 and 0.003 mmol g^{-1} concentration of EDTA, respectively. The standard deviation is shown in parentheses.

Spray sol.	$\text{Cu}^{2+}]^*/\text{mmol g}^{-1}$	Fabricated film	Annealing conditions;		Thickness (nm)	$^*\rho$ ($\Omega \text{ cm}$)
			temp. ($^{\circ}\text{C}$)	time (min)		
S'_1	0.006	F'_1	180	28	170	$8.90(2) \times 10^{-3}$
	0.003	F'_{1x}		25	150	$1.57(1) \times 10^{-3}$

5.3.4 Surface morphology, and the influence of chemical composition mainly atomic ratio of oxygen to copper on adhesion strength of thin films

The surface morphology and cross-sectional images of F_1 , F'_1 and F_2 are shown in Figure 5. These images indicated that the averaged particle sizes and film thicknesses of F'_1 are ca.

80 ± 60 and 170 ± 20 nm, respectively, and those of F_2 are 60 ± 20 nm and 130 ± 30 nm, respectively. While that of F_1 are indicated as ca. 100 ± 30 and 220 ± 40 nm, respectively.

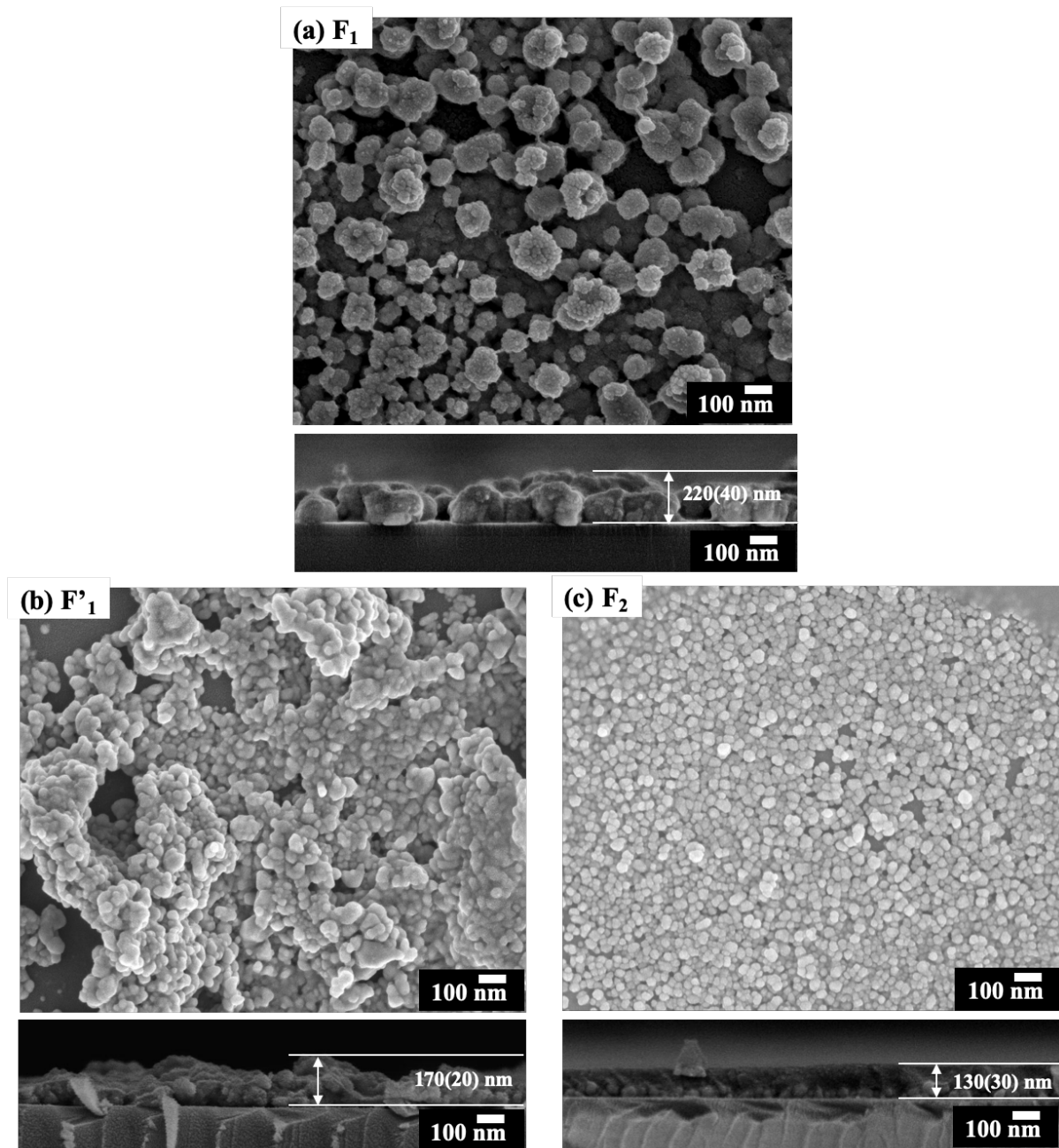


Figure 5. Surface morphologies and cross-sectional images of (a) F_1 , (b) F'_1 , and (c) F_2 fabricated by deposition of corresponding electrochemically prepared solutions onto quartz glass substrate at 180°C in air.

The tensile strength of the adhesion of F_1 , F'_1 and F_2 onto the quartz glass substrate were 40 ± 11 , 12 ± 7 , and 75 ± 7 MPa, respectively. The application of conductive Cu thin films in various technological fields strongly depends on their mechanical properties [17]. The adhesion strength, thickness and particle sizes of the films are summarized in Table 2.

Table 2. Adhesion strength, thickness, and particle sizes of fabricated films by MPM *via* spray deposition of corresponding electrochemically prepared precursor solution, onto quartz glass substrate at 180 °C in air. The standard deviations are shown in parentheses.

Films	Adhesion strength (MPa)	Thickness (nm)	Particle sizes (nm)
F_1	40 ± 11	220(± 40)	100(± 30)
F'_1	12 ± 7	170(± 20)	80(± 30)
PF'_1	15 ± 9	100	60(± 20)
F_2	75 ± 7	130(± 30)	60(± 20)
PF_2	64 ± 4	60	50(± 20)

The tensile strength of F_1 and F_2 indicates that they are strongly adhered onto their substrates than F'_1 . The tensile strength of F'_1 is expectedly 32 times lower than that of F_1 because of the strong bonding between the majority amount of Cu cations and O^{2-} belonging to Cu_2O and SiO_2 at their interference layer [16]. As shown in Figure 3, the F'_1 is of pure metallic Cu phase, hence the describe bonding at interference layer is very weak if not lacking in the film causing its weakly adherence to the substrate.

Figs. 6(a) and 6(b) show the Auger spectra of F'_1 and F_2 , respectively. The peaks are observed at approximately 264 eV for carbon, 273 eV for nitrogen, 509 eV for oxygen, and 764, 835, 914 eV for copper atoms in the wide scan spectra of both films. The atomic ratios of Cu, O, C and N in F'_1 were calculated to be 55, 11, 28 and 7 %, respectively, and those in F_2 were determined as 24, 19, 49, and 12 %, respectively.

Previously, the resultant metallic Cu thin films were achieved by MPM through the formation of intermediate Cu_2O phase which first appeared after heat-treatment of corresponding precursor films at 350°C for 15 and 50 minutes, respectively [16, 17]. Consequently, it was confirmed that the bond between trace amount of Cu cations belonging to the Cu_2O that remained locally at the interface in their film and O^{2-} belonging to the quartz

glass substrate assisted the formation of a robust interface between them [16]. Based on AES results, there is 0.2 and 0.8 are ratios of O to Cu in F'_1 and F_2 . The high amount of oxygen left in F_2 than in F'_1 strengthens their film adherence to its coated substrate *via* the above described identical bonding mechanism. The described bond is expected to be even stronger in Cu_2O thin film; F_1 whose lattice is made up by a network Cu and Oxygen atom.

F'_1 is weakly adherence onto its substrate, also due to its lower annealing temperature of $180^\circ C$ in air in comparison to other high temperature fabricated metallic Cu thin films with thickness and tensile strength of 40 nm, 36(12) MPa [16]; and 100 nm, 37(7) MPa [17], fabricated by MPM at $350^\circ C$ and $400^\circ C$, respectively. Additionally, it is noteworthy, that the tensile strength of F'_1 is seven times higher than that of 1.7(5) MPa obtained from a metallic copper thin film fabricated by physical vapor deposition [16].

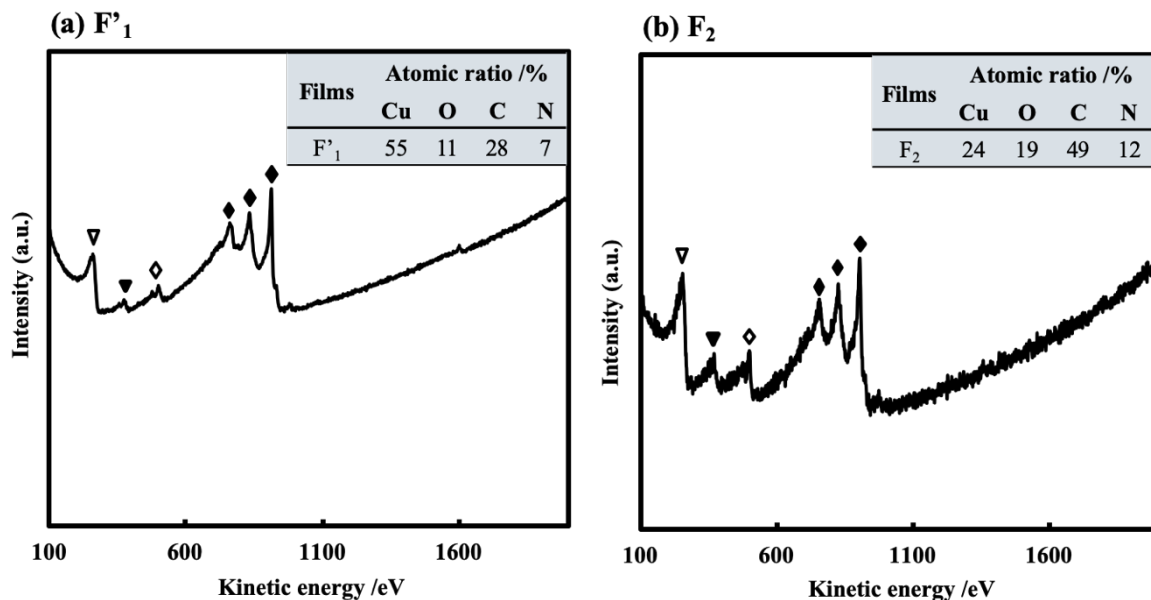


Figure 6. Auger spectra of (a) F'_1 and (b) F_2 fabricated by MPM *via* spray deposition of corresponding electrochemically prepared precursor solution onto quartz glass substrate at $180^\circ C$ in air. The peaks are denoted as follows; ∇ : C, \blacktriangledown : N, \diamond : O, \blacklozenge : Cu.

5.3.5. The influence of chemical composition mainly, atomic ratio of carbon to copper on the electrical resistivity of the thin films

The electrical resistivity of F'_1 was obtained as $8.9(2) \times 10^{-3} \Omega \text{ cm}$. From figure 5(b), the Cu grains in F'_1 were aggregated and it is for that reason such electrical resistivity was obtained.

The high concentration of remaining carbon in F'_1 , whose ratio to Cu is 0.5 was found not to have excessively disrupted its electrical resistivity. It may be accepted that the remaining carbon is rather useful to prevent the film from oxidation because the spray coating was performed in air. Expectedly, the electrical resistivity of F'_1 was very high in comparison to those of Cu thin films previously fabricated by MPM respectively at 350°C and 400°C *via* spin-coating method [16] and spray-coating one [17], respectively. On the basis of the effective post-annealing in those previous works, the identical treatment of F'_1 was performed as described above. As a result, the metallic Cu thin film PF'_1 with thickness and electrical resistivity of 100 nm and $5.13(1) \times 10^{-5} \Omega \text{ cm}$ could be obtained and these values are in close agreement to the previously reported film with 100 nm and $3.8(8) \times 10^{-5} \Omega \text{ cm}$, respectively. It can be accepted that the decrease in the electrical resistivity is ascribed to the decrease of carbon atoms in the film by further annealing treatment.

Although the crystalline Cu appeared in F_2 , the electrical resistivity of the sprayed thin film was over $10^6 \Omega \text{ cm}$. It is assumed that the low concentration of Cu(II) ions in the spray solution S_2 caused the large amount of remained carbon in F_2 whose ratio to Cu was 2.0, as observed by the abovementioned AES results.

S'_1 and S_2 contain an identical amount of carbon. However, the carbon atoms in F_2 remained four times higher than of F'_1 . It is suggested that the present EDTA in the solution had to coordinate with the copper as observed in S'_1 for the formation of the conductive copper F'_1 at a lower temperature of 180°C in air.

5.4. Photocatalytic activity of F_1 fabricated using electrochemically prepared precursor solution

The fabrication of visible light responsive *p*-type Cu_2O photocatalyst was achieved by coating electrochemically prepared Cu_2O precursor solution onto quartz substrate at 180°C in air. The coating solution was obtained by dissolution of copper plates in ammoniacal aqueous solution. Whose sufficient concentration of the Cu^{2+} in the precursor solution; S_1 , and equivalent to that in S_{14} was obtained by electrolytic reaction time of about 2 h. In comparison to F_{14} Cu_2O thin film which was fabricated using aqueous precursor solution whose starting material and source of Cu^{2+} was copper salt of ammonium formate, the photocatalytic and other measurable properties of the F_1 thin film are in close agreement to these of F_{14} . Table 3 describe such comparison and the traced change in absorbance and MO degradation efficiency under visible and dark conditions are shown in Figs. 7(a)–7(c). The ratio was calculated using equation 8 describe in chapter 2. The close agreement of the results implies that electrochemical

method can indeed achieve the preparation of coating solution for the fabrication of a Cu₂O thin film with identical properties as these fabricated using coating solution prepared by counterpart chemical convective MPM.

Table 3 Comparison of photocatalytic and other properties of F₁ and F14 thin film to these of F14 previously fabricated by spray coating in chapter 3.

Properties of Cu₂O thin film	F₁	F14
Thickness nm	230	350
Adhesion strength N	6.6	5.6
Carrier mobility cm ² v ⁻¹ s ⁻¹	0.92(6)	0.56(6)
Carrier concentration cm ⁻³	5.07(6) × 10 ¹⁶	3.00(6) × 10 ¹⁶
Resistivity Ω cm	3.38(1) × 10 ²	4.80(1) × 10 ²
Photocatalytic efficiency of MO /%	54	52

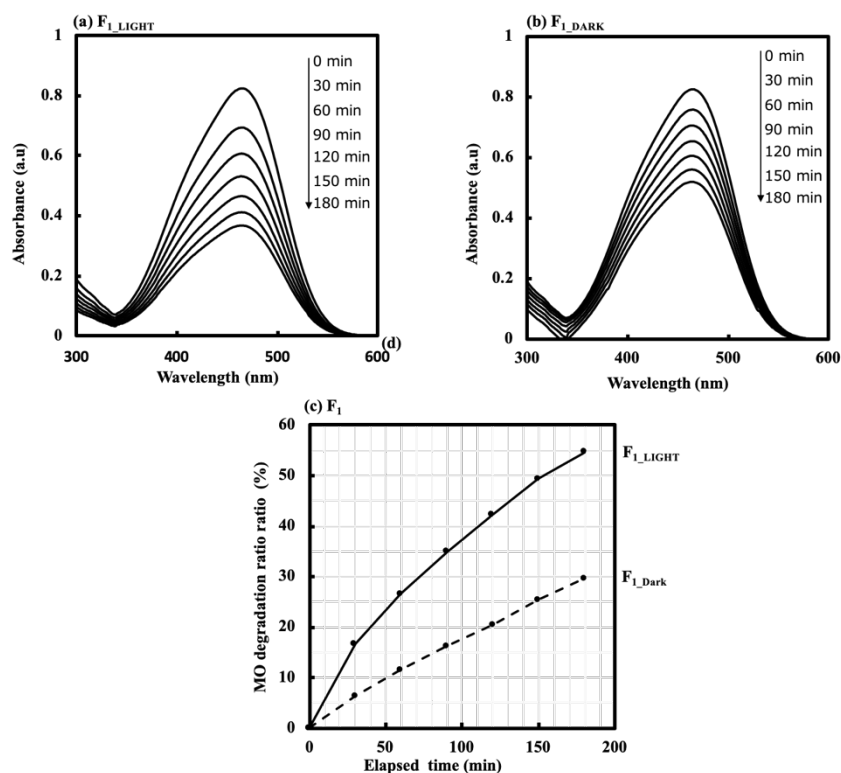


Figure 7. Photocatalytic properties of Cu₂O thin films *via* traced by reduction in absorbance spectra of MO concentration (a) under visible light irradiation (b) dark and their respective (c) degradation ratio.

5.4.1. The effect of irradiation time and increased sprayed area of Cu₂O thin films on the photocatalytic activity of the Cu₂O thin films under visible light

The films sizes were increased from (20 × 20 mm²) to (60 × 60 mm²). Their exposure time to visible light irradiation and dark condition was also increased to 4.5 h. The resultant thin films obtained after light irradiation and kept in dark condition were denoted as F_{1x4.5_LIGHT} and F_{1x4.5_DARK}, respectively. The photocatalytic evaluation of F_{1x4.5_LIGHT} and F_{1x4.5_DARK} reveals a high discoloration test of MO under both visible light and dark exposures. The discoloration of MO under dark condition by F_{1x4.5_DARK} is due to the identical mechanism of F₁₄ under same irradiation condition as described in chapter 3. Figs. 8(a)–8(c) shows the accelerated reduction of MO concentration under both irradiation conditions and their degradation efficiency ratio.

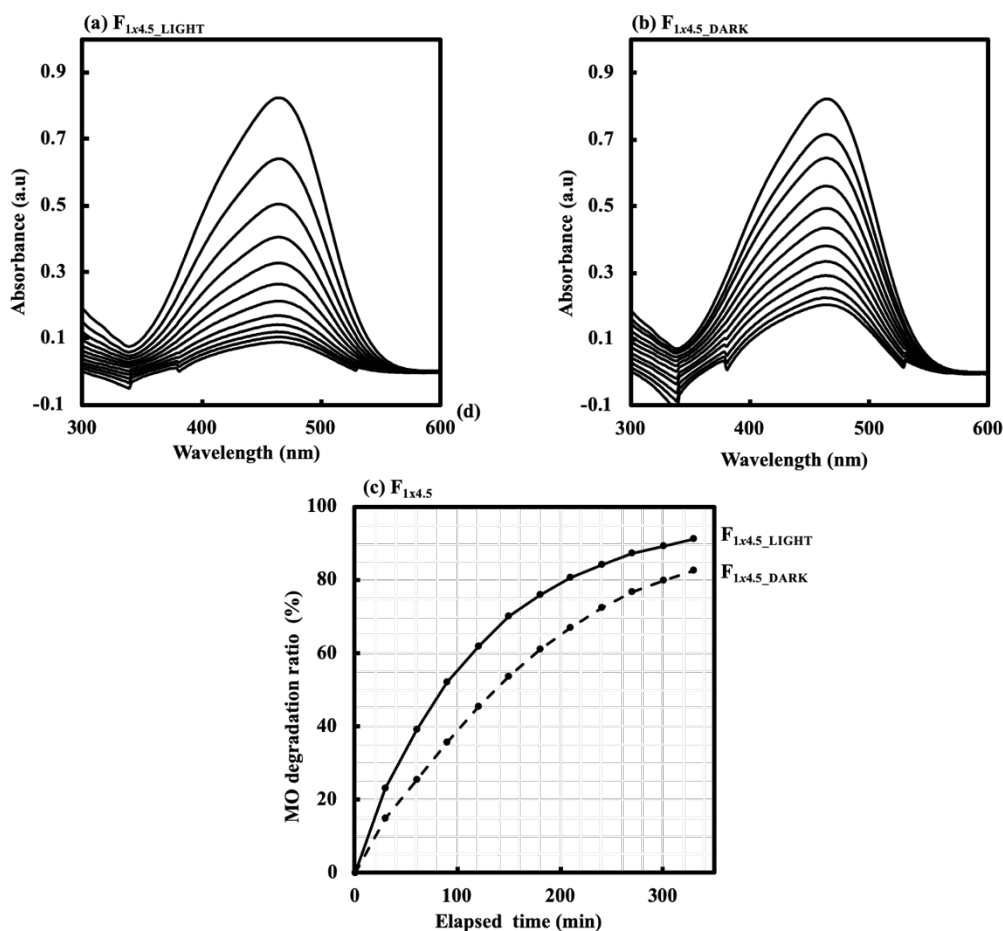


Figure 8. Photocatalytic properties of Cu₂O thin films *via* traced by reduction in absorbance spectra of MO concentration (a) under visible light irradiation (b) dark and their respective (c) degradation ratio.

5.4.2. The effect of pH on the photocatalytic activity of the Cu₂O thin films under visible light

It was indicated in chapter 3 by the XRD patterns of F6 and F14 after photocatalytic test that these thin films were not stable in their respective soaked MO aqueous solution at neutral pH leading to their oxidation. From that point of view; the photocatalytic of the Cu₂O thin films *via* discoloration of MO was then further evaluated at various pH. The MO solution was adjusted to various pH by addition of few drops on NaOH buffer and the photocatalytic test was performed under identical conditions as these used to test for F0 – F14. Figure 9 shows the photodegradation ratio of F₁ Cu₂O thin films under visible light irradiation and kept in dark condition at various pH of MO aqueous solution and their XRD patterns taken before and after the test.

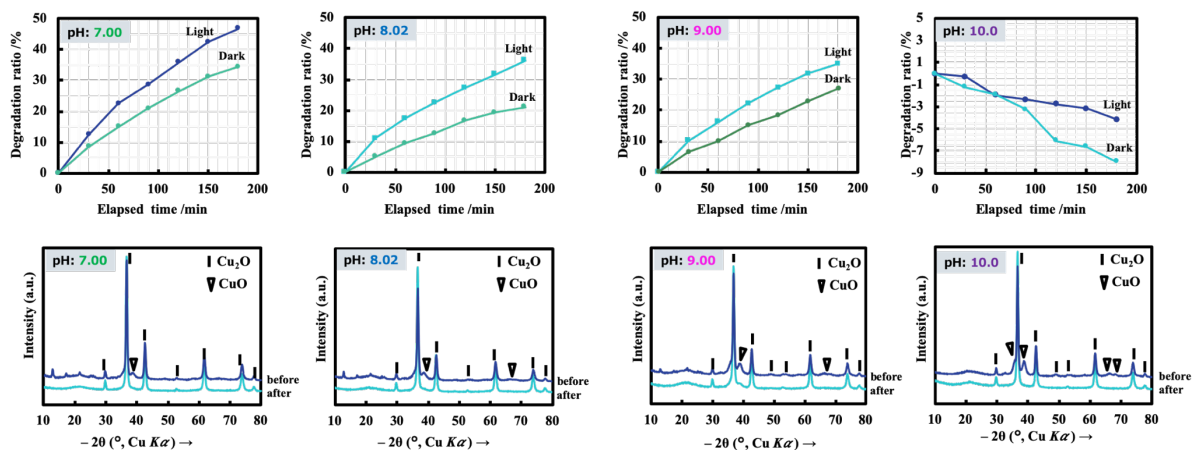


Figure 9. Photodegradation ratio of **F₁** Cu₂O thin films under visible light irradiation and kept in dark condition at various pH of MO aqueous solution and their XRD patterns taken before and after the test.

According to Figure 9, the degradation ratio of MO under visible light and dark conditions decreases as the pH increases, while the ratio remains higher under visible light irradiation than in dark conditions across all tested pH levels. Identical phenomena were observed for **F₁₄** at neutral pH, whose composition is identical to that of **F₁**. The **F₁** was expected to have a high adsorption ability for MO, which leads to its degradation when kept under dark conditions, primarily at pH 7–9. At pH 10, the film has no photocatalytic properties under both conditions due to its high stability. After the discoloration test, the pH of the MO solution also decreased, which is expected for pH 10. This implies that oxygen from water will react with Cu₂O thin film to oxidize it to CuO, as shown in their XRD patterns, and H⁺ ions will decompose MO. The excess amount of generated H⁺ ions further reduces the pH of the MO solution after the discoloration test. The stability of the **F₁** decreases and increases at low and high pH, respectively, resulting in increased and decreased peak intensities of oxidized CuO phases under those measurement conditions. Overall, the **F₁** film is less photocatalytically active at its most stable form under high pH of MO and visible light irradiation.

5.5. Fabrication of Cu₂O thin film at spraying temperature of 100 – 150°C

In order to investigate the influence of spray temperature on the formation of crystalline Cu₂O using the spray method, the deposition temperature was reduced from 180°C to 100 and 150°C to form a precursor film onto a quartz substrate in air. The electrochemically prepared Cu₂O aqueous solution was periodically spray coated onto the substrate using identical spray conditions, with the substrate temperature reduced to 100 and 150°C. The fabricated films using

spray temperature of 100 and 150°C in air were denoted as **SF₁₀₀** and **SF₁₅₀**, respectively. Only XRD patterns of the reduced temperature fabricated **SF₁₅₀** shows a crystal of Cu₂O single phase while that of the obtained **SF₁₀₀** indicated an amorphous precursor film as shown in Figs. 10(a)–(b). Even though, 150°C was sufficient to transits the Cu²⁺ in precursor solution into Cu⁺ in resultant **SF₁₅₀** with the assistant of HCOONH₄ reductant, the film was not electrically conductive. In order to improve the conductivity of **SF₁₅₀** it was further irradiated with UV-light (intensity of 4 mW cm⁻² at 254 nm) for a 24, 26 and 48 h to obtain **IF_{150x_24}**, **IF_{150x_26}**, and **IF_{150x_48}**, respectively. The film remained of single Cu₂O phase after UV irradiation for 24 – 26 h, and after 48 h a minor CuO was observed in the XRD patterns in Figure 10(b). The electrical resistivity of the films showed a decreased with an increased UV-irradiation time as shown in Table 4. A much-reduced temperature of 100°C provided insufficient minimum energy to induce crystallization, of the deposited droplets of precursor solution. To induce crystallization of **SF₁₀₀** the sprayed films were irradiated with identical UV-light intensity for 12, 16, 20 and 48 h to obtain **IF_{100x_12}**, **F_{100x_16}**, **F_{100x_20}**, and **IF_{100x_48}**, respectively. Figure 10(a) shows the XRD patterns of the thin films sprayed at reduced temperature of 100°C followed by UV-irradiation. The precursor film crystallized to Cu₂O single phase after its UV-irradiation for 12, 16, 20 and 48 h and their electrical resistivity which also decreased with an increase in irradiation time are shown in Table 5.

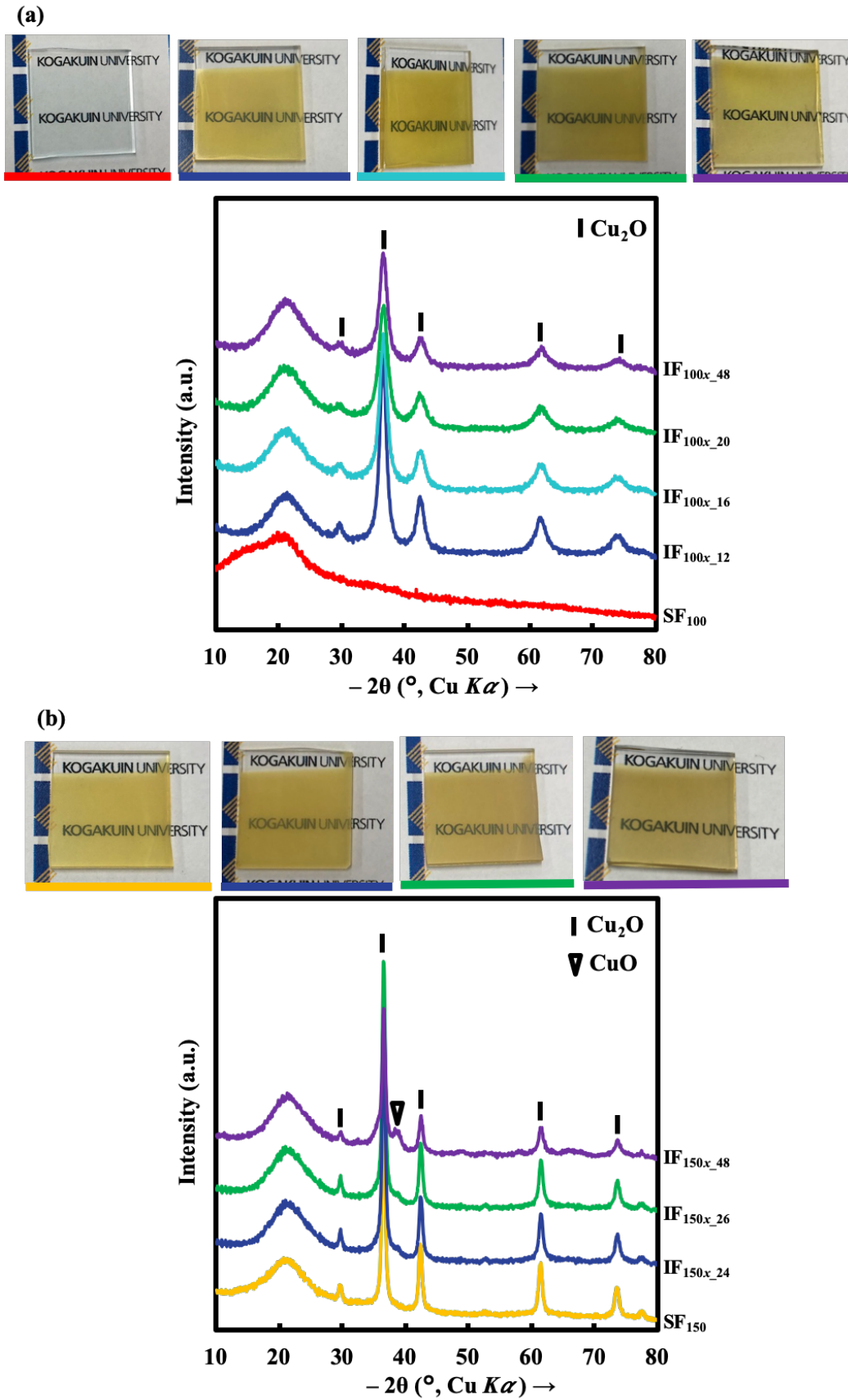


Figure 10. XRD patterns of (a) SF₁₀₀, IF_{100x_12}, F_{100x_16}, F_{100x_20}, and IF_{100x_48} (b) SF₁₅₀, IF_{150x_24}, and IF_{150x_26}, IF_{150x_48}.

Table 4 Crystallite size, thickness and electrical resistivity of reduced temperature fabricated Cu₂O thin films by spray coating at 150°C in air and UV-irradiated at various time.

Fabricated films	Crystallite size /nm	Thickness /nm	Resistance /M Ω
SF ₁₅₀	15.5	80	-
IF ₂₄	15.9	70	4.5(6) × 10 ²
IF ₂₆	14.5	70	3.6(4) × 10 ²
IF ₄₈	15.4	60	1.3(2) × 10 ²

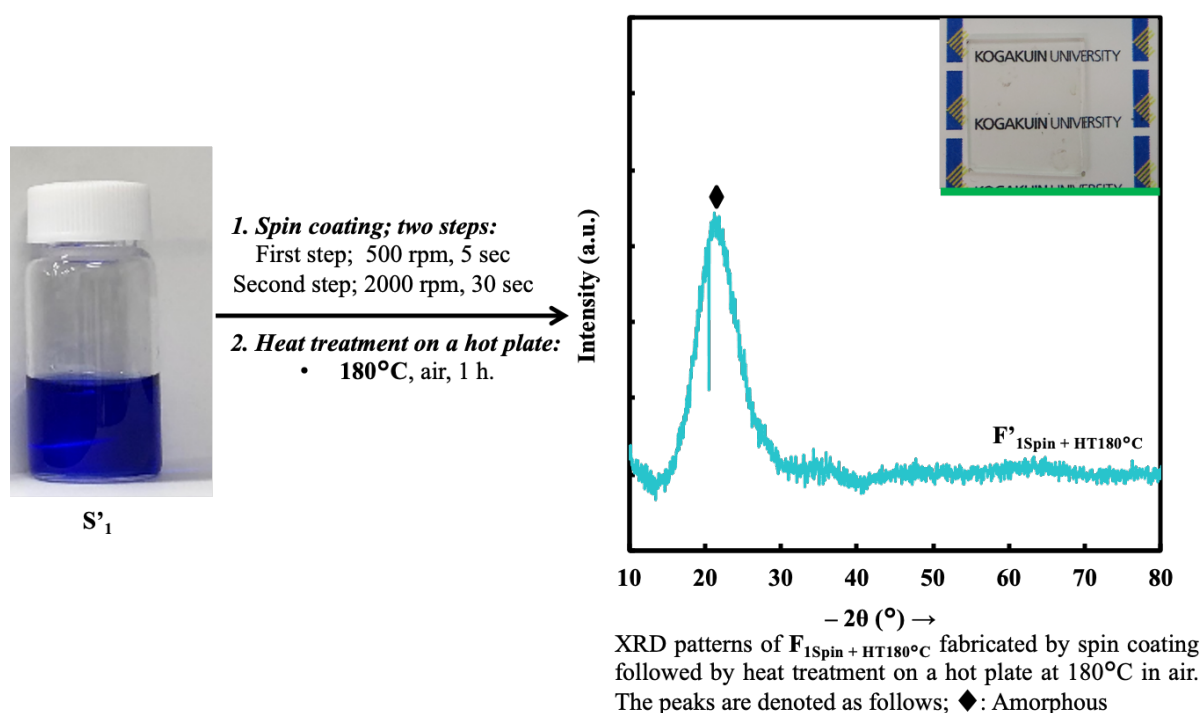
Table 5 Crystallite size, thickness and electrical resistivity of reduced temperature fabricated Cu₂O thin films by spray coating at 100°C in air and UV-irradiated at various time.

Fabricated films	Crystallite size /nm	Thickness /nm	Resistance /M Ω
IF ₁₂	6.8	110	3.0(6) × 10 ²
IF ₁₆	5.9	80	2.7(6) × 10 ²
IF ₂₀	4.8	80	2.3(4) × 10 ²
IF ₄₈	5.7	70	1.2(2) × 10 ²

5.6. Merit of Spray coating for fabrication of thin films at low temperature

Spray coating method was compared to spin coating in order to investigate its usefulness for the fabrication of metallic Cu thin films. About 200 μL of S₁ was spin coated onto quartz glass substrate using double mode steps of 500 rpm for 5 sec followed by 2000 rpm for 30 sec. The formed precursor film was pre-heated in an oven set at 70°C for 10 minutes and finally placed on a hot plate pre-heated at 180°C in air for ca. 1 h. The obtained precursor film; F_{1spin} + HT180°C was amorphous as shown by its XRD pattern in scheme 3. The formation of Cu [16] and Cu₂O [19] thin films by so far has only been reported by MPM *via* spin coating alcohol-based precursor solution onto substrate. Previous evidences indicated that spin coating favors only volatile organic solvent because aqueous solutions are generally inadequate to spread onto various substrates due to high surface tension [18]. The present study therefore confirmed that spray coating which has also been previous reported as only a coating procedure for the high

temperature formation of highly conductive Cu thin film [17] is significantly effective and sufficient to form conductive Cu thin film at 180°C in air. The merit of spray coating is highlighted by continuous deposition of small droplets of aqueous precursor solution that continuously crystallize and grows into a film after 5 seconds of spray for every 20 seconds. Some of its operational advantages, in contrast to spin coating aqueous solution is that the substrate is being kept at a stationary position and temperature throughout the period of spraying. Scheme 3 shows the formation of amorphous film by spin coating aqueous precursor film and heating it on a hot plate at 180°C in air.



Scheme 3. Formation of F'_{1Spin + HT180°C} by spin coating aqueous precursor film and heating it on a hot plate at 180°C in air

5.7. Summary

Fabrication of the conductive metallic Cu thin film by MPM *via* spray deposition of S'₁ containing Cu(II) of EDTA and amine, which was electrochemically prepared at ambient temperature was achieved at 180°C in air. The film has a thickness, adhesion strength and electrical resistivity of 170 nm, 12 ± 7 MPa and 8.9(2) × 10⁻³ Ω cm, respectively. The adhesion strength of the fabricated conductive metallic Cu thin film was weak in comparison to these previously fabricated by MPM due to its weak annealing temperature of 180°C and lacking of bonding between film and substrate, that is usually promoted by potential minor Cu₂O phase locally remaining at their interface. However, the film electrical resistivity of the order 10⁻³ Ω

cm was interesting to be achieved at 180°C in air. Furthermore, when identical annealing conditions to these of previously high temperature fabricated films by spray coating [17] is applied, its electrical resistivity reduces, and in close agreement to its counterpart film. The fabricated metallic Cu thin film whose corresponding electrolytic ES₂ initially contain EDTA was not electrically conductive. From that point of view the electrical resistivity of the film was established to be due to remaining amount of carbon in the film whose ratio to copper was 4 times high than that found in F'₁ based on their chemical composition which was analyzed by AES. While S₁ fabricated from ES₁ with no addition of EDTA is a Cu₂O thin film, hence the presence of EDTA is important as a source of carbon that is responsible for reduction of Cu²⁺ in solution to Cu⁺ in thin film. The photocatalytic activity of F₁ was in close agreement to that of its counterpart F14 containing identical chemical composition. While its stability depends on the pH of aqueous MO solution, it was indicated that the film was less photocatalytic active at its stable form under high pH of MO and visible light irradiation. Images of some of the fabricated thin films are shown in Figure 11.

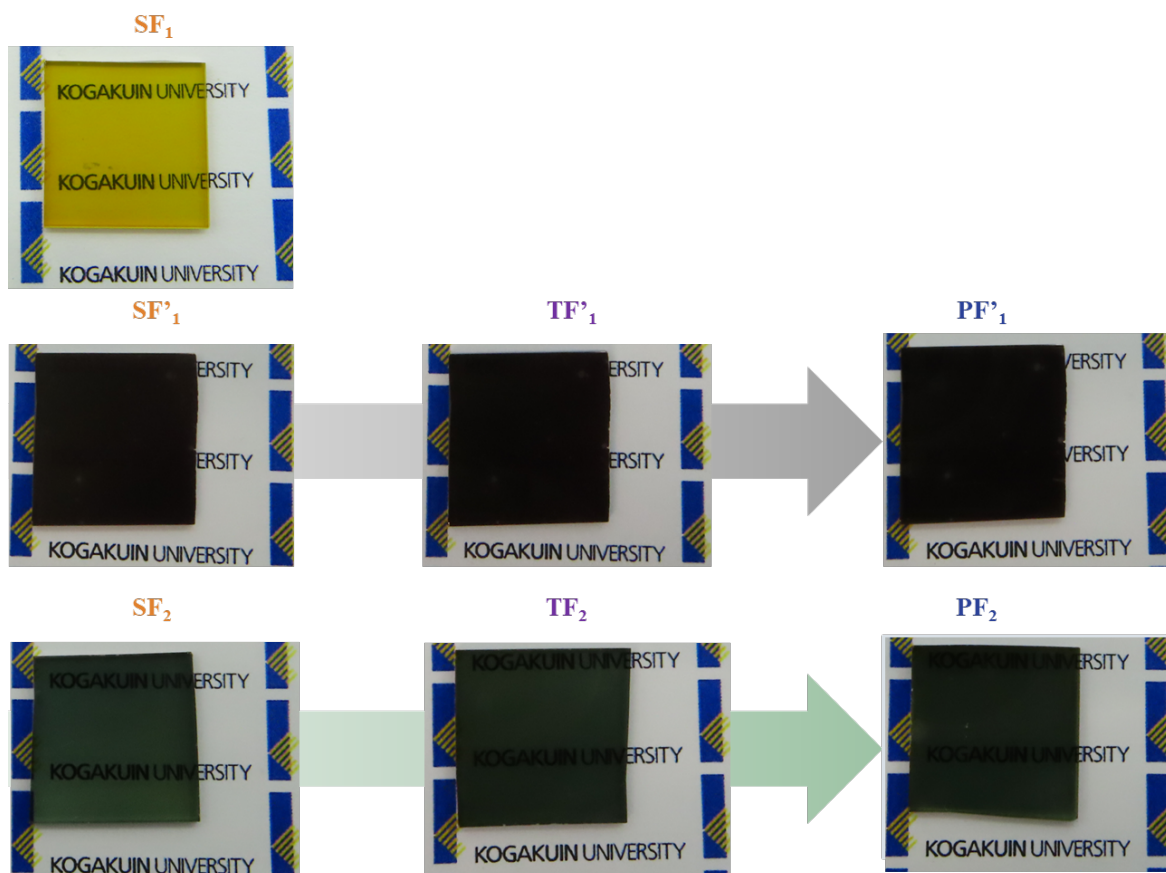


Figure 11. Images of some of the fabricated thin films.

Reference

- [1] Hashemipour, H.; Zadeh, M.E.; Pourakbari, R.; et al. Investigation on synthesis and size control of copper nanoparticle via electrochemical and chemical reduction method. *Int. J. Phys. Sci.* **2011**, *6*, 4331–4336.
- [2] Yu, L.; Sun, H.; He, J.; et al. Electro-reduction of cuprous chloride powder to copper nanoparticles in an ionic liquid. *Electrochemistry Communications.* **2007**, *9*, 1374–1381.
- [3] Yener, S.C.; Cerezci, O. Material analysis and application for radio frequency electromagnetic wave shielding. *Acta Phys. Pol. A.* **2016**, *129*, 635–638.
- [4] Duran, D.; Kadoğlu, H. Research on electromagnetic shielding with copper core yarns. *Tekst. ve Konfeksiyon.* **2012**, *22*, 354–359.
- [5] Tai, M.F.; Kok, S.L.; Mukai, K.; et al. EMI shielding performance for varies frequency by metal plating on mold compound. *Adv. Sci. Technol. Eng. Syst.*, **2017**, *2*, 1159–1164.
- [6] Ahmed, R.A. Synthesis of Copper Nanoparticles with Various Sizes and Shapes: Application as a Superior Non-Enzymatic Sensor and Antibacterial Agent. *Int. J. Electrochem. Sci.* **2016**, *11*, 4712–4723.
- [7] Song, X.; Sun, S.; Zhang, W.; et al. A method for the synthesis of spherical copper nanoparticles in the organic phase. **2004**, *273*, 463–469.
- [8] Lee, Y.; Choi, J.; Lee, K.J.; et al. Large-scale synthesis of copper nanoparticles by chemically controlled reduction for applications of inkjet-printed electronics. *Nanotechnology.* **2008**, *19*, 1–7.
- [9] Tegoni, M.; Valensin, D.; Toso, L.; et al. Copper Chelators: Chemical Properties and Bio-medical Applications. *Current Medicinal Chemistry.* **2014**, *21*, 3785–3818.
- [10] Touabi, N.; Martinez, S.; Bounoughaz, M. Optimization of Electrochemical Copper Recovery Process : Effect of the Rotation Speed in Chloride Medium of pH = 3. *Int. J. Electrochem. Sci.* **2015**, *10*, 7227–7240.
- [11] Yang, X.; Chen, S.; Zhao, S.; et al. Synthesis of copper nanorods using electrochemical methods. *J.Serb.Chem.Soc.* **2003**, *68*, 843–847.
- [12] Hojabri, A.; Hajakbari, F.; Moazzen, M.; Kadkhodaei S. Effect of Thickness on Properties of Copper Thin Films Growth on Glass by DC Planar Magnetron Sputtering. *Sid.Ir.* **2012**, *2*, 107–112.
http://www.sid.ir/en/VEWSSID/J_pdf/102902012JUN113.pdf.
- [13] Aadim, K.A.; Hussain, A.A.K.; Abdulameer, M.R. Effect of Laser Pulse Energy on the

- Optical Properties of Cu₂O Films by Pulsed Laser Deposition. *Acta Phys. Pol.* **2015**, *128*, 419–422.
- [14] Norziehana, N.; Isa, C. Electrodeposition and Characterization of Copper Coating on Stainless Steel Substrate from Alkaline Copper Solution Containing Ethylenediaminetetraacetate (EDTA). *J. Mech. Eng.* **2017**, *2*, 127–138.
- [15] Koyama, K.; Tanaka, M.; Miyasaka, Y.; et al. Electrolytic Copper Deposition from Ammoniacal Alkaline Solution Containing Cu (I). *Material Transactions.* **2006**, *47*, 2076–2080.
- [16] Nagai, H.; Mita, S.; Takano, I.; et al. Conductive and semi-transparent Cu thin film fabricated using molecular precursor solutions. *Mater. Lett.* **2015**, *141*, 235–237.
- [17] Hishimone, P.; Nagai, H.; Morita, M.; et al. Highly-Conductive and Well-Adhered Cu Thin Film Fabricated on Quartz Glass by Heat Treatment of a Precursor Film Obtained Via Spray-Coating of an Aqueous Solution Involving Cu(II) Complexes. *Coatings.* **2018**, *8*(10), 1–10.
- [18] Nagai, H.; Sato, M. Molecular Precursor Method for Fabricating *p*-Type Cu₂O and Metallic Cu Thin Films. *Mod. Technol. Creat. Thin-film Syst. Coatings.* 2017.
- [19] Nagai, H.; Suzuki, T.; Hara, H.; et al. Chemical fabrication of *p*-type Cu₂O transparent thin film using molecular precursor method. *Mater. Chem. Phys.* **2012**, *137*, 252–257.
- [20] Wu, H.; Tomiyama, N.; Nagai, H.; et al. Fabrication of a *p*-type Cu₂O thin- film via UV-irradiation of a patternable molecular-precursor film containing Cu(II) complexes. *Journal of Crystal Growth.* **2019**, *509*, 112–117.
- [21] Armelao, L.; Barreca, D.; Bertapelle, M.; et al. A sol-gel approach to nanophasic copper oxide thin films. *Thin Solid Film.* **2003**, *442*, 48–52.
- [22] Nordin, N.; Hasan, S.Z.; Zakaria, Z.; et al. Effect of applied voltage on slow-release of Cu(II) ions on the synthesis of Copper(II) stearate complex by electrochemical technique. *J. Braz. Chem. Soc.* **2015**, *26*, 1115–1123.
- [23] Kuprum, P.; Karboksilat, I.I.; Berasaskan, O.; et al. Synthesis and Characterization of Copper(II) Carboxylate with Palm-Based Oleic Acid by Electrochemical Technique. *Malaysian Journal of Analytical Science.* **2015**, *19*, 236–243.
- [24] Bejerrum, J.; Agarwala, B.V. Metal Amine Formation in Solution. XIX. On the Formation of Tetraamminedi- μ -hydroxodicopper(II) and Hydroxotetra-ammine Complexes in Ammoniacal Copper(II) Solutions. *Acta Chemica. Scandivanica A.* **1980**, *34*, 475–481.
- [25] Haram, S.K.; Mahadeshwar, A.R.; Dixit, S.G. Synthesis and characterization of copper

- sulphide nanoparticles in aqueous surfactant solutions. *Adsorpt. Sci. Technol.* **1998**, *16*, 667–677.
- [26] Prenesti, E.; Daniele, P.G.; Toso, S. Visible spectrophotometric determination of metal ions: The influence of structure on molar absorptivity value of copper(II) complexes in aqueous solution. *Anal. Chim. Acta.* **2002**, *459*, 323–336.
- [27] Prenesti, E.; Daniele, P.G.; Berto, S.; et al. Spectrum-structure correlation for visible absorption spectra of copper(II) complexes showing axial co-ordination in aqueous solution. *Polyhedron.* **2006**, *25*, 2815–2823.
- [28] Inoue, F.; Philipsen, H.; Radisic, A.; et al. Electroless Copper Bath Stability Monitoring with UV-VIS Spectroscopy, pH, and Mixed Potential Measurements. *J. Electrochem. Soc.* **2012**, *159*, D437–D441.

CHAPTER 6
Summary and Future Developments

CHAPTER 6: Summary and Future Developments

Under this study low temperature of 180°C and atmospheric air were considered effective conditions for the fabrication of functional thin films of copper oxide and metallic copper *via* spray coating by MPM. Precursor aqueous based coating solutions involving Cu(II) complexes were prepared by two main methods of conventional chemical synthesis and electrochemical employing copper salts and metal plates, respectively as starting materials. The highly photocatalytic *p*-type Cu₂O and conductive metallic Cu thin films were fabricated by depositing conventional chemical synthesized and electrochemical prepared precursor aqueous solutions, respectively onto a quartz glass substrate at 180°C in air. Both thin films were fabricated using spray coating method at atmospheric conditions, which is a well-developed coating application process for aqueous based precursor solutions deposition on various substrates within MPM.

The *p*-type Cu₂O thin films are potential candidates in various energy requiring technological devices such as thin film solar cells and transistors while Cu thin films are potential candidates in electric circuit boards, thermal collector tubes and as antibacterial material surfaces. The fabrication conditions of these thin films mainly low temperature and atmospheric conditions from precursor aqueous solutions is considered to promote sustainable development through reduced raw material, cost, energy consumption and CO₂ emission. Sustainable development goals encourage the scientific research due to an alarmingly increase of the world population that its average is estimated to be of 81 million people per year. The population demand and need for utilization of advanced technological devices is also increasing, therefore formation of functional Cu₂O and metallic Cu thin films by environmental conservative methods is significantly necessary.

The Cu₂O precursor aqueous solution prepared from metallic copper plate by electrochemical method. The solution was used selectively fabricate *P*-type Cu₂O and Cu thin films of which selectivity was determined by the presence or absences of added EDTA in the electrolytic solution of dissolved HCOONH₄ in aqueous ammonia. The electrochemically prepared aqueous solution was prepared from dissolution of anode copper metal plates electrodes *via* electrolysis, which were used a model electrode in this study. Crude copper locally mined in Namibia will be utilized as a permanent electrode for source of Cu²⁺ during

electrolysis. Namibia is rich in Natural resources such as Diamond, Uranium, Zinc and Copper. Copper contributes 50% to the country's annual export earnings. Copper is exported to foreign countries in its raw forms for processing into finished final products, of which Namibians buy a high price, without being used in the research and industrial fields inside the country. It's from that point of view that considering the fabrication of functional thin films at low temperature in air using a conservative spray method for precursor aqueous solution will contribute to the sustainable development, add value to the Namibia crude copper and promote its local industrialization.

The main results which were featured in the published articles from this study are summarized in the next two sections, as well as the future development of the entire research work.

6.1. Fabrication of Highly photocatalytic *p*-type Cu₂O semiconductor at low temperature from the chemical synthesized precursor aqueous solution

A *p*-type Cu₂O thin films on a quartz glass substrate were facilely fabricated at 180°C in air by spraying aqueous precursor solutions. The spray solutions were prepared in a diluted ammonia solution by dissolving Cu(II) formate and ammonium formate whose molar ratios to Cu(II) ion were 0, 2, 6 and 14. The prepared precursor solutions were stable and could be stored at usual environmental conditions for longer than 4 months. According to the XRD patterns, Cu₂O single phase thin films were obtained from coating precursor solutions whose molar ratio of added ammonium formate was 2, 6 and 14. The varied added ammonium formate was a reductant for transformation of divalent copper in various precursor solution into monovalent copper in the corresponding resultant Cu₂O thin films. Whereas, in the case of 0 added amount of ammonium formate, the resultant thin film was partially oxidized to CuO due to lack of reductant in corresponding precursor solution.

The photocatalytic activity of all the fabricated thin films was investigated *via* discoloration test of MO under visible light at ambient temperature. The thin films whose added amount of ammonium formate in their corresponding coating solutions were; 0, 2, 6 and 14 discoloration rate constants of MO solution under the visible-light irradiation were determined to be in the following order of 0.004, 0.004, 0.003, 0.042 and 0.087 min⁻¹. Whereas from time-dependence of MO concentration in dark condition, the rate constant of MO adsorption onto the thin films

and substrates could be also determined as 0.002, 0.002, 0.001, 0.002 and 0.056 min⁻¹. Based on the thin films pseudo-first-order rate constants, whose precursor solutions of contains added molar ratios at 6 and 14, with 140 and 350 nm thickness respectively indicated a highly photocatalytic activity under visible-light irradiation of 0.45 mW cm⁻². The photocatalytic activities of these thin films were majorly attributed to their O-defect site found in their Raman spectra. In addition, FE-SEM of the thin films provided the important information on the morphology directly relevant to the adsorption ability of the film with photocatalytic properties of which the thin film resulting from 14 times amount of added ammonium formate was more porous structured than all the fabricated thin films. The O-defect site and porous structure were indicated by this study to be the important factors to fabricate a highly photocatalytic Cu₂O thin film having high adsorption ability and whose adhesion strength onto the quartz substrate were larger than 5.6 N. It was linked that the photocatalytic activity of the obtained Cu₂O thin film depends on the amount of added ammonium formate into the spray solutions. The 6 times molar ratio of added ammonium formate against Cu(II) ion is a threshold to provide the photocatalytic activity to the resultant Cu-deficient Cu₂O thin films.

The immobilized Cu₂O thin films facilely fabricated at low temperature can be used to remove organic pollutants as a convenient photocatalyst under visible light irradiation. This study demonstrated a procedure with simple instrumentation and required no further heat-treatment of the sprayed thin films to obtain crystalline highly photocatalytic *p*-type Cu₂O thin films. The chemical component, and optical and electrical properties were also examined in detail and found not to significantly be related to their photocatalytic activity.

6.1.1 Recommendations and future development

The fabrication of photocatalytic *p*-type Cu₂O thin films at 180°C in air by spray coating precursor aqueous solution onto a larger substrate surface, than a 20 × 20 mm². The coating of Cu₂O can be attempted on a different substrates and shapes such as polycarbonate because it was indicated that the functional thin films can be formed at low temperature.

6.2. Selective fabrication of Cu₂O and Cu thin films at low temperature from electrochemically prepared precursor aqueous solution

The previous sections described the formation of aqueous coating solution of Cu(II) complex prepared from starting material of metal salts, in a two-step preparation of coating solution within the MPM. In a typical MPM, the preparation of coating solution usually involves two steps; of which the first is the isolation of solid metal complex using various copper salts. And the second step is the dissolution of the synthesized metal complex into appropriate solvent to result in a stable precursor coating solution. This study attempted the preparation of Cu(II) complex coating solution in a one-step process. The preparation of Cu₂O precursor solution was achieved from direct conversion of Cu metal into Cu(II) complexes with no isolation process of solid Cu(II) complexes or salts, via electrochemical process in an electrolytic solution involving dissolved ammonium formate in dilute ammonia aqueous solution. The solution was spray coated onto quartz glass substrate at 180°C in air to result in a *p*-type Cu₂O thin films whose properties were identical to that of highly photocatalytic *p*-type Cu₂O thin films fabricated in previous section whose added ammonium formate molar ratio to Cu²⁺ was 14.

It was revealed that by adding EDTA in the electrochemically prepared precursor solution and coating it onto a quartz glass substrate at identical condition will result in the formation of conductive metallic Cu thin film. While preparation of Cu precursor aqueous solution by electrolyzing copper plate in identical electrolytic solution initially involving EDTA will result in a non-conductive metallic Cu thin film. Hence EDTA was identified as an inhibiting factor for the dissolution of Cu²⁺ ion in respective electrolytic solutions, whose concentration was 0.033 and 0.018 mmol g⁻¹, respectively for initially excluding and including EDTA in electrolytic solution.

A conductive Cu thin film with a thickness of 170 nm, electrical resistivity of $8.9(2) \times 10^{-3}$ Ω cm and adhesion strength of 12(7) MPa was fabricated at 180°C in air. The surface morphology image of resultant Cu thin film, observed by a field emission scanning electron microscope revealed closely distributed Cu grains with particle sizes of ca. 80 ± 30 nm. It was indicated that the Cu complex containing EDTA ligand in the spray solution plays important roles to (1) provide enough amount of carbon atoms as a reducing agent for phase transition of its coordinated Cu²⁺ to crystalline Cu⁰ and (2) prevent the product from oxidation under atmospheric O₂ during spray-coating.

6.2.1. Recommendations and future development

As described in the opening introduction of this Chapter. Copper is one of abundant natural resources in Namibia. The future development of this work is the replacing of metallic copper plates used as starting material for preparation of coating solution, with a crude copper locally mined in Namibia. The solution can be coated onto quartz glass substrate and other various substrates at 180°C in air for the fabrication of both functional *p*-type Cu₂O or conductive metallic Cu thin films, based on the inclusion or exclusion of EDTA in the starting electrolytic solution. The fabricated thin films will not only be applicable to materials in energy devices, but mostly for their application such as their formation of antibacterial materials for environmental purification and immobilized photocatalysts. The utilization of crude copper mined in Namibia will contribute to the local industrialization of the country's raw material and its economic development.

Figure 1 shows the proposed experimental design for the preparation of precursor aqueous solutions and its application in spray coating for the selective fabrications of copper oxide and metallic Cu thin films on quartz glass substrate at 180°C in air by MPM. Two types of spray solutions namely; **S**_{1BRSTR} and **S'**_{1BRSTR} are electrochemically prepared using the identical electrolysis procedures as that described in chapter 4 and 5. The obtained **S**_{1BRSTR} and **S'**_{1BRSTR} precursor solutions are correspondence of **S**₁ and **S'**₁ electrochemically prepared using copper plate as electrodes. The prepared spray solutions are further spray coated onto quartz glass substrate at 180°C in air to obtain **F**_{1BRSTR} and **F'**_{1BRSTR} thin films.

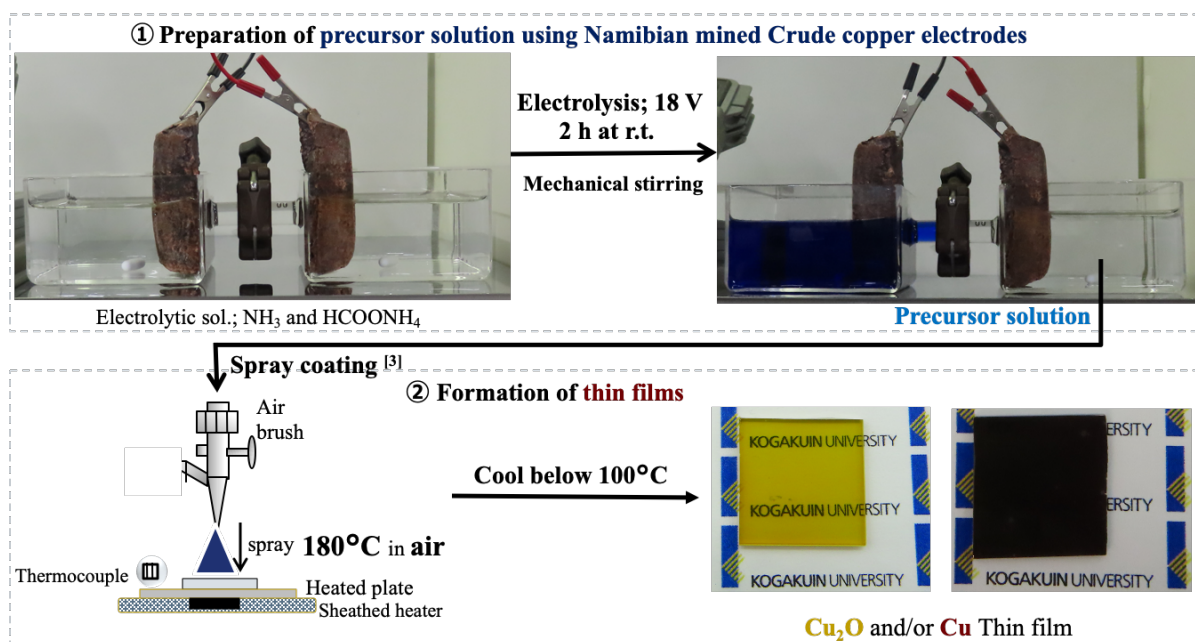


Figure 1. A schematic route for the preparation of aqueous precursor solution and selective fabrication of Cu_2O or metallic Cu copper thin films *via* spray coating at 180°C in air by MPM.

6.3. Preliminary results and discussion

6.3.1 Absorption spectra of spray solution electrochemically prepared from Cu blister

Figure 2 shows the UV-vis absorption spectra of the electrochemically prepared precursor solution using the Cu blister. The maximum absorption peak position of $S_{1\text{BRSTR}}$ and $S'_{1\text{BRSTR}}$ are observed at ca. 604 and 614 nm, which are in close agreement with these of S_1 and S'_1 as discussed in chapter 5. This implies that both copper plate and blister can electrolytically produce identical precursor solution considering the purity of Cu blister as only 98.9 %.

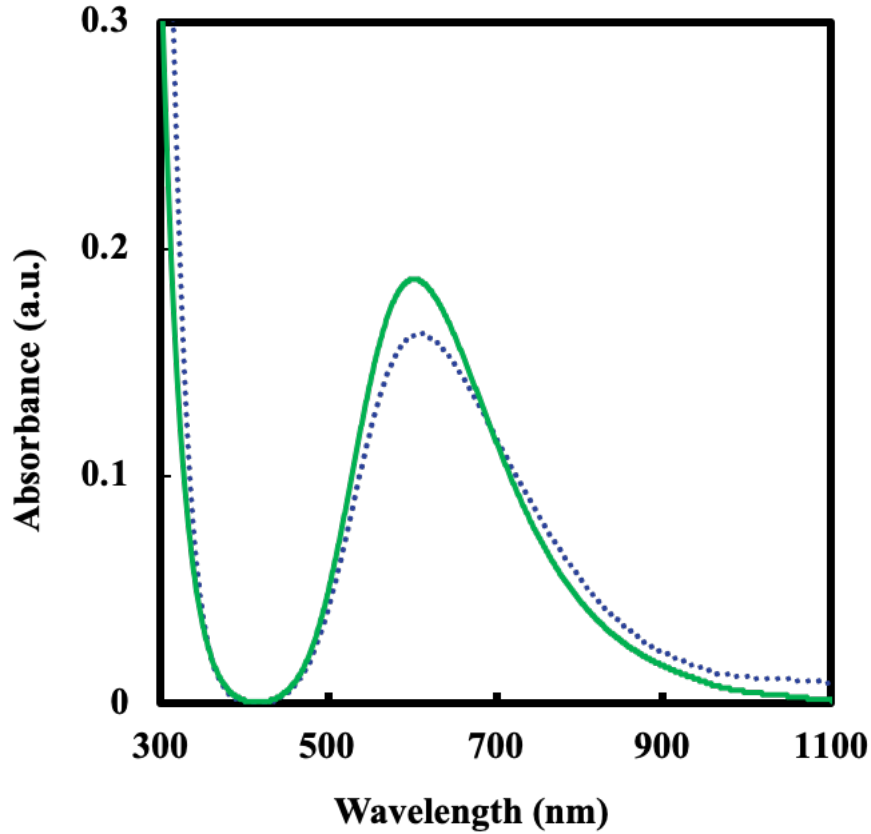


Figure 2. Absorption spectra of S_{1BLSTR} and S'_{1BLSTR} spray precursor solutions. The lines are labelled as; dotted blue line: S_{1BLSTR} and solid green line: S'_{1BLSTR} .

6.3.2. XRD patterns and electrical properties of fabricated F_{1BRSTR} and F'_{1BRSTR} .

Figure 3 shows the XRD patterns of the F_{1BRSTR} and F'_{1BRSTR} . Expectedly both S_{1BRSTR} and S'_{1BRSTR} results in a Cu_2O and Cu single phases, respectively. The hereof fabricated films showed no any other different elemental crystal phase from its corresponding F_1 and F'_1 discussed in chapter 5. Therefore, the potential impurities in S_{1BRSTR} and S'_{1BRSTR} precursor solution did not alter the crystals phases of the resulted thin film obtained after their spraying onto substrate at $180^\circ C$ in air. The electrical properties of the films were also evaluated and indicated that both obtained films were electrically conductive after spraying onto substrate at $180^\circ C$ in air. Table 1 shows the electrical properties and thickness of the fabricated thin films.

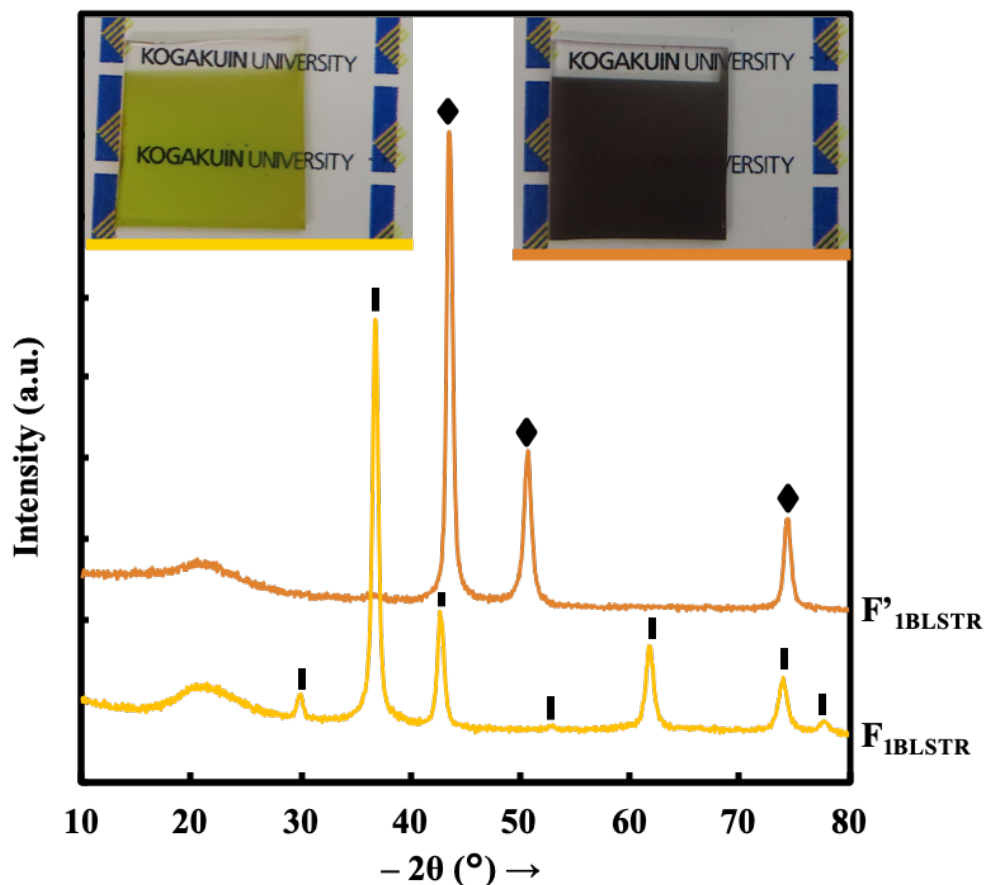


Figure 3. XRD patterns of F_{1BLSTR} , and F'_{1BLSTR} fabricated by MPM *via* spray deposition of corresponding electrochemically prepared S_{1BLSTR} and S'_{1BLSTR} onto quartz glass substrate at 180°C in air. The peaks are denoted as follows; ◆: Cu and |: Cu_2O .

Table 1 Averaged thickness and electrical resistivity of the fabricated F_{1BLSTR} and F'_{1BLSTR} using corresponding precursor solutions. The standard deviation is shown in parentheses.

Fabricated films	Annealing conditions;		Thickness (nm)	ρ (Ω cm)
	temp. ($^{\circ}C$)	time (min)		
F_{1BLSTR}	180	22	140	-
F'_{1BLSTR}		23	190	$1.85(1) \times 10^{-3}$

研究業績書

I. 審査付論文

番号を付して、著書名(学位申請者にアンダーライン)、論文名、学協会誌名、巻(号)、最初と最後のページ、発表年(西暦)を記載すること。

II. その他の研究論文(著書、学術雑誌、研究機関への研究報告、解説など)

番号を付して、著書名(学位申請者にアンダーライン)、論文名、学協会誌名、巻(号)、最初と最後のページ、発表年(西暦)を記載すること。

III. 口頭研究発表

国外と国内に分けて、番号を付して、研究者名(学位申請者にアンダーライン)、学会名、開催地、発表年月日を記載すること。

IV. 学会(委員会関係も含む)および社会における活動状況等

活動期間と学会、委員会名を記載すること。

I. 審査付論文

1. A. Uusiku, H. Nagai, and M. Sato, Highly photocatalytic *p*-type Cu₂O thin films fabricated on a quartz glass substrate at 180°C in air, by spraying aqueous precursor solutions involving Cu(II) complexes. *Material Technology*, Published online: 30 Dec 2019. DOI: 10.1080/10667857.2019.1710333.
2. A. Uusiku, H. Nagai, and M. Sato, Selective deposition *p*-type Cu₂O or conductive Cu thin film at 180°C in air on a quartz glass substrate: Development of an aqueous spray solution using two-compartment electrolysis system. *Functional Materials Letters*, Published online: 16 Mar 2020 as a full-length article. DOI: 10.1142/S1793604720510121.

III. 口頭研究発表

国外

International conference, Oral

1. A. Uusiku, H. Nagai, and M. Sato, Direct preparation of aqueous solutions involving Cu(II) complex of EDTA, from copper plates by electrochemical process, The 24th International SPACC Symposium, Auckland, New Zealand, 2017/11/22–25.
2. A. Uusiku, H. Nagai, and M. Sato, Fabrication of conductive Cu thin film by Molecular Precursor Method using electrochemically prepared precursor solution, The 25th International SPACC Symposium, Okinawa, Japan, 2018/11/ 23–25.

International conference, Poster

1. A. Uusiku, M. R. Kiremire, L. S. Daniel, Synthesis and characterization of metal complexes of di-2-pyridyl ketone Schiff base ligands derived from *s*-methylthiocarbamate fragment, The 22nd International SPACC Symposium, Windhoek, Namibia. 2015/11/15–17.
2. A. Uusiku, H. Nagai, and M. Sato, Effect of applied voltage on the synthesis of Cu(II) complex of EDTA in aqueous solutions, from copper plates by electrochemical process, The 16th International Symposium on Advanced Technology, Tokyo, Japan, 2017/11/01–02.

国内

Domestic conference, Oral

1. A. Uusiku, M. R. Kiremire, L. S. Daniel, Synthesis and characterization of metal complexes of 2-benzoylpyridine and di-2-pyridyl ketone schiff base ligands derived from *s*-methylthiocarbamate, 2nd Annual Science Research Conference, Windhoek, Namibia, 2014/10/30–31.

4. A. Uusiku, E. M. R. Kiremire, L. S. Daniel, The study of metal complexes of di-2-pyridyl ketone Schiff base ligands derived from s-methyldithiocarbamate fragment and its application to biological activity toward *P. Falciparum*, 3rd Annual Science Research Conference. Windhoek, Namibia, 2015/11.

V . その他の業績

1. Best Poster Presentation Certificate, University of Namibia (The 22nd International SPACC Symposium, Windhoek, Namibia, 2015/11/15–17)
2. Best Poster Presentation Certificate, Kogakuin University of Technology and Engineering, (The 16th International Symposium on Advanced Technology, Tokyo, Japan, 2017/11/01–02)

ACKNOWLEDGEMENTS

I am grateful to the Ministry of Education, Culture, Sport, Science and Technology (MEXT) for awarding me a full study scholarship that enabled me to advance my knowledge in scientific research, for the long-term goal of contributing to the development of my country, Namibia through scientific research. I am equally grateful to Kogakuin University, specifically Graduate School of Engineering for accepting me in their program of Applied Chemistry and Chemical Engineering to conduct my Ph. D. research studies.

I express my sincere gratitude to my supervisors. **Prof. Mitsunobu Sato** for guiding me throughout the entire research from its title selections, his unique teaching toward searching of meaningful and reproduceable results, his immense knowledge, constant motivation and patience has led to the production of efficient and accurate research findings in a simple approach. You have alarmingly shaped my research scientific writing skills. Thank you for being a good mentor and advisor for my Ph. D. studies. Indeed “Simple is the best” _ Prof. Sato.

Prof. Hiroki Nagai, I am indebted to you for accessing and monitoring my research works on a daily basis. Your teaching approach, daily hard-working dedication and guidance onto my research work has made me a better researcher and had always stimulated me to do more better every day during my research at your laboratory. You were always ready to give insightful suggestions and encouragements. Thank you for making my daily access to all the laboratory instruments and reagents easily accessible even when I could not read Japanese. Thank you for building a great team and creating a conducive working environment for all of your laboratory students every year. You remain an exemptional teacher in my academic journey.

To **Dr. Chihiro Mochuzuki**, thank you for always providing me with the research materials, reagents, some equipment, specifically spraying air brushes that produced all the thin films under this study. You have showed your sincere support in all kinds of ways you could possible do. Thank you for assisting me with other life-requiring advances and emergency outside my research scope and the university.

Much appreciation to Kogakuin Professors; **Prof. Takeyoshi Onuma**, **Prof. Tomohiro Yamaguchi**, **Prof. Tohru Honda**, **Prof. Ichiro Takano** for your continued support,

encouragements and making your laboratory measuring instruments available for use in this research at all the times.

I am grateful to all the internal examiners **Prof. Toshinori Okura** and **Prof. Hidetaka Aso**, external examiner **Prof. Kazuaki Kudo** from University of Tokyo for making time out of your busy schedules to examine my research thesis. Thank you for providing important comments that had resulted in a huge improvement of the final thesis.

I would like to express my sincere gratitude to all laboratory members of applied chemistry and chemical engineering at the period of September 2016 – March 2020. Mostly to; Dr Hsiang – Jung Wu, Mr Tatsuya Suzuki, Mr. Yutaka Suwazono, Mr. Yuuki Fukuda, Mr. Gen Nakayama, Mr. Masayuki Ishii, Mr. Nobuyuki Takei and Mr. Nayoki Ogawa for their assistance with some measurements and studying of Japanese manuals of many instruments used in this research.

I would like to extend my gratitude to all the employees at the international student support center of Kogakuin university for their continued assistance, in finding housing, reminders for monthly scholarship signature, for providing meaningful school events and gatherings and trips that helped me learn the Japanese culture and made valuable friends in the process.

To my Namibian senior Dr Daniel S. Likius, I am grateful for the opportunity of introducing me to Japan. Thank you for your continued encouragement during my research studies. To my friend and former Laboratory mate at UNAM and Kogakuin University Dr. Phillipus N. Hishimone, I am grateful for all the laboratory assistance you offered me during all the years we studied together. Your hard work and dedication to the research has inspired me to work hard during my Ph. D. studies.

Many thanks to my fellow Namibia students, Mr Paulus Shigwedha and Mr. Natangue Shafuda for studying together in Kogakuin University, your hard work toward your own various researches had kept me motivated to work extra hard during this research studies.

I am grateful for the support and continued encouragement from all staff members of Chemistry and Biochemistry department of faculty of scient at UNAM. Specifically, to Prof, Veikko Uahengo, Dr. Martha Kandawa Shulz, Dr. Petrina Kapewangolo, Ms. Teopolina Tomas, Ms. Natalia Anannias and Ms. Lea Nashipolo. I am indebted to my mentor **Prof. Enos M. R.**

Kiremire for introducing me to scientific research through my Msci. studies and for his continued support and encouragements during this research study.

To UNAM former vice-chancellor Prof. Lazarus Hangula and current vice-chancellor Prof. Kenneth Matengu your immense support and upholds toward the partnership collaboration your university has created with KU has given me an opportunity to further my research and had motivated me throughout this study. To the current presidents of the Republic of Namibia Dr. Hage G. Geingob, I was honored to had a chance of meeting you at TICAD7 during the time of my research study in Japan. Your brief words of encouragements had motivated me to complete my research studies.

To the former and current Namibian ambassadors to Japan; Ambassador Sofia Namwandi and Ambassador Morven M. Luswenyo, I am thankful for all the diplomatic assistances your office had provided me during my studies in Japan. Additionally, I extend my greatest gratitude for the assistance I received from all the employee at the Namibian embassy in Japan during this study. To the former Japanese Ambassador to Namibia; Ambassador Hamada Shinichi and his first secretary Mrs. Yokotani Kaoru I am thankful for all the assistance you provided me with all the paper works preparations including obtaining of study visa and itinerary, for all the emails of encouragement sent from your office during my time of this study. To the all the staff members of the **University of Electrocommunication (UEC), Tokyo, Japan** (April – September 2016). I am grateful for the opportunity you granted me by accepting me in your prestigious University to learn Japanese language for 6 months, which had helped me navigated my life and research studies in Japan.

I am thankful to great people I have meet during my period of study in Japan. They have helped me learn the Japanese culture and have always supported me during this study: Many special thanks to Ms. Mariko Mori, Ms. Kumi Yamamoto, Mr. Hiroki Hara and to the Akimoto and Matsuda families.

To my beloved siblings; Angula Uusiku, Petrus K. Uusiku, Hilma K. Uusiku, Makende Uusiku, Alma Uusiku, Maria L. Uusiku, Lazarus K. Uusiku, Kaino Uusiku, Petrina M. Uusiku, Helena N. Uusiku and Daniel Uusiku (RIP), my unconditional love for all of you had kept me close to you and had motivated me to work hard every day during this studies. To my biological mother **Alina Ndakondjelwapo Sheepo**, I will forever be grateful for your love, support and always believing in me. You are my biggest role model in everything I have done so far including this

research studies. To my second mother **Alma Nangula Johanness** (1945-2013), I am forever grateful for your teaching of hard work that you had installed in me at my very young age. It had encouraged me to continue working hard during my entire academic journey, specifically during this research studies, may your soul continue to rest in peace. To my late father, **Lazarus Kambata Uusiku**, thank you for always watching over me from heaven, this work is dedicated to you and mom.

To my aunt and uncles Albertina M. Nashandi and uncles Nicky P. Nashandi, Jacob K. Iiyambo, and Lazarus M. K. Iindongo thank you for taking me in your houses with your huge families during my earliest year of research studies and for always supporting and taking care of me. You have always encouraged me to work very hard during this study.

To my beloved cousins Nangula, Penda, Nambuli, and Netumbo Nashandi, Sylvia K. Amakali, Lovisa Iita, Hileni D. Kuumbwa, Alina Iiyambo, Josef K. Kamati, nieces Johanna, and Albertina Sheepo, Linea T. Nghinyemata, and nephews Hallelujah and Josef Uusiku, your constant reminder of your love for me, has kept me focused and progressive throughout this research studies. To my friends turned family; Saara L. Hamunyela, Hilma N. Shomongula Akweetelela, Rauna N. Nghitwikwa Absalom, Wilhemina Nawela, and Aina Kapulwa your continued support during my studies is greatly appreciated.